

AN ANALYSIS OF THE TRANSIENT PRESSURE BEHAVIOR OF  
A WELL SITUATED BETWEEN TWO SEALING FAULTS AND  
ITS APPLICATION TO SUBSURFACE FAULT MAPPING  
USING THE RESERVOIR LIMIT TEST

---

A Thesis  
Presented to  
the Faculty of the Department of Petroleum Engineering  
University of Houston

---

In Partial Fulfillment  
of the Requirements for the Degree  
Master of Science in Petroleum Engineering

---

by  
John R.D. Tidmarsh  
June 1966

347749

## ACKNOWLEDGEMENTS

The author wishes to thank the Board and Management of BP (Trinidad) Limited for making available the facilities to undertake this work. He is also grateful to the late Park J. Jones for guidance during the early stages; and to John Saint, who not only read the manuscript, but made many criticisms and useful suggestions. He has received invaluable assistance from Nazeer Mohammed, Julien Rampersad, Fazal Khan and Oscar Nesbit in the preparation of the final copy. He is especially indebted to his wife for her constant encouragement, patience and understanding.

AN ANALYSIS OF THE TRANSIENT PRESSURE BEHAVIOR OF  
A WELL SITUATED BETWEEN TWO SEALING FAULTS AND  
ITS APPLICATION TO SUBSURFACE FAULT MAPPING  
USING THE RESERVOIR LIMIT TEST

---

An Abstract of a Thesis  
Presented to  
the Faculty of the Department of Petroleum Engineering  
University of Houston

---

In Partial Fulfillment  
of the Requirements for the Degree  
Master of Science in Petroleum Engineering

---

by  
John R.D. Tidmarsh  
June 1966

The transient pressure behavior of a well situated between two sealing faults, and producing at a constant reservoir production rate, has been analyzed, using the line sink solution of the diffusivity equation and the method of images.

The study has been restricted to single phase flow through homogeneous isotropic reservoirs.

The angle of intersection between the faults and the position of the well within each fault block have been varied, to determine the effects upon the dimensionless drawdown curve.

It has been found that the shape of the curve, for a given angle of intersection, depends only on the ratio of the distances between the producing well and the two faults; and that the slope of the final straight-line portion of the curve is a function solely of the angle at which the faults intersect.

A library of type dimensionless drawdown curves has been prepared. By comparing these curves with one constructed from field data obtained during a Reservoir Limit Test, it is possible to determine whether or not the well is situated between two sealing faults; the angle of intersection between the faults; and the ratio of the distances between the faults and the well.

Furthermore, by measuring the dimensionless times at which straight-line portions of the curve intersect, the distance to each fault may be read off charts specially constructed for the purpose.

## TABLE OF CONTENTS

CHAPTER	PAGE
I. INTRODUCTION AND SCOPE OF THE THESIS .....	1
II. FUNDAMENTAL EQUATIONS .....	3
One Ideal Well in an Infinite Reservoir .....	3
Several Ideal Wells in an Infinite Reservoir .	5
The Skin Effect .....	7
III. CALCULATION OF RESISTIVITY, DIFFUSIVITY AND	
SKIN EFFECT, USING THE RESERVOIR LIMIT TEST .	10
Resistivity and Diffusivity .....	10
The Skin Effect .....	14
IV. THE METHOD OF IMAGES AND ITS APPLICATION TO	
SUBSURFACE FAULT MAPPING .....	17
V. THE TRANSIENT PRESSURE BEHAVIOR OF A WELL	
SITUATED BETWEEN TWO SEALING FAULTS .....	23
30° Fault Block .....	23
The image system .....	23
Dimensionless drawdown equations .....	28
Characteristics of dimensionless	
drawdown curves .....	29
Intersection-time equations .....	35
180° Fault Block .....	36
120° Fault Block .....	37
90° Fault Block .....	38
72° Fault Block .....	40
60° Fault Block .....	41

CHAPTER	PAGE
45° Fault Block .....	43
15° Fault Block .....	45
Parallel Faults .....	48
The Effect of the Skin .....	50
VI. SUBSURFACE FAULT MAPPING USING THE RESERVOIR	
LIMIT TEST .....	54
The Basis of Subsurface Fault Mapping .....	54
Method of Analysis .....	56
Example number 1 .....	58
Measured data .....	58
Calculation of resistivity, diffusivity and skin effect .....	59
Conversion of field data to ideal dimensionless data .....	62
Analysis of the dimensionless drawdown curve .....	64
Discussion of results .....	65
Example number 2 .....	68
Measured data .....	68
Calculation of resistivity, diffusivity and skin effect .....	69
Conversion of field data to ideal dimensionless data .....	71
Analysis of the dimensionless drawdown curve .....	72

CHAPTER	PAGE
Discussion of results .....	76
Example number 3 .....	76
Measured data .....	76
Calculation of resistivity, diffusivity and skin effect; and interpretation of the drawdown curve .....	78
Discussion of results .....	82
Example number 4 .....	83
Measured data .....	83
Calculation of resistivity, diffusivity and skin effect .....	84
Conversion of field data to ideal dimensionless data .....	87
Analysis of the dimensionless drawdown curve .....	87
Discussion of results .....	89
Example number 5 .....	89
Measured data .....	89
Calculation of resistivity, diffusivity and skin effect .....	91
Conversion of field data to ideal dimensionless data .....	94
Analysis of the dimensionless drawdown curve .....	94
Discussion of results .....	96

CHAPTER	PAGE
VII. AN APPRAISAL OF THE RESERVOIR LIMIT TEST, AND CONCLUSIONS .....	99
BIBLIOGRAPHY .....	101
APPENDIX A. Nomenclature .....	103
APPENDIX B. The Well Function .....	106
APPENDIX C. Image Systems .....	111
APPENDIX D. Computer Programs for Ideal Dimensionless Drawdown Curves .....	122
APPENDIX E. Library of Type Dimensionless Drawdown Curves .....	133
APPENDIX F. Charts for Subsurface Fault Mapping ....	144



## LIST OF FIGURES

FIGURE	PAGE
1. Pressure Distribution in a Reservoir Showing the Skin Effect .....	9
2. Drawdown for an Ideal Well in an Infinite Reservoir .....	13
3. Drawdown for a Well in an Infinite Reservoir Showing the Skin Effect .....	16
4. Well Situated in a $90^{\circ}$ Fault Block .....	18
5. Image System for a $90^{\circ}$ Fault Block .....	18
6. Image System for a $30^{\circ}$ Fault Block .....	25
7. $30^{\circ}$ Fault Block. Typical Computer Output for Ideal Dimensionless Drawdown Curve .....	30
8. $30^{\circ}$ Fault Block. Ideal Dimensionless Drawdown Curve .....	32
9. Parallel Faults. Typical Computer Output for Ideal Dimensionless Drawdown Curve .....	51
10. $60^{\circ}$ Fault Block. Dimensionless Drawdown Curves for an Ideal Well and a Well with a Skin .....	53
11. Subsurface Fault Mapping. Example No. 1. Drawdown Curve .....	60
12. Subsurface Fault Mapping. Example No. 1. Ideal Dimensionless Drawdown Curve .....	63
13. Subsurface Fault Mapping. Solution to Example No. 1 .....	66

FIGURE	PAGE
14. Subsurface Fault Mapping. Example No. 2.	
Drawdown Curve .....	70
15. Subsurface Fault Mapping. Example No. 2.	
Ideal Dimensionless Drawdown Curve for	
Solution No. 1 .....	73
16. Subsurface Fault Mapping. Example No. 2.	
Ideal Dimensionless Drawdown Curve for	
Solution No. 2 .....	75
17. Subsurface Fault Mapping. Solutions to	
Example No. 2 .....	77
18. Subsurface Fault Mapping. Example No. 3.	
Drawdown Curve .....	80
19. Subsurface Fault Mapping. Solution to	
Example No. 3 .....	81
20. Subsurface Fault Mapping. Example No. 4.	
Drawdown Curve .....	85
21. Subsurface Fault Mapping. Example No. 4.	
Ideal Dimensionless Drawdown Curve .....	88
22. Subsurface Fault Mapping. Solution to	
Example No. 4 .....	90
23. Subsurface Fault Mapping. Example No. 5.	
Drawdown Curve .....	92
24. Subsurface Fault Mapping. Example No. 5.	
Ideal Dimensionless Drawdown Curve .....	95
25. Subsurface Fault Mapping. Solution to	
Example No. 5 .....	97

## CHAPTER I

### INTRODUCTION AND SCOPE OF THE THESIS

The Reservoir Limit Test, developed by Park J. Jones, is a transient-flow, formation evaluation technique, whereby a well is produced at a constant reservoir production rate and a quantitative analysis made of the curve obtained by plotting the pressure drawdown versus the log of producing time.

From such an analysis, it is possible to calculate certain reservoir properties, including distances to impermeable productive limits, such as sealing faults, with which this thesis is concerned.

However, difficulties encountered during previous interpretations of drawdown curves have revealed the need for a library of type curves, which show the effects of one or more sealing faults on the drawdown in a producing well.

The transient pressure behavior of a well situated near one sealing fault, or between two faults, has therefore been investigated analytically, and a library of type curves constructed (Appendix E). A method for calculating the distances to the faults, and the angle of intersection between the faults, has been evolved, and results are presented in the form of simple charts (Appendix F). The study has been restricted to fault blocks for which image systems can be drawn, and only single phase flow through homogeneous isotropic reservoirs has been considered. Calculations were

performed on an IBM 709 digital computer.

Chapter II contains basic data pertaining to transient flow, from which the fundamental equations, upon which subsurface fault mapping is based, are derived.

Some aspects of the Reservoir Limit Test are discussed in Chapter III, wherein methods for finding the reservoir resistivity, reservoir diffusivity and skin effect are described.

In Chapter IV, the method of images and its application to subsurface fault mapping are explained.

Chapter V contains a detailed analysis of the transient pressure behavior of a well producing at a constant reservoir production rate, and situated between two sealing faults at varying angles of intersection.

In Chapter VI, methods for determining the angle of intersection between the faults and the distances to the faults are developed, and examples are worked. The limitations of the Reservoir Limit Test are also discussed, both from a theoretical and practical point of view.

The last chapter is devoted to a brief appraisal of the Reservoir Limit Test as a formation evaluation technique; and areas in which further study is necessary are mentioned.

## CHAPTER II

### FUNDAMENTAL EQUATIONS

#### I. ONE IDEAL WELL IN AN INFINITE RESERVOIR

Consider an ideal well, that is a well with no skin, situated within an infinite homogeneous isotropic reservoir. When that well is placed on production, a pressure drop, known as the drawdown, occurs in the vicinity of the well-bore.

The magnitude of the drawdown depends mainly upon :

( i ) The reservoir production rate,  $BQ^*$  barrels per day

and (ii) The reservoir resistivity,  $D$ , defined as follows :

$$D = \frac{0.1412\mu}{hk} \text{ psi/bpd} \dots\dots\dots (\text{II} - 1)$$

At a given time after commencement of production, the rate of propagation of perceptible drawdown into the reservoir is a function of the diffusivity,  $\eta$ , defined as follows :

$$\eta = \frac{6.328k}{\mu c\phi} \text{ sq. ft/day} \dots\dots\dots (\text{II} - 2)$$

The drawdown  $j$  psi, at radius  $r$  ft. from the well-bore, at time  $t$  days after commencement of production, is governed by the basic diffusivity equation for radial trans-

---

\* Nomenclature is given in Appendix A

ient flow, which is :

$$\frac{\partial^2 j}{\partial r^2} + \frac{1}{r} \frac{\partial j}{\partial r} = \frac{1}{\eta} \frac{\partial j}{\partial t} \dots\dots\dots (II - 3)$$

For a constant reservoir production rate, BQ , Kelvin's line sink solution of equation (II - 3), after Carslaw and Jaeger (1 : 261) \*, is :

$$j(r,t) \equiv j = \frac{BDQ}{2} W(u) \dots\dots\dots (II - 4)$$

where :

$$u = \frac{r^2}{4\eta t} \dots\dots\dots (II - 5)$$

and W(u) is the Well Function of u , defined and described in Appendix B.

When u is less than 0.01, W(u) may be replaced by its logarithmic approximation. Under these conditions, the drawdown is given by :

$$j = 1.15BDQ \log \frac{2.25\eta t}{r^2} \dots (II - 6)$$

From equations (II - 4) and (II - 5) , the self-drawdown in a producing well with no skin is given by :

$$j_i = \frac{BDQ}{2} W\left(\frac{r_w^2}{4\eta t}\right) \dots\dots\dots (II - 7)$$

where  $r_w$  is the radius of the wellbore, that is the radius of the bit used to drill the well, in feet.

However,  $\frac{r_w^2}{4\eta t}$  is usually less than 0.01 after a

---

\* The American Educational Research Association system of reference.

few minutes of production. Thus, for practical purposes, the self-drawdown in an ideal well may be expressed as :

$$j_i = 1.15BDQ \log \frac{2.25\eta t}{r_w^2} \dots \text{ (II - 8)}$$

## II. SEVERAL IDEAL WELLS IN AN INFINITE RESERVOIR

Now consider  $(n + 1)$  wells, which have been produced at the same reservoir flow rate,  $BQ$ , from an infinite reservoir since zero time. Then, by the method of superposition, the drawdown in any one of those wells is equal to its self-drawdown plus the drawdown due to the  $n$  other wells.

Therefore, from equations (II - 4), (II - 5) and (II - 7), the total drawdown is given by :

$$j_{i(n+1)\text{wells}} = \frac{BDQ}{2} \left[ W\left(\frac{r_w^2}{4\eta t}\right) + \sum_{y=1}^n W\left(\frac{r_y^2}{4\eta t}\right) \right] \dots \text{ (II - 9)}$$

where  $r_y$  is the distance, in feet, between the well in question and the  $y^{\text{th}}$  of the  $n$  other wells.

It is convenient to express equations (II - 8) and (II - 9) in terms of dimensionless quantities.

Putting :

$$j_{Di} = \frac{j_i}{BDQ} \dots \text{ (II - 10)}$$

$$t_D = \frac{\eta t}{r_w^2} \dots \text{ (II - 11)}$$

$$\text{and } r_{Dy} = \frac{r_y}{2r_w} \dots \text{ (II - 12)}$$

equation (II - 8) becomes :

$$j_{Di} = 1.15 \log 2.25t_D \dots\dots\dots (II - 13)$$

and equation (II - 9) becomes :

$$j_{Di(n+1)\text{wells}} = \frac{1}{2} \left[ W\left(\frac{1}{4t_D}\right) + \sum_{y=1}^n W\left(\frac{r_{Dy}^2}{t_D}\right) \right] \dots\dots (II - 14)$$

Equation (II - 14) therefore gives the ideal dimensionless drawdown, at any dimensionless time, in any one of  $(n + 1)$  wells, which have been produced at the same reservoir flow rate since zero time from an infinite, homogeneous, isotropic reservoir, where  $r_{Dy}$  is the dimensionless distance between the well in question and the  $y^{\text{th}}$  of the  $n$  other wells.

Jones (5 : 2) has shown that the time, at which perceptible interference from the  $y^{\text{th}}$  of the  $n$  other wells reaches the well in question, is given by :

$$t_{\text{int}(y)} = \frac{r_y^2}{16\eta} \dots\dots\dots (II - 15)$$

Therefore, from equations (II - 11) and (II - 12) :

$$t_{D\text{int}(y)} = \frac{r_{Dy}^2}{4} \dots\dots\dots (II - 16)$$

That is, for values of  $t_D$  less than  $r_{Dy}^2/4$ , the  $y^{\text{th}}$  of the  $n$  other wells has no effect upon the drawdown observed in the well in question.



### III. THE SKIN EFFECT

The drawdown observed in a producing well is usually greater than that indicated by equation (II - 8) or (II - 9) , due to a reduction in permeability in the immediate vicinity of the wellbore. This may be caused by such effects as mud filtration, swelling of clay particles in silty sands, formation collapse, contamination by cement and chemical precipitation.

In some instances, the observed drawdown is less than the ideal drawdown, indicating a zone of increased (or stimulated) permeability around the wellbore.

The difference between the actual drawdown and the ideal drawdown is known as the skin effect,  $j_s$  , first investigated by van Everdingen (2 : 171) and Hurst (3 : B - 6).

By definition :

$$j_s \equiv j_w - j_i = \text{BDQS} \dots\dots\dots \text{(II - 17)}$$

where  $S$  , a dimensionless quantity, is known as the skin.

Occasionally, an additional pressure drop occurs near the wellbore, due to the occurrence of non-Darcy (turbulent) flow, for which the basic diffusivity equation (II - 3) is not valid. This may be treated as a flow-rate dependent skin effect, and evaluated as described by Ramey (8 : 223).

The drawdown due to the skin occurs in the immediate vicinity of the wellbore, and is not transmitted into the

reservoir, as illustrated in Figure 1, after Hurst (3 : B - 6). Thus, the skin effect in a given producing well has no effect upon the drawdown observed in any other well producing from the same reservoir.

From equations (II - 8) and (II - 17), the self-drawdown in a producing well with a skin is given by :

$$j_w = BDQ \left[ 1.15 \log \frac{2.25\eta t}{r_w^2} + S \right] \dots\dots (II - 18)$$

Similarly, from equations (II - 9) and (II - 17), the drawdown in any one of (n+1) wells, which have been produced at the same reservoir rate since zero time, is :

$$j_{w(n+1)\text{wells}} = \frac{BDQ}{2} \left[ W\left(\frac{r_w^2}{4\eta t}\right) + \sum_{y=1}^n W\left(\frac{r_y^2}{4\eta t}\right) + 2S \right] \dots (II - 19)$$

The corresponding dimensionless equations are :

$$j_{Dw} = 1.15 \log 2.25t_D + S \dots\dots\dots (II - 20)$$

and :

$$j_{Dw(n+1)\text{wells}} = \frac{1}{2} \left[ W\left(\frac{1}{4t_D}\right) + \sum_{y=1}^n W\left(\frac{r_{Dy}^2}{t_D}\right) + 2S \right] \dots (II - 21)$$

Equations (II - 13) , (II - 14) , (II - 16) , (II - 20) and (II - 21) are the fundamental equations upon which subsurface fault mapping is based, as will be shown in Chapters IV, V and VI.

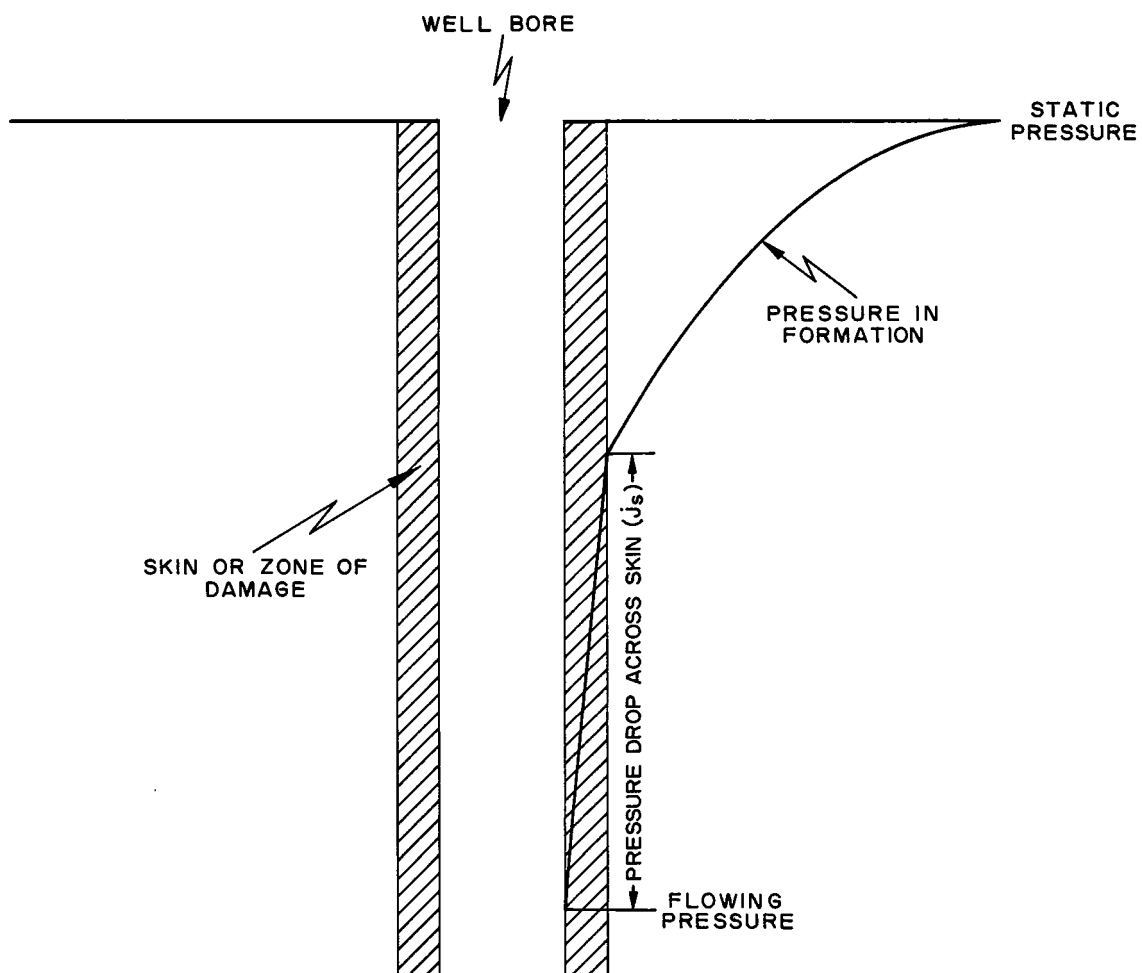


FIGURE 1

PRESSURE DISTRIBUTION IN A RESERVOIR  
SHOWING THE SKIN EFFECT

## CHAPTER III

### CALCULATION OF RESISTIVITY, DIFFUSIVITY AND SKIN EFFECT, USING THE RESERVOIR LIMIT TEST

The methods presented in this chapter were developed by Park Jones (5 : 1). However, part of his nomenclature has been modified to conform with that used throughout the thesis. Methods for finding the reservoir resistivity, reservoir diffusivity and the skin effect are described.

#### I. RESISTIVITY AND DIFFUSIVITY

During a Reservoir Limit Test, a well is produced at a constant reservoir production rate and the bottom-hole pressure continually recorded. The difference between the initial static pressure,  $p_{ws}$ , and the bottom-hole flowing pressure,  $p_{wf}$ , is termed the drawdown, which is given by equation (II - 18) :

$$p_{ws} - p_{wf} \equiv j_w = BDQ \left[ 1.15 \log \frac{2.25\eta t}{r_w^2} + s \right]$$

provided no interference from reservoir limits or other producing wells has been felt.

If  $j_w$  is plotted versus  $\log t$ , the slope  $m$  is defined by :

$$m = \frac{\partial j_w}{\partial (\log t)} = 1.15BDQ \text{ psi/log cycle ... (III - 1)}$$

The slope in an ideal well is also given by equation (III - 1) , as can be seen by inspection of equation (II - 8).

Since BQ and D are constant, m is constant, and the plot of  $j_w$  or  $j_i$  versus  $\log t$  is a straight line. Knowing the slope and formation flow rate, the resistivity, D , may be found :

$$D = \frac{m}{1.15 BQ} \dots\dots\dots (III - 2)$$

From equations (II - 1) and (III - 2) :

$$k = \frac{0.1626 \mu BQ}{hm} \dots\dots\dots (III - 3)$$

from which the effective permeability may be calculated.

From equations (II - 1) and (II - 2) :

$$\eta = \frac{0.8935}{Dhc\phi} \dots\dots\dots (III - 4)$$

Thus, knowing the resistivity, the diffusivity,  $\eta$  , may be calculated, since values of the formation thickness, average coefficient of compressibility and porosity are usually known or can be estimated fairly accurately.

In an ideal well, the drawdown is given by equation (II - 8) :

$$\begin{aligned} j_i &= 1.15BDQ \log \frac{2.25\eta t}{r_w^2} \\ &= 1.15BDQ \left[ \log t - \log \frac{r_w^2}{2.25\eta} \right] \dots\dots (III - 5) \end{aligned}$$

In this case, the diffusivity may be obtained by extrapolating the line of slope  $m$  back to zero drawdown at time  $t_{1,0}$  days.

Putting :

$$j_1 = 0 \text{ and } t = t_{1,0}$$

into equation (III - 5) , it is seen that :

$$\log t_{1,0} = \log \frac{r_w^2}{2.25\eta}$$

from which :

$$\eta = \frac{r_w^2}{2.25t_{1,0}} \dots\dots\dots (III - 6)$$

It is emphasized that equation (III - 6) applies to an ideal well only.

Figure 2 shows the drawdown in an ideal well completed in an infinite reservoir, where :

$$BQ = 125 \text{ res. bpd}$$

$$D = 0.16 \text{ psi/res. bpd}$$

$$\eta = 1.25 \times 10^5 \text{ sq.ft./day}$$

$$\text{and } r_w = 0.25 \text{ ft.}$$

The curve was plotted, using equation (II - 8) .

From equation (III - 1) , the slope of the curve is :

$$\begin{aligned} m &= 1.15 \times 125 \times 0.16 \text{ psi/log cycle} \\ &= 23 \text{ psi/log cycle} \end{aligned}$$

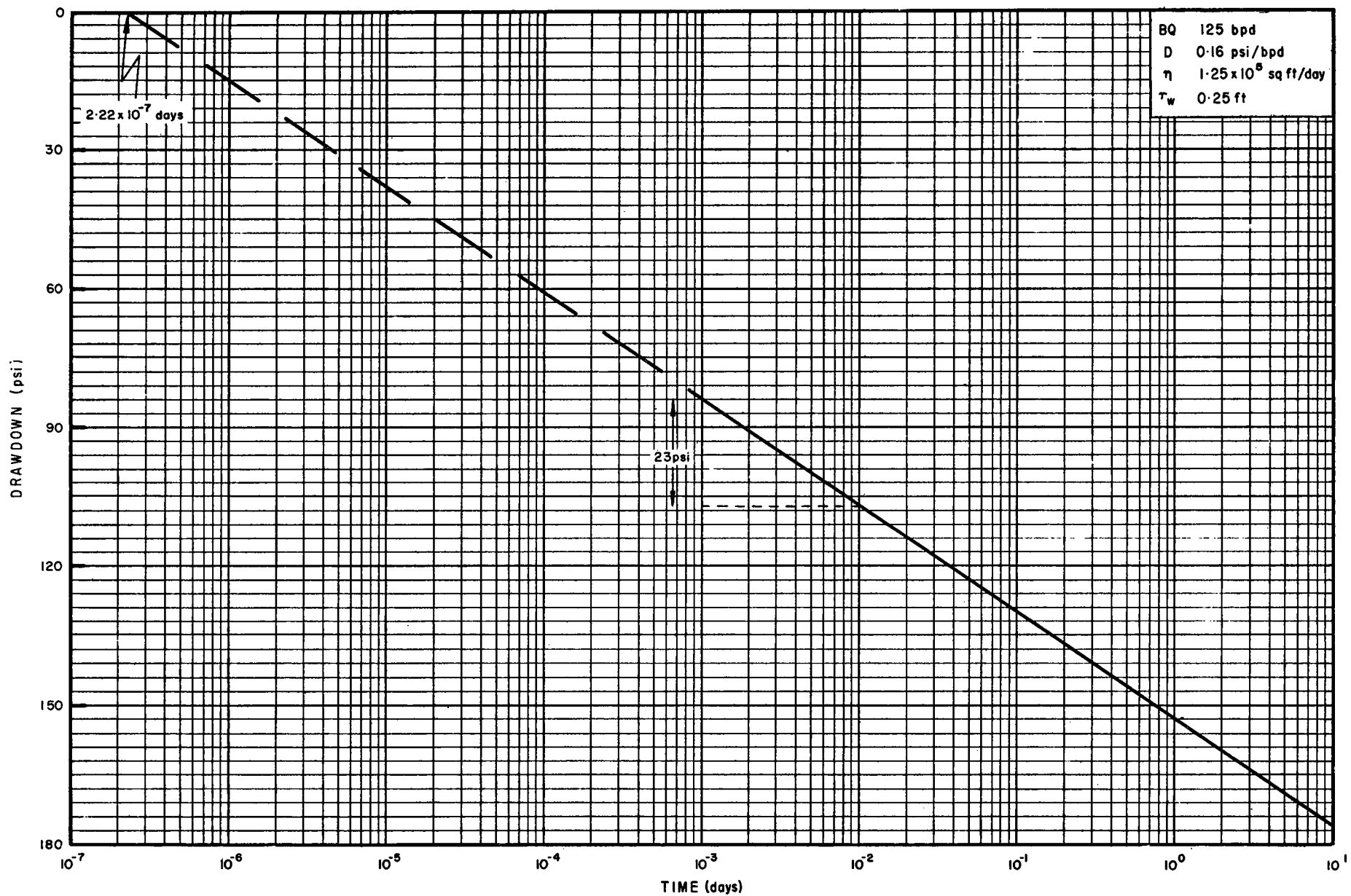


FIGURE 2

DRAWDOWN FOR AN IDEAL WELL IN AN INFINITE RESERVOIR

From equation (III - 6) , the intercept of the line on zero drawdown is given by :

$$\begin{aligned} t_{1,0} &= \frac{r_w^2}{2.25\eta} \\ &= \frac{(0.25)^2}{2.25 \times 1.25 \times 10^5} \\ &= 2.22 \times 10^{-7} \text{ days} \end{aligned}$$

As will be shown later, the straight line of slope  $m$  may not be seen if the well is situated near an impermeable productive limit. In this case, an approximate value of the permeability is required from some other source before an interpretation of the drawdown curve can be made. This is illustrated in examples in Chapter VI.

## II. THE SKIN EFFECT

The skin effect, defined in Chapter II, depends upon the permeability of the skin, the radius of the skin and the permeability of the reservoir beyond the skin.

The following equation, which was developed by Jones (5 : 4) from an expression derived by Hurst (4 : 175) , gives the drawdown in a well with a skin :

$$j_w = \frac{kBDQ}{2k_s} \left[ W\left(\frac{kr_w^2}{4k_s\eta t}\right) - W\left(\frac{kr_s^2}{4k_s\eta t}\right) + \frac{k_s}{k} W\left(\frac{r_s^2}{4\eta t}\right) \right] \dots\dots\dots \text{(III - 7)}$$



Using this equation, and the values of production rate, resistivity, diffusivity and wellbore radius used for the ideal curve in Figure 2 , a drawdown curve was constructed for a well with a skin, in which :

$$k_s = 1 \text{ md}$$

$$r_s = 4 \text{ ft}$$

$$\text{and } k = 10 \text{ md}$$

This curve and part of the ideal curve are shown in Figure 3.

It can be seen that the ideal curve is displaced downwards by an amount equal to the skin effect, BDQS .

The first part of the curve represents the drawdown due to the skin,  $j_s$  , and the second part the drawdown due to the reservoir,  $j_{res}$ .

The skin is evaluated by calculating the constants,  $D$  and  $\gamma$  , from the  $j_{res}$  line, as described above. The ideal drawdown at a convenient time, say one day, is then calculated from equation (II - 8). Subtraction of the calculated ideal drawdown from the observed actual drawdown yields the skin effect, BDQS , from which the skin may be calculated.

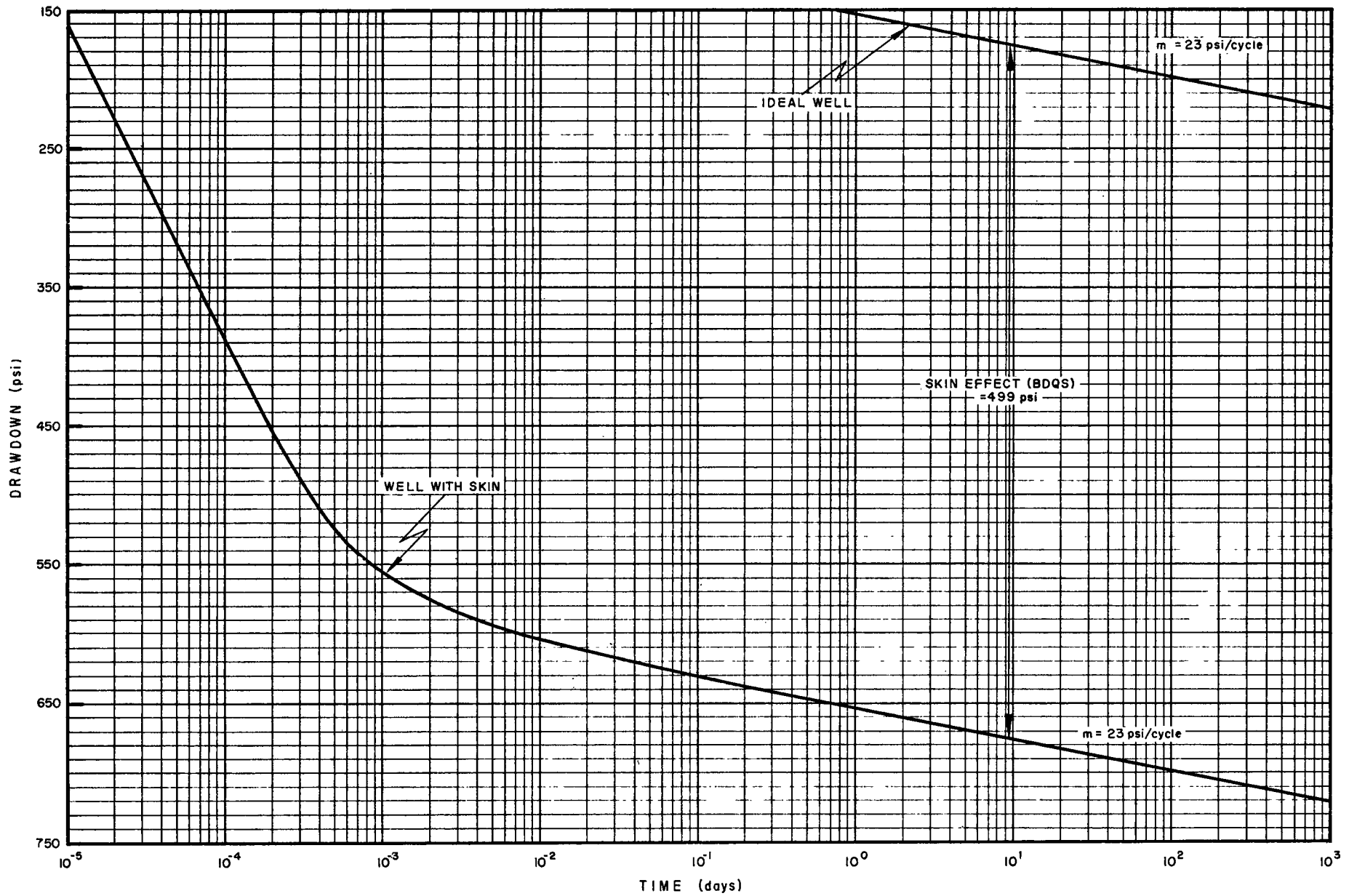


FIGURE 3  
DRAWDOWN FOR A WELL IN AN INFINITE RESERVOIR  
SHOWING THE SKIN EFFECT

## CHAPTER IV

### THE METHOD OF IMAGES AND ITS APPLICATION TO SUBSURFACE FAULT MAPPING

Although the equations presented in Chapter II were developed for flow in an infinite reservoir, they may be used to predict the transient pressure behavior of a well situated near impermeable productive limits such as sealing faults. This is achieved by using the method of images which was first applied to fluid flow problems by Muskat in 1937 (6 : 175).

For example, consider a single ideal producing well, situated between two sealing faults which intersect at  $90^\circ$ , as shown in Figure 4. Distances from the well to the two "no flow boundaries" are  $g_1$  and  $g_2$  feet. The reservoir is infinite in the north-easterly direction.

This configuration may be replaced by an image system of four wells situated in an infinite reservoir, as shown in Figure 5, where each well has been "produced" at the same reservoir flow rate since zero time. The two broken lines represent the original positions of the faults. The faults have been "removed" but the image wells have been placed in such a way that no fluid flow takes place across the original fault positions.

Starting with the producing well, image wells are located by means of successive reflection across alternate faults, as in a mirror. The image system is complete when

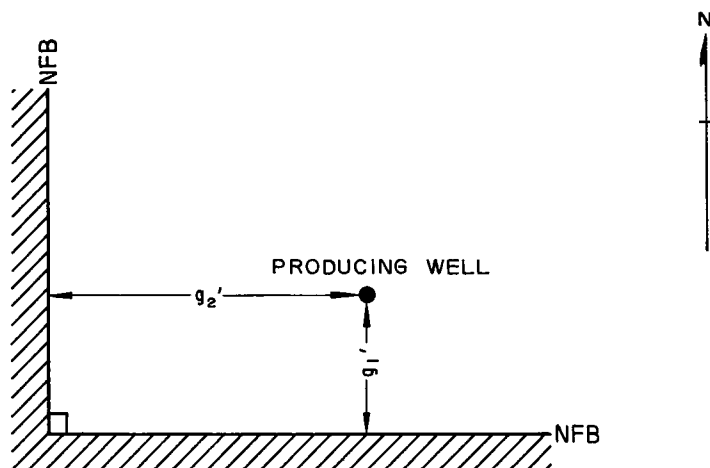


FIGURE 4

WELL SITUATED IN A 90° FAULT BLOCK

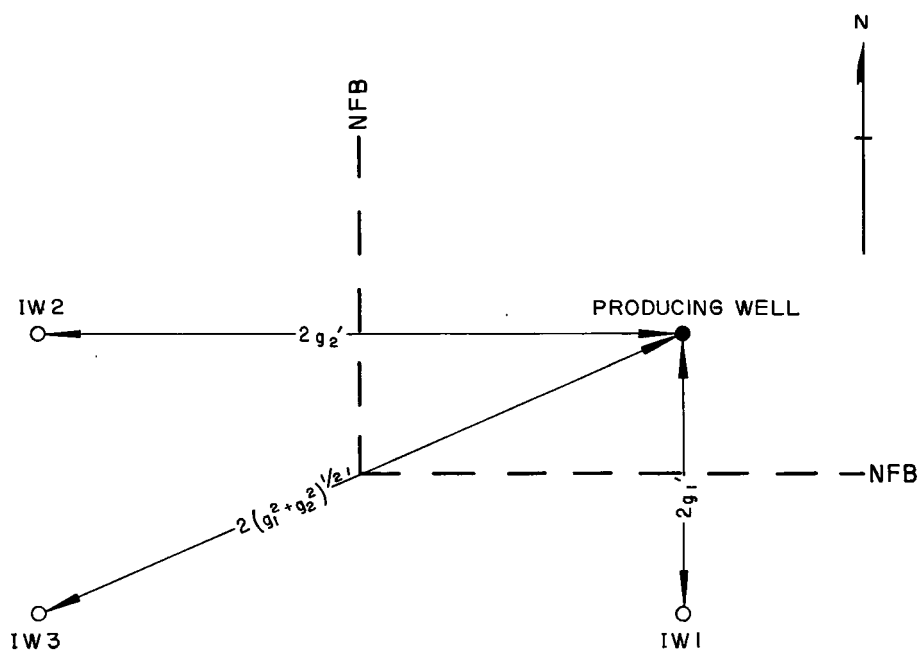


FIGURE 5

IMAGE SYSTEM FOR A 90° FAULT BLOCK

each well has its own two image wells, one for each fault. Finally, image wells are numbered according to their distances from the well in question, beginning with the nearest well.

From equation (II - 4) , and using the method of superposition, the drawdown immediately to the east of any point on the north-south line in Figure 5 , due to the well in question and image well 1, is equal to the drawdown immediately to the west of that same point, due to image wells 2 and 3. There is therefore no drawdown gradient across the line, which is therefore a no flow boundary. The same is true of the east-west line, drawdown to the north, due to the well in question and image well 2 , being equal to drawdown to the south due to image wells 1 and 3.

The two systems shown in Figures 4 and 5 are therefore identical, with respect to drawdown measured in the producing well.

Knowing the distance to each fault, it is possible to calculate the distances between the producing well and image wells. The dimensionless drawdown at any dimensionless time may then be calculated from equation (II - 14) , developed earlier for  $(n+1)$  wells situated in an infinite reservoir. In the case of a  $90^\circ$  fault block :

$$j_{Di_{90^\circ}} = \frac{1}{2} \left[ W\left(\frac{1}{4t_D}\right) + \sum_{y=1}^3 W\left(\frac{r_{Dy}^2}{t_D}\right) \right] \dots\dots\dots (IV - 1)$$

where :

$$r_{D1} = \frac{g_1}{r_w} \dots\dots\dots (IV - 2)$$

$$r_{D2} = \frac{g_2}{r_w} \dots\dots\dots (IV - 3)$$

$$\text{and } r_{D3} = \frac{(g_1^2 + g_2^2)^{\frac{1}{2}}}{r_w} \dots\dots\dots (IV - 4)$$

Conversely, knowing the drawdown, distances to faults may be calculated, and this is the whole basis of subsurface fault mapping using the Reservoir Limit Test.

When the producing well is situated against one of the faults, the effects of image well 1 are felt immediately, and the drawdown, from commencement of production, is twice that due to a well situated in an infinite reservoir. The dimensionless distance to image well 2 is given by equation (IV - 3) above and the dimensionless distance to image well 3 is found by substituting  $g_1 = 0$  into equation (IV - 4).

When the well is situated against both faults, the effects of all image wells are felt from commencement of production, and the drawdown is four times that due to a well situated in an infinite reservoir, i.e. :

$$j_{Di_{90^\circ}}(r_{D1}=r_{D2}=0) = 2W \left( \frac{1}{4t_D} \right) \dots\dots\dots (IV - 5)$$

In general, for a well situated against two faults which intersect at  $\theta^\circ$  :

$$j_{Di_{\theta^\circ}}(r_{D1}=r_{D2}=0) = \frac{b}{2} W \left( \frac{1}{4t_D} \right) \dots\dots\dots (IV - 6)$$

where  $b$  is the total number of wells in the image system, including the well in question.

Image systems may be drawn for other angles of intersection ( $\theta$ ) between two faults, according to the following three rules :

$$(i) \text{ If } \frac{360}{\theta} = 2\ell$$

where  $\ell$  is a positive integer, an image system may be drawn, for any position of the well between the faults.

$$(ii) \text{ If } \frac{360}{\theta} = 2\ell - 1$$

where  $\ell$  is a positive integer, an image system may be drawn, but only when the well lies on the perpendicular bisector of the angle between the faults.

and (iii) When  $\frac{360}{\theta}$  is not an integer, an image system can not be drawn.

In cases (i) and (ii), the number of image wells,  $n$ , is given by :

$$n = \frac{360}{\theta} - 1 \dots\dots\dots (IV - 7)$$

All wells in any system lie on a circle of radius  $R$ , with its center at the intersection of the two faults.

For  $0 < \theta \leq 90^\circ$  :

$$R = \left[ g_1^2 + (g_1 \cot \theta + g_2 \operatorname{cosec} \theta)^2 \right]^{\frac{1}{2}} \dots (IV - 8)$$

or :

$$R = \left[ g_2^2 + (g_2 \cot \theta + g_1 \operatorname{cosec} \theta)^2 \right]^{\frac{1}{2}} \quad \text{.. (IV - 9)}$$

The method of images is used in Chapter V , to investigate the transient pressure behavior of a well situated between two sealing faults. Image systems of the fault blocks considered are shown in Appendix C.



## CHAPTER V

### THE TRANSIENT PRESSURE BEHAVIOR OF A WELL SITUATED BETWEEN TWO SEALING FAULTS

This chapter contains a mathematical analysis of the transient pressure behavior of a well situated near one or two sealing faults. The following cases are considered :

- ( i ) A single linear fault i.e.  $180^\circ$  fault block
- (ii) Two linear faults intersecting at  $120^\circ$ ,  $90^\circ$ ,  $72^\circ$ ,  $60^\circ$ ,  $45^\circ$ ,  $30^\circ$  and  $15^\circ$
- and (iii) Two linear parallel faults.

The  $30^\circ$  fault block is investigated first, followed by other analyses, in order of increasing number of image wells. Since the methods of analysis are similar in each case, detailed workings are omitted for all fault blocks, except the first. Equations pertaining to an ideal well are developed after which the effect of the skin is discussed.

#### I. $30^\circ$ FAULT BLOCK

##### The image system

The image system, consisting of the producing well and eleven image wells, is shown in Appendix C - 7. All wells lie on a circle of radius  $R$  , where  $R$  , from equation (IV - 8) or (IV - 9) , is given by :

$$R = 2 \left( g_1^2 + g_2^2 + \sqrt{3} g_1 g_2 \right)^{\frac{1}{2}} \dots\dots\dots (V - 1)$$

Distances from the producing well to the eleven image wells are calculated as follows :

Let the angle subtended at the center of the circle by the producing well and the first fault be  $\alpha^\circ$ , and the angle subtended by the producing well and the second fault be  $\beta^\circ$ , as shown in Figure 6.

Then :

$$\alpha + \beta = 30^\circ \dots\dots\dots (V - 2)$$

Bearing in mind that image wells are located by reflection across alternate faults, it is easily shown that the angles subtended at the center of the circle by adjacent image wells are as shown in Figure 6.

It is also apparent that :

$$\sin \alpha = \frac{g_1}{R} \dots\dots\dots (V - 3)$$

$$\cos \alpha = \frac{(R^2 - g_1^2)^{\frac{1}{2}}}{R} \dots\dots\dots (V - 4)$$

$$\sin \beta = \frac{g_2}{R} \dots\dots\dots (V - 5)$$

$$\text{and } \cos \beta = \frac{(R^2 - g_2^2)^{\frac{1}{2}}}{R} \dots\dots\dots (V - 6)$$

Now, the length of a chord  $\ell$ , subtending an angle  $\phi$ , at the center of a circle, of radius  $R$ , is given by :

$$\ell = 2R \sin \frac{\phi}{2} \dots\dots\dots (V - 7)$$

Distances between the producing well and image wells are derived from equations (V - 1) to (V - 7).

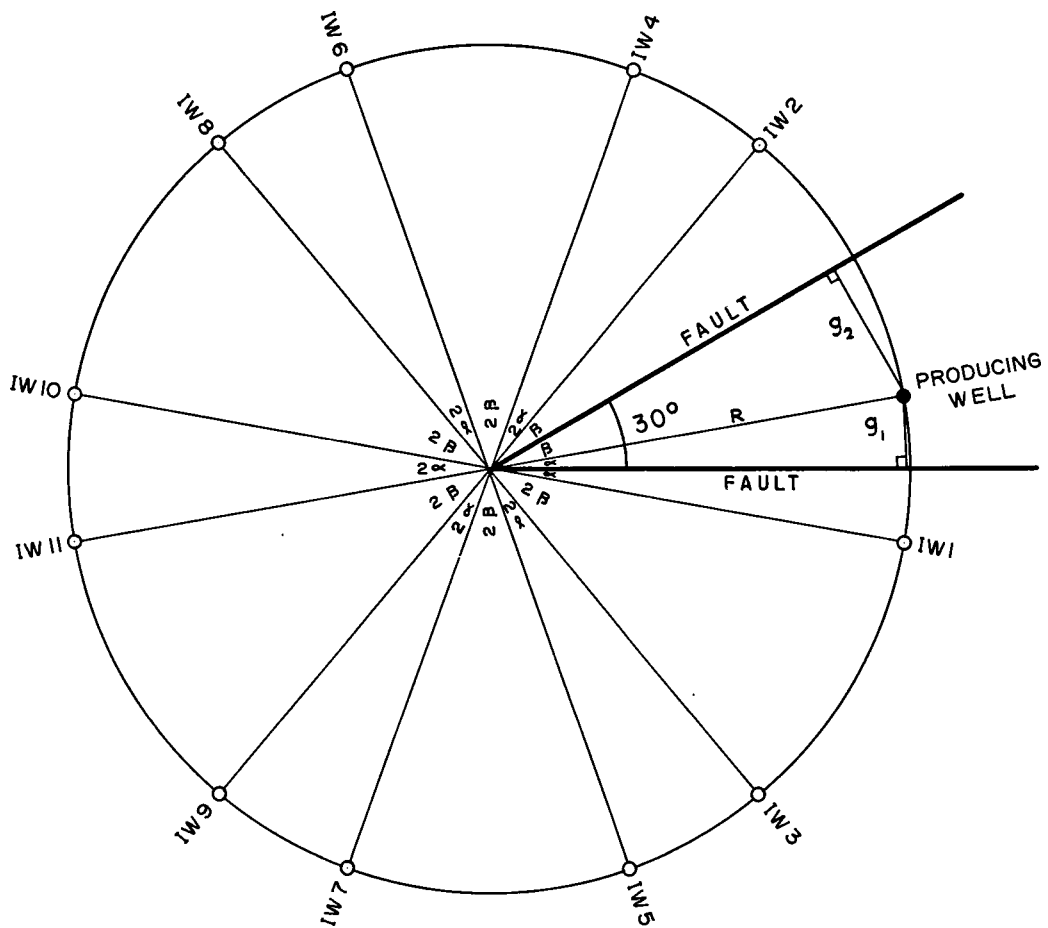


FIGURE 6

IMAGE SYSTEM FOR A 30° FAULT BLOCK

Since image well number 1 is formed by reflection of the producing well in the first fault, the distance to this image well is given by :

$$r_1 = 2g_1 \dots\dots\dots (V - 8)$$

Similarly :

$$r_2 = 2g_2 \dots\dots\dots (V - 9)$$

The angle subtended at the center of the circle by the producing well and image well number 3 (see Figure 6 ) is  $2(\alpha + \beta) = 60^\circ$ . Therefore, from equations (V - 7) , (V - 1) , (V - 8) and (V - 9) :

$$\begin{aligned} r_3 &= 2R \sin \frac{60}{2} \\ &= R \\ &= 2 \left( g_1^2 + g_2^2 + \sqrt{3} g_1 g_2 \right)^{\frac{1}{2}} \\ &= \left( r_1^2 + r_2^2 + 1.732 r_1 r_2 \right)^{\frac{1}{2}} \dots\dots\dots (V - 10) \end{aligned}$$

Similarly :

$$r_4 = \left( r_1^2 + r_2^2 + 1.732 r_1 r_2 \right)^{\frac{1}{2}} \dots\dots\dots (V - 11)$$

The angle subtended at the center of the circle by the producing well and image well number 5 is  $\left[ 2(\alpha + \beta) + 2\alpha \right] = (60 + 2\alpha)$ . Therefore, from equations (V - 7) , (V - 4) , (V - 3) , (V - 1) , (V - 8) and (V - 9) :

$$\begin{aligned} r_5 &= 2R \sin \frac{(60 + 2\alpha)}{2} \\ &= 2R (\sin 30 \cos \alpha + \cos 30 \sin \alpha) \end{aligned}$$

$$\begin{aligned}
&= 2R \left[ \frac{(R^2 - g_1^2)^{\frac{1}{2}}}{2R} + \frac{\sqrt{3} g_1}{2R} \right] \\
&= 2 (\sqrt{3} g_1 + g_2) \\
&= 1.732 r_1 + r_2 \dots\dots\dots (V - 12)
\end{aligned}$$

Similarly, distances to other image wells are as follows :

$$r_6 = r_1 + 1.732 r_2 \dots\dots\dots (V - 13)$$

$$\begin{aligned}
r_7 &= r_8 \\
&= 1.732 (r_1^2 + r_2^2 + 1.732 r_1 r_2)^{\frac{1}{2}} \dots\dots (V - 14)
\end{aligned}$$

$$r_9 = 2 r_1 + 1.732 r_2 \dots\dots\dots (V - 15)$$

$$r_{10} = 1.732 r_1 + 2 r_2 \dots\dots\dots (V - 16)$$

$$\text{and } r_{11} = 2 (r_1^2 + r_2^2 + 1.732 r_1 r_2)^{\frac{1}{2}} \dots\dots (V - 17)$$

Dividing each side of equations (V - 8) to (V - 17) by  $2 r_w$ , and applying equation (II - 12), we obtain :

$$r_{D1} = \frac{g_1}{r_w} \dots\dots\dots (V - 18)$$

$$r_{D2} = \frac{g_2}{r_w} \dots\dots\dots (V - 19)$$

$$\begin{aligned}
r_{D3} &= r_{D4} \\
&= (r_{D1}^2 + r_{D2}^2 + 1.732 r_{D1} r_{D2})^{\frac{1}{2}} \dots\dots\dots (V - 20)
\end{aligned}$$

$$r_{D5} = 1.732 r_{D1} + r_{D2} \dots\dots\dots (V - 21)$$

$$r_{D6} = r_{D1} + 1.732 r_{D2} \dots\dots\dots (V - 22)$$

$$\begin{aligned} r_{D7} &= r_{D8} \\ &= 1.732 \left( r_{D1}^2 + r_{D2}^2 + 1.732 r_{D1} r_{D2} \right)^{\frac{1}{2}} \dots\dots (V - 23) \end{aligned}$$

$$r_{D9} = 2r_{D1} + 1.732r_{D2} \dots\dots\dots (V - 24)$$

$$r_{D10} = 1.732r_{D1} + 2r_{D2} \dots\dots\dots (V - 25)$$

$$\text{and } r_{D11} = 2 \left( r_{D1}^2 + r_{D2}^2 + 1.732 r_{D1} r_{D2} \right)^{\frac{1}{2}} \dots\dots\dots (V - 26)$$

### Dimensionless drawdown equations

From equation (II - 14) , the ideal dimensionless drawdown in the producing well is given by :

$$j_{Di_{30^\circ}} = \frac{1}{2} \left[ W \left( \frac{1}{4t_D} \right) + \sum_{y=1}^{11} W \left( \frac{r_{Dy}^2}{t_D} \right) \right] \dots\dots\dots (V - 27)$$

Therefore, from equations (V - 18) to (V - 26) :

$$\begin{aligned} j_{Di_{30^\circ}} &= \frac{1}{2} \left\{ W \left[ \frac{1}{4t_D} \right] + W \left[ \frac{r_{D1}^2}{t_D} \right] + W \left[ \frac{r_{D2}^2}{t_D} \right] \right. \\ &+ 2W \left[ \frac{r_{D1}^2 + r_{D2}^2 + 1.732 r_{D1} r_{D2}}{t_D} \right] + W \left[ \frac{(1.732 r_{D1} + r_{D2})^2}{t_D} \right] \\ &+ W \left[ \frac{(r_{D1} + 1.732 r_{D2})^2}{t_D} \right] + 2W \left[ \frac{3(r_{D1}^2 + r_{D2}^2 + 1.732 r_{D1} r_{D2})}{t_D} \right] \\ &+ W \left[ \frac{(2r_{D1} + 1.732 r_{D2})^2}{t_D} \right] + W \left[ \frac{(1.732 r_{D1} + 2r_{D2})^2}{t_D} \right] \\ &\left. + W \left[ \frac{4(r_{D1}^2 + r_{D2}^2 + 1.732 r_{D1} r_{D2})}{t_D} \right] \right\} \dots\dots\dots (V - 28) \end{aligned}$$

When the well is situated against one of the faults :

$$j_{Di_{30}^0}(r_{D1}=0) = W\left(\frac{1}{4t_D}\right) + 2W\left(\frac{r_{D2}^2}{t_D}\right) \\ + 2W\left(\frac{3r_{D2}^2}{t_D}\right) + W\left(\frac{4r_{D2}^2}{t_D}\right) \dots\dots\dots (V - 29)$$

From equation (IV - 6) , when the well is situated against both faults :

$$j_{Di_{30}^0}(r_{D1}=r_{D2}=0) = 6W\left(\frac{1}{4t_D}\right) \dots\dots\dots (V - 30)$$

Equations (V - 28) and (V - 29) were programmed in the MAD language, for use on an IBM 709 digital computer, as shown in Appendix D - 7. The Well Function was programmed as an external function, as shown in Appendix B.

Using these programs, dimensionless drawdown curves were constructed for values of  $r_{D2}$  ranging from 100 to 8000 and  $r_{D2}/r_{D1}$  ranging from 1 to  $\infty$  (i.e.  $r_{D1} = 0$ ). Type curves are shown in Appendix E - 7, and discussed below and in Chapter VI. Typical computer output is illustrated in Figure 7.

#### Characteristics of dimensionless drawdown curves

Before interference from any of the image wells is felt, the producing well behaves as though it were situated in an infinite reservoir. Therefore, from equation (II - 13) :

$$j_{Di_1} = 1.15 \log \frac{t_D}{0.445} \dots\dots\dots (V - 31)$$

## THIRTY DEGREE FAULT BLOCK

RD2 = 500.00

RD1 = 250.00

TD	JD
.1E 02	1.57
.2E 02	1.91
.5E 02	2.36
.1E 03	2.71
.2E 03	3.05
.5E 03	3.51
.1E 04	3.86
.2E 04	4.20
.5E 04	4.66
.1E 05	5.01
.2E 05	5.36
.5E 05	5.89
.1E 06	6.39
.2E 06	7.04
.5E 06	8.32
.1E 07	9.86
.2E 07	12.11
.5E 07	16.14
.1E 08	19.73
.2E 08	23.59
.5E 08	28.90
.1E 09	32.99
.2E 09	37.11
.5E 09	42.59
.1E 10	46.75
.2E 10	50.91
.5E 10	56.41
.1E 11	60.57
.2E 11	64.73
.5E 11	70.22
.1E 12	74.38
.2E 12	78.54
.5E 12	84.04
.1E 13	88.20

FIGURE 7

30° FAULT BLOCK

TYPICAL COMPUTER OUTPUT FOR  
IDEAL DIMENSIONLESS DRAWDOWN CURVE



The plot of  $j_{Di_1}$  versus  $\log t_D$  is a straight line with slope equal to 1.15 units per log cycle, denoted by  $m_D$  in Figure 8. This applies to any fault block, provided no interference from image wells has been felt.

After interference from the first image well is felt, the dimensionless drawdown is given by :

$$j_{Di_2} = 1.15 \log \frac{t_D}{0.445} + \frac{1}{2}W\left(\frac{r_{D1}^2}{t_D}\right) \dots\dots\dots (V - 32)$$

For sufficiently large values of  $t_D$ , the Well Function may be replaced by its logarithmic approximation, and equation (V - 32) becomes :

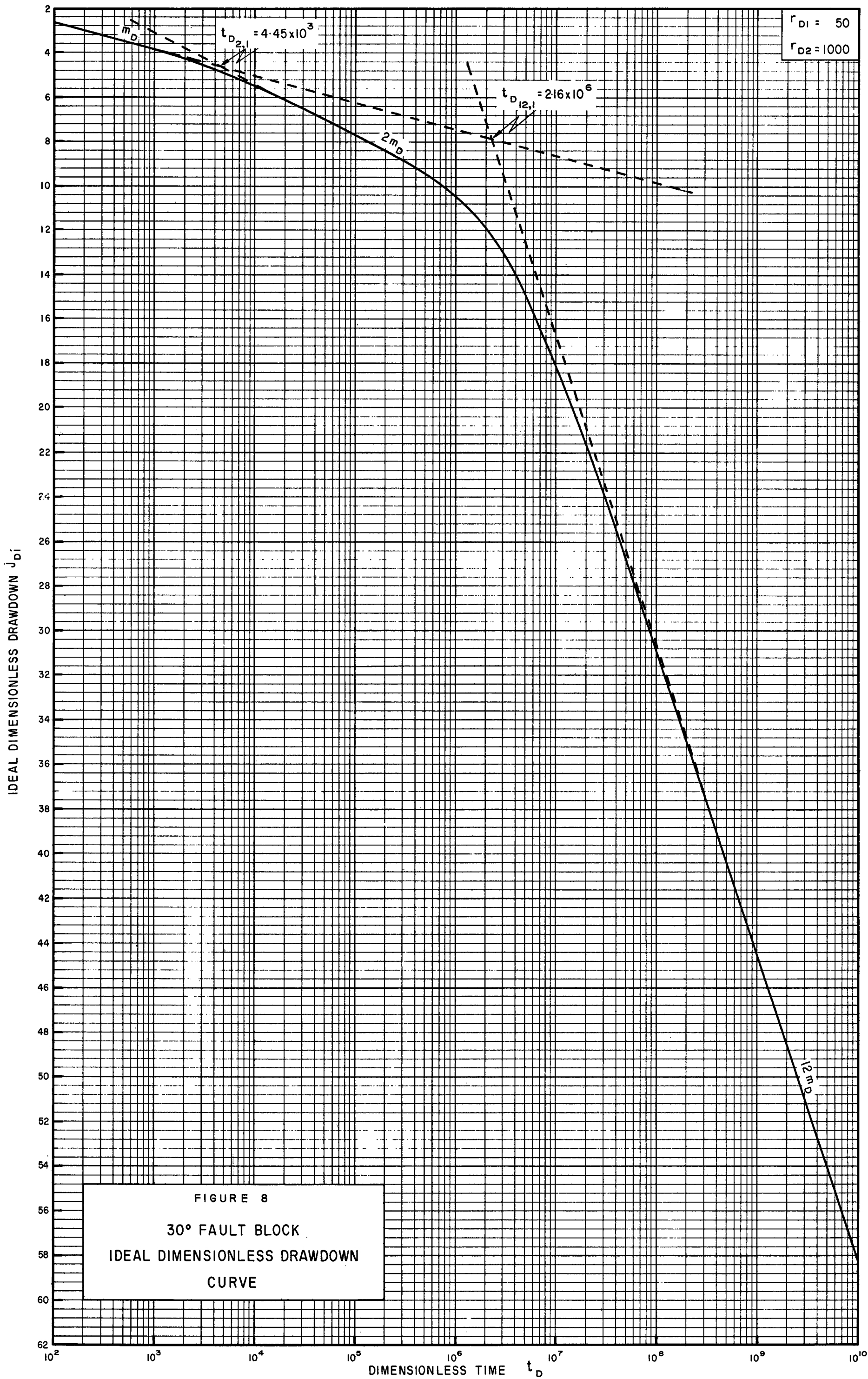
$$j_{Di_2} = 1.15 \log \frac{t_D}{0.445} + 1.15 \log \frac{t_D}{1.78r_{D1}^2} \dots\dots\dots (V - 33)$$

which simplifies to :

$$j_{Di_2} = 2.3 \log \frac{t_D}{0.89r_{D1}^2} \dots\dots\dots (V - 34)$$

Therefore, for sufficiently large values of  $t_D$ , the plot of  $j_{Di_2}$  versus  $\log t_D$  is a straight line with slope equal to 2.3 units per log cycle, i.e.  $2m_D$ , provided no interference from image wells 3 to 11 has reached the producing well. The change in slope from  $m_D$  to  $2m_D$  occurs gradually, resulting in a smooth curve, as shown in Figure 8.

After interference from all image wells has reached the producing well, the dimensionless drawdown is given by equation (V - 28). Replacing the Well Functions by their logarithmic



approximations, and simplifying, equation (V - 28) becomes :

$$j_{Di_{12}} = 13.8 \log \frac{t_D}{2.138 \left\{ (r_{D1}^2 + r_{D2}^2 + 1.732 r_{D1} r_{D2})^{5/12} \left[ r_{D1} r_{D2} (1.732 r_{D1} + r_{D2}) (r_{D1} + 1.732 r_{D2}) \right. \right.} \quad (V - 35)$$

$$\left. \left. (2 r_{D1} + 1.732 r_{D2}) (1.732 r_{D1} + 2 r_{D2}) \right]^{1/6} \right\}}$$

Therefore, for sufficiently large values of  $t_D$ , the plot of  $j_{Di_{12}}$  versus  $\log t_D$  is a straight line with slope equal to 13.8 units per log cycle, i.e.  $12m_D$ . Once again, the change in slope from  $2m_D$  to  $12m_D$  occurs gradually, as shown in Figure 8.

When the producing well is situated against one of the faults, the effects of image well 1 are felt from commencement of production, and the drawdown is twice that due to a well situated in an infinite reservoir. Therefore, from equation (V - 31), the straight line of slope  $2m_D$  is defined by :

$$j_{Di_2}(r_{D1}=0) = 2.3 \log \frac{t_D}{0.445} \dots\dots\dots (V - 36)$$

From equation (V - 29), the straight line of slope  $12m_D$ , due to all wells in the image system, is given by :

$$j_{Di_{12}}(r_{D1}=0) = 13.8 \log \frac{t_D}{2.567 r_{D2}^{5/3}} \dots\dots\dots (V - 37)$$

When the well is situated against both faults, the effects of all image wells are felt from commencement of production, and the straight line of slope  $12m_D$  is defined

by :

$$j_{D1} j_{D2} (r_{D1}=r_{D2}=0) = 13.8 \log \frac{t_D}{0.445} \dots\dots\dots (V - 38)$$

It is apparent that all three straight lines will not always be present on the dimensionless drawdown curve. If the well is situated against one of the faults, the curve will begin with a slope of  $2m_D$ , and the  $m_D$  line will be absent. If the well is situated against both faults, the  $m_D$  and  $2m_D$  lines will be absent, and the curve will possess a slope of  $12m_D$  units per log cycle throughout. Furthermore, examination of the type curves (Appendix E - 7) indicates that for  $r_{D1} > 0$ , the line of slope  $2m_D$  will only be seen when  $r_{D2}/r_{D1} \geq 20$ . For smaller values of  $r_{D2}/r_{D1}$ , the  $2m_D$  line has insufficient time to develop, because interference from image wells 3 to 11 is felt too soon after interference from image well 2. Lastly, the final slope of  $12m_D$  will only be present if the duration of the test is sufficiently long.

The slope of any straight-line portion of the curve depends only on the number of wells contributing to the drawdown along that line i.e. a straight line of slope  $nm_D$  is caused by  $n$  wells, namely the producing well and  $(n-1)$  image wells. But, from equation (IV - 7), the number of image wells is given by :

$$n-1 = \frac{360}{\theta} - 1$$

from which :

$$n = \frac{360}{\theta}$$

Therefore, the final slope on the dimensionless draw-down curve is given by :

$$\text{Final slope} = \frac{360}{\theta} \cdot m_D \dots\dots\dots (V - 39)$$

where  $\theta$  is the angle of intersection between the two faults.

From an examination of the dimensionless drawdown curves, which were all drawn on the same scale, it was found that identical shapes were obtained for constant values of  $r_{D2}/r_{D1}$ , irrespective of the values of  $r_{D1}$  and  $r_{D2}$ . This is of fundamental importance and facilitates rapid calculation of the distances between the producing well and the two faults, as will be shown in Chapter VI.

#### Intersection-time equations

The two straight lines, of slope  $m_D$  and  $2m_D$ , intersect at a dimensionless time  $t_{D2,1}$ , at which  $j_{Di_1} = j_{Di_2}$ , as shown in Figure 8. Therefore, from equations (V - 31) and (V - 34) :

$$t_{D2,1} = 1.78 r_{D1}^2 \dots\dots\dots (V - 40)$$

Similarly, from equations (V - 31) and (V - 35), the two lines, of slope  $m_D$  and  $12m_D$ , intersect at a dimensionless time  $t_{D12,1}$ , given by :

$$t_{D12,1} = 2.465 \left\{ (r_{D1}^2 + r_{D2}^2 + 1.732 r_{D1} r_{D2})^{5/11} \right. \\ \left. \left[ r_{D1} r_{D2} (1.732 r_{D1} + r_{D2}) (r_{D1} + 1.732 r_{D2}) \right. \right. \\ \left. \left. (2 r_{D1} + 1.732 r_{D2}) (1.732 r_{D1} + 2 r_{D2}) \right]^{2/11} \right\} \dots \quad (V - 41)$$

From equations (V - 36) and (V - 37), when the well is situated against one of the faults :

$$t_{D12,2}(r_{D1}=0) = 3.645 r_{D2}^2 \dots \dots \dots (V - 42)$$

Dividing equation (V - 41) by equation (V - 40), and putting  $r_{D2}/r_{D1} = x$ , we obtain :

$$\frac{t_{D12,1}}{t_{D2,1}} = 1.385 \left\{ (1 + x^2 + 1.732x)^{5/11} \right. \\ \left. [x(1.732 + x)(1 + 1.732x)(2 + 1.732x)(1.732 + 2x)]^{2/11} \right\} \\ \dots \dots \dots (V - 43)$$

Equations (V - 40), (V - 42) and (V - 43) are incorporated in Appendices F - 1 and F - 2, the use of which is described in Chapter VI.

## II. 180° FAULT BLOCK

The image system, consisting of the producing well and one image well, is shown in Appendix C - 1, where  $g$  is the distance between the producing well and the fault.

From equation (II - 14), the dimensionless drawdown in the producing well is given by :

$$j_{Di180^\circ} = \frac{1}{2} \left[ W\left(\frac{1}{4t_D}\right) + W\left(\frac{r_D^2}{t_D}\right) \right] \dots \dots \dots (V - 44)$$

where :

$$r_D = \frac{g}{r_w} \dots\dots\dots (V - 45)$$

When the well is situated against the fault :

$$j_{Di180^\circ}(r_D=0) = W\left(\frac{1}{4t_D}\right) \dots\dots\dots (V - 46)$$

Equation (V - 44) was programmed for use on an IBM 709 digital computer, as shown in Appendix D - 1, and dimensionless drawdown curves were constructed for  $r_D$  varying between 100 and 8000. The type curve is shown in Appendix E - 1.

After interference from the fault has been felt, the slope of the curve changes gradually from  $m_D$  to  $2m_D$ , and remains constant thereafter.

The two straight lines intersect at a dimensionless time,  $t_{D2,1}$ , which is a function of  $r_D$ , as derived above (equation (V - 40)).

### III. $120^\circ$ FAULT BLOCK

The image system, consisting of the producing well and two image wells, can only be drawn when the distances to the two faults are equal, i.e.  $g_1 = g_2 = g$ , as shown in Appendix C - 2.

From equation (II - 14), the dimensionless drawdown is given by :

$$j_{Di_{120^\circ}} = \frac{1}{2} W\left(\frac{1}{4t_D}\right) + W\left(\frac{r_D^2}{t_D}\right) \dots\dots\dots (V - 47)$$

where  $r_D$  is defined by equation (V - 45).

When the well is situated at the intersection of the faults :

$$j_{Di_{120^\circ}}(r_D=0) = \frac{3}{2} W\left(\frac{1}{4t_D}\right) \dots\dots\dots (V - 48)$$

The computer program and type curve, pertaining to equation (V - 47) , are shown in Appendices D - 2 and E - 2 respectively.

From equation (V - 47) , the straight-line portion of the curve, due to all three wells in the system, is given by :

$$j_{Di_3} = 3.45 \log \frac{t_D}{1.121r_D^{4/3}} \dots\dots\dots (V - 49)$$

Solving for  $t_{D3,1}$  from equations (V - 31) and (V - 49) , and dividing by equation (V - 40) , we obtain :

$$\frac{t_{D3,1}}{t_{D2,1}} = 1 \dots\dots\dots (V - 50)$$

Equation (V - 50) is incorporated in Appendix F - 1, but it is emphasized that this is only valid when the distances to the two faults are equal.

#### IV. $90^\circ$ FAULT BLOCK

The image system, consisting of the producing well and three image wells, is shown in Appendix C - 3. All wells lie



on a circle of radius  $R$  , where :

$$R = (g_1^2 + g_2^2)^{\frac{1}{2}} \dots\dots\dots (V - 51)$$

From equation (II - 14) , the dimensionless drawdown is given by :

$$j_{Di90^\circ} = \frac{1}{2} \left[ W\left(\frac{1}{4t_D}\right) + W\left(\frac{r_{D1}^2}{t_D}\right) + W\left(\frac{r_{D2}^2}{t_D}\right) + W\left(\frac{r_{D1}^2 + r_{D2}^2}{t_D}\right) \right] \dots\dots\dots (V - 52)$$

where  $r_{D1}$  and  $r_{D2}$  are defined by equations (V - 18) and (V - 19) respectively.

When the well is situated against one of the faults :

$$j_{Di90^\circ}(r_{D1}=0) = W\left(\frac{1}{4t_D}\right) + W\left(\frac{r_{D2}^2}{t_D}\right) \dots\dots\dots (V - 53)$$

When the well is situated against both faults :

$$j_{Di90^\circ}(r_{D1}=r_{D2}=0) = 2W\left(\frac{1}{4t_D}\right) \dots\dots\dots (V - 54)$$

The computer program and type curves, pertaining to equations (V - 52) and (V - 53) , are shown in Appendices D - 3 and E - 3 respectively.

From equation (V - 52) , for  $r_{D1} > 0$  , the straight-line portion of the curve, due to all four wells in the system, is given by :

$$j_{Di4} = 4.6 \log \frac{t_D}{1.259(r_{D1}r_{D2})^{\frac{1}{2}} (r_{D1}^2 + r_{D2}^2)^{\frac{1}{4}}} \dots\dots (V - 55)$$

Solving for  $t_{D4,1}$  from equations (V - 31) and (V - 55) , dividing by equation (V - 40) , and putting  $r_{D2}/r_{D1} = \alpha$  , we obtain :

$$\frac{t_{D4,1}}{t_{D2,1}} = \left[ \alpha^2 (1 + \alpha^2) \right]^{1/3} \dots\dots\dots (V - 56)$$

From equation (V - 53) , when the well is situated against one of the faults, the straight-line portion of the curve, due to all wells in the system, is given by :

$$j_{Di4}(r_{D1}=0) = 4.6 \log \frac{t_D}{0.89r_{D2}} \dots\dots\dots (V - 57)$$

Therefore, from equations (V - 36) and (V - 57) :

$$t_{D4,2}(r_{D1}=0) = 1.78 r_{D2}^2 \dots\dots\dots (V - 58)$$

Equations (V - 56) and (V - 58) are incorporated in Appendices F - 1 and F - 2 respectively.

## V. 72° FAULT BLOCK

The image system, consisting of the producing well and four image wells, can only be drawn when the distances to the two faults are equal, i.e.  $g_1 = g_2 = g$  , as shown in Appendix C - 4.

All wells lie on a circle of radius  $R$  , where :

$$R = 1.701 g \dots\dots\dots (V - 59)$$

From equation (II - 14) , the dimensionless drawdown is given by :

$$j_{Di72^{\circ}} = \frac{1}{2} W\left(\frac{1}{4t_D}\right) + W\left(\frac{r_D^2}{t_D}\right) + W\left(\frac{2.616r_D^2}{t_D}\right) \dots (V - 60)$$

where  $r_D$  is defined by equation (V - 45).

When the well is situated at the intersection of the faults :

$$j_{Di72^{\circ}}(r_D=0) = \frac{5}{2} W\left(\frac{1}{4t_D}\right) \dots (V - 61)$$

The computer program and type curve, pertaining to equation (V - 60) , are shown in Appendices D - 4 and E - 4 respectively.

From equation (V - 60) , the straight-line portion of the curve, due to all five wells in the system, is given by :

$$j_{Di5} = 5.75 \log \frac{t_D}{1.982r_D^{8/5}} \dots (V - 62)$$

Solving for  $t_{D5,1}$  from equations (V - 31) and (V - 62) , and dividing by equation (V - 40) , we obtain :

$$\frac{t_{D5,1}}{t_{D2,1}} = 1.617 \dots (V - 63)$$

Equation (V - 63) is incorporated in Appendix F - 1 , but it is emphasized that this is only valid when the distances to the two faults are equal.

## VI. 60° FAULT BLOCK

The image system, consisting of the producing well and

five image wells, is shown in Appendix C - 5. All wells lie on a circle of radius  $R$ , where :

$$R = \frac{2}{\sqrt{3}} \left( g_1^2 + g_1 g_2 + g_2^2 \right)^{\frac{1}{2}} \dots\dots\dots (V - 64)$$

From equation (II - 14), the dimensionless drawdown is given by :

$$\begin{aligned} j_{Di60^\circ} = \frac{1}{2} \left\{ W \left[ \frac{1}{4t_D} \right] + W \left[ \frac{r_{D1}^2}{t_D} \right] + W \left[ \frac{r_{D2}^2}{t_D} \right] \right. \\ \left. + 2W \left[ \frac{r_{D1}^2 + r_{D1} r_{D2} + r_{D2}^2}{t_D} \right] + W \left[ \frac{(r_{D1} + r_{D2})^2}{t_D} \right] \right\} \dots (V - 65) \end{aligned}$$

where  $r_{D1}$  and  $r_{D2}$  are defined by equations (V - 18) and (V - 19) respectively.

When the well is situated against one of the faults :

$$j_{Di60^\circ}(r_{D1}=0) = W \left( \frac{1}{4t_D} \right) + 2W \left( \frac{r_{D2}^2}{t_D} \right) \dots\dots\dots (V - 66)$$

When the well is situated against both faults :

$$j_{Di60^\circ}(r_{D1}=r_{D2}=0) = 3W \left( \frac{1}{4t_D} \right) \dots\dots\dots (V - 67)$$

The computer program and type curves, pertaining to equations (V - 65) and (V - 66), are shown in Appendices D - 5 and E - 5 respectively.

From equation (V - 65), for  $r_{D1} > 0$ , the straight-line portion of the curve, due to all six wells in the system, is given by :

$$j_{Di6} = 6.9 \log \frac{t_D}{1.413 \left[ r_{D1} r_{D2} (r_{D1} + r_{D2}) (r_{D1}^2 + r_{D1} r_{D2} + r_{D2}^2) \right]^{1/3}} \dots\dots\dots (V - 68)$$

Solving for  $t_{D6,1}$  from equations (V - 31) and (V - 68), dividing by equation (V - 40), and putting  $r_{D2}/r_{D1} = x$ , we obtain :

$$\frac{t_{D6,1}}{t_{D2,1}} = \left[ x(1+x)(1+x+x^2) \right]^{2/5} \dots\dots\dots (V - 69)$$

From equation (V - 66), when the well is situated against one of the faults, the straight-line portion of the curve, due to all wells in the system, is given by :

$$j_{Di6}(r_{D1}=0) = 6.9 \log \frac{t_D}{1.121 r_{D2}^{4/3}} \dots\dots\dots (V - 70)$$

Therefore, from equations (V - 36) and (V - 70) :

$$t_{D6,2}(r_{D1}=0) = 1.78 r_{D2}^2 \dots\dots\dots (V - 71)$$

Equations (V - 69) and (V - 71) are incorporated in Appendices F - 1 and F - 2 respectively.

## VII. 45° FAULT BLOCK

The image system, consisting of the producing well and seven image wells, is shown in Appendix C - 6. All wells lie on a circle of radius  $R$ , where :

$$R = \left[ 2 \left( g_1^2 + g_2^2 + \sqrt{2} g_1 g_2 \right) \right]^{\frac{1}{2}} \dots\dots\dots (V - 72)$$

From equation (II - 14) , the dimensionless drawdown is given by :

$$\begin{aligned} j_{Di_{45^\circ}} = & \frac{1}{2} \left\{ W \left[ \frac{1}{4t_D} \right] + W \left[ \frac{r_{D1}^2}{t_D} \right] + W \left[ \frac{r_{D2}^2}{t_D} \right] \right. \\ & + 2W \left[ \frac{r_{D1}^2 + r_{D2}^2 + 1.414 r_{D1} r_{D2}}{t_D} \right] + W \left[ \frac{(1.414 r_{D1} + r_{D2})^2}{t_D} \right] \\ & \left. + W \left[ \frac{(r_{D1} + 1.414 r_{D2})^2}{t_D} \right] + W \left[ \frac{2(r_{D1}^2 + r_{D2}^2 + 1.414 r_{D1} r_{D2})}{t_D} \right] \right\} \\ & \dots (V - 73) \end{aligned}$$

where  $r_{D1}$  and  $r_{D2}$  are defined by equations (V - 18) and (V - 19) respectively.

When the well is situated against one of the faults :

$$j_{Di_{45^\circ}}(r_{D1}=0) = W \left( \frac{1}{4t_D} \right) + 2W \left( \frac{r_{D2}^2}{t_D} \right) + W \left( \frac{2r_{D2}^2}{t_D} \right) \dots\dots (V - 74)$$

When the well is situated against both faults :

$$j_{Di_{45^\circ}}(r_{D1}=r_{D2}=0) = 4W \left( \frac{1}{4t_D} \right) \dots\dots\dots (V - 75)$$

The computer program and type curves, pertaining to equations (V - 73) and (V - 74) , are shown in Appendices D - 6 and E - 6 respectively.

From equation (V - 73) , for  $r_{D1} > 0$  , the straight-line portion of the curve, due to all eight wells in the system, is given by :

$$j_{Di8} = 9.2 \log \frac{t_D}{1.631 \left\{ \left[ r_{D1} r_{D2} (1.414 r_{D1} + r_{D2}) (r_{D1} + 1.414 r_{D2}) \right]^{\frac{1}{4}} \right.} \\ \left. (r_{D1}^2 + r_{D2}^2 + 1.414 r_{D1} r_{D2})^{\frac{3}{8}} \right\}} \dots\dots\dots (V - 76)$$

Solving for  $t_{D8,1}$  from equations (V - 31) and (V - 76), dividing by equation (V - 40), and putting  $r_{D2}/r_{D1} = \alpha$ , we obtain :

$$\frac{t_{D8,1}}{t_{D2,1}} = 1.104 \left\{ \left[ \alpha (1.414 + \alpha) (1 + 1.414 \alpha) \right]^{2/7} (1 + \alpha^2 + 1.414 \alpha)^{3/7} \right\} \dots\dots\dots (V - 77)$$

From equation (V - 74), when the well is situated against one of the faults, the straight-line portion of the curve, due to all wells in the system, is given by :

$$j_{Di8}(r_{D1}=0) = 9.2 \log \frac{t_D}{1.497 r_{D2}^{3/2}} \dots\dots\dots (V - 78)$$

Therefore, from equations (V - 36) and (V - 78) :

$$t_{D8,2}(r_{D1}=0) = 2.243 r_{D2}^2 \dots\dots\dots (V - 79)$$

Equations (V - 77) and (V - 79) are incorporated in Appendices F - 1 and F - 2 respectively.

## VIII. 15° FAULT BLOCK

The image system, consisting of the producing well and twenty three image wells, is shown in Appendix C - 8. All

wells lie on a circle of radius  $R$  , where :

$$R = \left( 14.928g_1^2 + 14.928g_2^2 + 28.839g_1g_2 \right)^{\frac{1}{2}} \dots\dots (V - 80)$$

From equation (II - 14) , the dimensionless drawdown is given by :

$$\begin{aligned} j_{Di_{15}^o} = & \frac{1}{2} \left\{ W \left[ \frac{1}{4t_D} \right] + W \left[ \frac{r_{D1}^2}{t_D} \right] + W \left[ \frac{r_{D2}^2}{t_D} \right] \right. \\ & + 2 W \left[ \frac{0.067X}{t_D} \right] + W \left[ \frac{(1.932r_{D1} + r_{D2})^2}{t_D} \right] + W \left[ \frac{(r_{D1} + 1.932r_{D2})^2}{t_D} \right] \\ & + 2 W \left[ \frac{0.25X}{t_D} \right] + W \left[ \frac{(2.732r_{D1} + 1.932r_{D2})^2}{t_D} \right] \\ & + W \left[ \frac{(1.932r_{D1} + 2.732r_{D2})^2}{t_D} \right] + 2 W \left[ \frac{0.5X}{t_D} \right] \\ & + W \left[ \frac{(3.346r_{D1} + 2.732r_{D2})^2}{t_D} \right] + W \left[ \frac{(2.732r_{D1} + 3.346r_{D2})^2}{t_D} \right] \\ & + 2 W \left[ \frac{0.75X}{t_D} \right] + W \left[ \frac{(3.732r_{D1} + 3.346r_{D2})^2}{t_D} \right] \\ & + W \left[ \frac{(3.346r_{D1} + 3.732r_{D2})^2}{t_D} \right] + 2 W \left[ \frac{0.933X}{t_D} \right] \\ & + W \left[ \frac{(3.864r_{D1} + 3.732r_{D2})^2}{t_D} \right] + W \left[ \frac{(3.732r_{D1} + 3.864r_{D2})^2}{t_D} \right] \\ & \left. + W \left[ \frac{X}{t_D} \right] \right\} \dots\dots\dots (V - 81) \end{aligned}$$

where  $r_{D1}$  and  $r_{D2}$  are defined by equations (V - 18) and (V - 19) respectively, and  $X$  is given by :



$$X = 14.928r_{D1}^2 + 14.928r_{D2}^2 + 28.839r_{D1}r_{D2} \quad \dots \quad (V - 82)$$

When the well is situated against one of the faults :

$$\begin{aligned} j_{Di15^0}(r_{D1}=0) = & W\left(\frac{1}{4t_D}\right) + 2 W\left(\frac{r_{D2}^2}{t_D}\right) \\ & + 2 W\left(\frac{3.732r_{D2}^2}{t_D}\right) + 2 W\left(\frac{7.464r_{D2}^2}{t_D}\right) \\ & + 2 W\left(\frac{11.196r_{D2}^2}{t_D}\right) + 2 W\left(\frac{13.928r_{D2}^2}{t_D}\right) \\ & + W\left(\frac{14.928r_{D2}^2}{t_D}\right) \dots\dots\dots (V - 83) \end{aligned}$$

When the well is situated against both faults :

$$j_{Di15^0}(r_{D1}=r_{D2}=0) = 12 W\left(\frac{1}{4t_D}\right) \dots\dots\dots (V - 84)$$

The computer program and type curves, pertaining to equations (V - 81) and (V - 83), are shown in Appendices D - 8 and E - 8 respectively.

From equation (V - 81), for  $r_{D1} > 0$ , the straight-line portion of the curve, due to all twenty four wells in the system, is given by :

$$\begin{aligned} j_{Di24} = 27.6 \log & \frac{t_D}{1.095 \left\{ [r_{D1}r_{D2}(1.932r_{D1}+r_{D2})(r_{D1}+1.932r_{D2}) \right.} \\ & (2.732r_{D1}+1.932r_{D2})(1.932r_{D1}+2.732r_{D2}) \\ & (3.346r_{D1}+2.732r_{D2})(2.732r_{D1}+3.346r_{D2}) \\ & (3.732r_{D1}+3.346r_{D2})(3.346r_{D1}+3.732r_{D2}) \\ & (3.864r_{D1}+3.732r_{D2})(3.732r_{D1}+3.864r_{D2})]^{1/12} \\ & \left. (14.928r_{D1}^2+14.928r_{D2}^2+28.839r_{D1}r_{D2})^{11/24} \right\}} \\ & \dots\dots\dots (V - 85) \end{aligned}$$

Solving for  $t_{D24,1}$  from equations (V - 31) and (V - 85) , dividing by equation (V - 40) , and putting  $r_{D2}/r_{D1} = x$  , we obtain :

$$\frac{t_{D24,1}}{t_{D2,1}} = 0.64 \left\{ \frac{[x(1.932+x)(1+1.932x)(2.732+1.932x)(1.932+2.732x)(3.346+2.732x)(2.732+3.346x)(3.732+3.346x)(3.346+3.732x)(3.864+3.732x)(3.732+3.864x)]^{2/23}}{(14.928+14.928x^2+28.839x)^{11/23}} \right\} \dots\dots\dots (V - 86)$$

From equation (V - 83) , when the well is situated against one of the faults, the straight-line portion of the curve, due to all wells in the system, is given by :

$$j_{Di24}(r_{D1}=0) = 27.6 \log \frac{t_D}{8.024 r_{D2}^{11/6}} \dots\dots\dots (V - 87)$$

Therefore, from equations (V - 36) and (V - 87) :

$$t_{D24,2}(r_{D1}=0) = 10.44 r_{D2}^2 \dots\dots\dots (V - 88)$$

Equations (V - 86) and (V - 88) are incorporated in Appendices F - 1 and F - 2 respectively.

## IX. PARALLEL FAULTS

The image system, part of which is shown in Appendix C - 9 , consists of the producing well and an infinite number of image wells, all of which lie on a straight line at right angles to the two faults.

The dimensionless drawdown is given by :

$$j_{Di_{Parallel}} = \frac{1}{2} \left[ W\left(\frac{1}{4t_D}\right) + \sum_{y=1}^{\infty} W\left(\frac{r_{Dy}^2}{t_D}\right) \right] \dots\dots\dots (V - 89)$$

where :

$$r_{D1} = \frac{g_1}{r_w} \dots\dots\dots (V - 90)$$

$$r_{D2} = \frac{g_2}{r_w} \dots\dots\dots (V - 91)$$

$$\begin{aligned} r_{D3} &= r_{D4} \\ &= r_{D1} + r_{D2} \dots\dots\dots (V - 92) \end{aligned}$$

$$r_{D5} = r_{D1} + (r_{D1} + r_{D2}) \dots\dots\dots (V - 93)$$

etc.

In general, for  $n > 4$  :

$$r_{Dn} = r_{D(n-4)} + (r_{D1} + r_{D2}) \dots\dots\dots (V - 94)$$

When the well is situated against one of the faults :

$$r_{D2} = r_{D3} = r_{D4} = r_{D5} \dots\dots\dots (V - 95)$$

$$r_{D6} = r_{D7} = r_{D8} = r_{D9} = 2r_{D2} \dots\dots (V - 96)$$

$$r_{D10} = r_{D11} = r_{D12} = r_{D13} = 3r_{D2} \dots\dots (V - 97)$$

etc.

In general, for  $n > 4$  :

$$r_{Dn} = r_{D(n-4)} + r_{D2} \dots\dots\dots (V - 98)$$

which is the same as equation (V - 94) in which  $r_{D1} = 0$  .

The computer program and type curves, pertaining to equation (V - 89) , are shown in Appendices D - 9 and E - 9

respectively. The computer program not only prints out the dimensionless drawdown versus dimensionless time for given values of  $r_{D1}$  and  $r_{D2}$ , but also calculates the number of image wells contributing to the drawdown at each dimensionless time. Typical output is illustrated in Figure 9.

Since there are an infinite number of image wells, there is no final straight-line portion on the dimensionless drawdown curve, the slope of which continues to increase with the log of time, as shown in Appendix E - 9. With increasing time, more and more image wells affect the drawdown, interference from the  $y^{\text{th}}$  image well being felt at a dimensionless time given by equation (II - 16), namely :

$$t_{D_{\text{int}}}(y) = \frac{r_{Dy}^2}{4} \dots\dots\dots (V - 99)$$

## X. THE EFFECT OF THE SKIN

As described in Chapters II and III, the skin has the effect of increasing or decreasing the ideal drawdown by an amount equal to the skin effect (BDQS). Similarly, the dimensionless drawdown is increased or decreased by the value of  $S$ , as can be seen from equation (II - 20) or (II - 21). Since the entire curve is displaced up or down by a constant amount, the library of type curves for a well situated between two faults (Appendix E) is still valid, provided the drawdown due to the skin is recognized and ignored, as illustrated in examples worked in Chapter VI. Similarly, the dimensionless times at which straight-line portions of the curve intersect

## PARALLEL FAULTS

RD2 = 1000.0

RD1 = 500.0

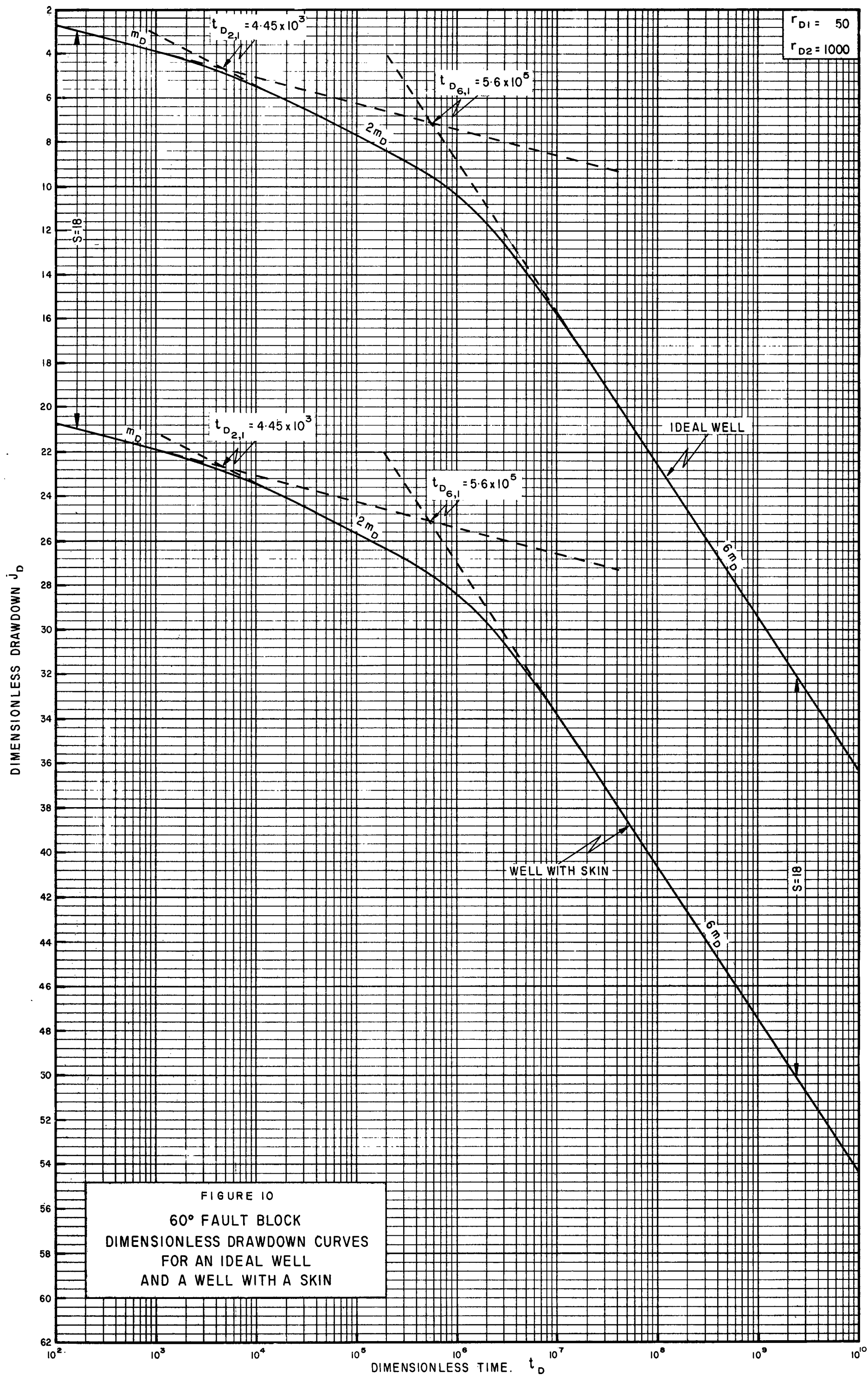
TD	JD	IMAGES
.1E 02	1.57	0
.2E 02	1.91	0
.5E 02	2.36	0
.1E 03	2.71	0
.2E 03	3.05	0
.5E 03	3.51	0
.1E 04	3.86	0
.2E 04	4.20	0
.5E 04	4.66	0
.1E 05	5.01	0
.2E 05	5.36	0
.5E 05	5.81	0
.1E 06	6.17	1
.2E 06	6.58	1
.5E 06	7.27	2
.1E 07	7.98	5
.2E 07	8.96	6
.5E 07	10.90	10
.1E 08	13.09	16
.2E 08	16.18	22
.5E 08	22.32	37
.1E 09	29.24	53
.2E 09	39.02	74
.5E 09	58.43	118
.1E 10	80.31	168

FIGURE 9

## PARALLEL FAULTS

TYPICAL COMPUTER OUTPUT FOR  
IDEAL DIMENSIONLESS DRAWDOWN CURVE

are unaffected by the skin, as illustrated in Figure 10 ,  
and Appendices F - 1 and F - 2 , which are graphical  
solutions of intersection-time equations, may still be used.



## CHAPTER VI

### SUBSURFACE FAULT MAPPING USING THE RESERVOIR LIMIT TEST

#### I. THE BASIS OF SUBSURFACE FAULT MAPPING

When a well is situated between two sealing faults, the angle of intersection between the faults and the distance to each fault may be rapidly found from data obtained during a successful Reservoir Limit Test, using Appendices E and F .

The method of approach is based upon the following fundamental conclusions obtained from the analyses of Chapter V :

- ( i) For an ideal well, the "shape" of the dimensionless drawdown curve is a function of two things only, namely :
    - (a) The angle of intersection between the two faults ( $\theta$ )
    - and (b) The ratio of the dimensionless distances to the two faults ( $r_{D2}/r_{D1}$ ) where  $r_{D1}$  and  $r_{D2}$  are defined by equations (V - 18) and (V - 19) respectively.
- Thus, if the ideal dimensionless drawdown curve obtained from field data is plotted on the same



scale as that used in Appendix E ,  $\theta$  and  $r_{D2}/r_{D1}$  may be readily found by determining which curve in the library of type curves has the same shape as that obtained in the field.

- ( ii) The above matching technique is independent of the skin, provided the part of the drawdown curve due to the skin is recognized and ignored.
- (iii) Provided the duration of the test is sufficiently long, the final slope on the dimensionless draw-down curve is given by equation (V - 39) , namely :

$$\text{Final slope} = \frac{360}{\theta} \cdot m_D$$

where  $\theta$  is the angle of intersection between the two faults and  $m_D$  is the slope of the dimensionless drawdown curve for a well situated in an infinite reservoir i.e. 1.15 units/log cycle.

- ( iv) The dimensionless times at which straight-line portions of the curve intersect are a function of the dimensionless distances to the two faults. The latter may be found by measuring the appropriate times of intersection and entering these in Appendix F - 1 or F - 2 . The former is for  $r_{D1} > 0$  while the latter is used when the well is situated at or close to one of the faults.

and ( v) The dimensionless time at which interference from the  $y^{\text{th}}$  image well reaches the producing well is given by equation (II - 16) , namely :

$$t_{\text{Dint}(y)} = \frac{r_{\text{Dy}}^2}{4}$$

## II. METHOD OF ANALYSIS

The complete procedure for subsurface fault mapping is as follows :

- ( i) Produce the well at a constant reservoir production rate and record the flowing bottom hole pressure versus time.
- ( ii) Plot the drawdown versus the log of time and draw a smooth curve through the points.
- (iii) Determine the resistivity, diffusivity and skin effect as described in Chapter III .
- ( iv) Convert the field data to ideal dimensionless data, using equations (II - 10) and (II - 11) , namely :

$$\begin{aligned} j_{\text{Di}} &= \frac{j_i}{\text{BDQ}} \\ &= \frac{j_w - j_s}{\text{BDQ}} \end{aligned}$$

$$\text{and } t_{\text{D}} = \frac{\eta^t}{r_w^2}$$

- ( v) Plot the ideal dimensionless drawdown versus the log of dimensionless time, on the same scale as

that used in Appendix E .

- ( vi) Determine the angle of intersection between the two faults, from the slope of the final straight-line portion of the dimensionless drawdown curve.
  - (vii) Compare the dimensionless field curve with the appropriate set(s) of curves in Appendix E to determine the value of  $r_{D2}/r_{D1}$  .
  - (viii) Measure the dimensionless times at which straight-line portions of the curve intersect, and enter these, if necessary together with the value of  $r_{D2}/r_{D1}$  , in either Appendix F - 1 or F - 2 to solve for  $r_{D1}$  and  $r_{D2}$  . If times of intersection can not be measured, use dimensionless times of interference and solve for  $r_{D1}$  and/or  $r_{D2}$  using equation (II - 16) . The latter method is less reliable than the former, due to the difficulty of accurately selecting the dimensionless times of interference, and should be avoided wherever possible.
- and ( ix) Calculate the distances to the two faults, using equations (V - 18) and (V - 19) as follows :

$$g_1 = r_{D1}r_w$$

$$\text{and } g_2 = r_{D2}r_w$$

If desired, the appropriate computer program from Appendix D may be run, using the values of  $r_{D1}$  and  $r_{D2}$  found in step (viii) above, to obtain the theoretical ideal

dimensionless drawdown curve for comparison with that constructed from field data. This offers a final check of the validity of the interpretation.

The above method is best illustrated by means of examples. The following have been specially selected in order to illustrate not only the method of analysis, but also some of the difficulties associated with the Reservoir Limit Test. These difficulties have been experienced by BP (Trinidad) Limited during the running of several tests in their fields in Trinidad, West Indies.

It will be seen that a knowledge of many reservoir rock and fluid properties is necessary in each example. Methods for obtaining these properties are not described since these are based upon well known techniques which have been widely published and generally accepted by the petroleum industry.

#### Example number 1

Measured data. An oil well was produced at a constant reservoir production rate of 100 barrels per day and the bottom hole pressure was continually recorded for 300 days as follows :

<u>Time</u> (days)	<u>Bottom hole pressure</u> (psig)	<u>Drawdown</u> (psi)
0.000	2500	Initial shut-in pressure
0.001	2465	35
0.002	2464	36
0.005	2461	39
0.01	2459	41
0.02	2456	44
0.05	2452	48
0.1	2448	52

<u>Time</u> (days)	<u>Bottom hole pressure</u> (psig)	<u>Drawdown</u> (psi)
0.2	2445	55
0.5	2440	60
1.0	2436	64
2.0	2433	67
5.0	2427	73
10.0	2422	78
20.0	2414	86
50.0	2400	100
100.0	2387	113
200.0	2373	127
300.0	2364	136

The following data were known from other sources  
(PVT, core analysis, log interpretation, etc.) :

$$\phi = 30\%$$

$$h = 62 \text{ ft.}$$

$$\mu = 5.25 \text{ cps.}$$

$$c = 8.0 \times 10^{-6} \text{ vol/vol/psi}$$

$$r_w = 0.333 \text{ ft.}$$

Calculation of resistivity, diffusivity and skin effect.

The drawdown measurements are plotted in Figure 11 which contains three straight-line portions as indicated. It is evident that the well is situated between two sealing faults. Furthermore, since the final slope is eight times the initial slope, the angle of intersection between the faults is given by :

$$\begin{aligned} \theta &= \frac{360}{8} \\ &= 45^\circ \end{aligned}$$

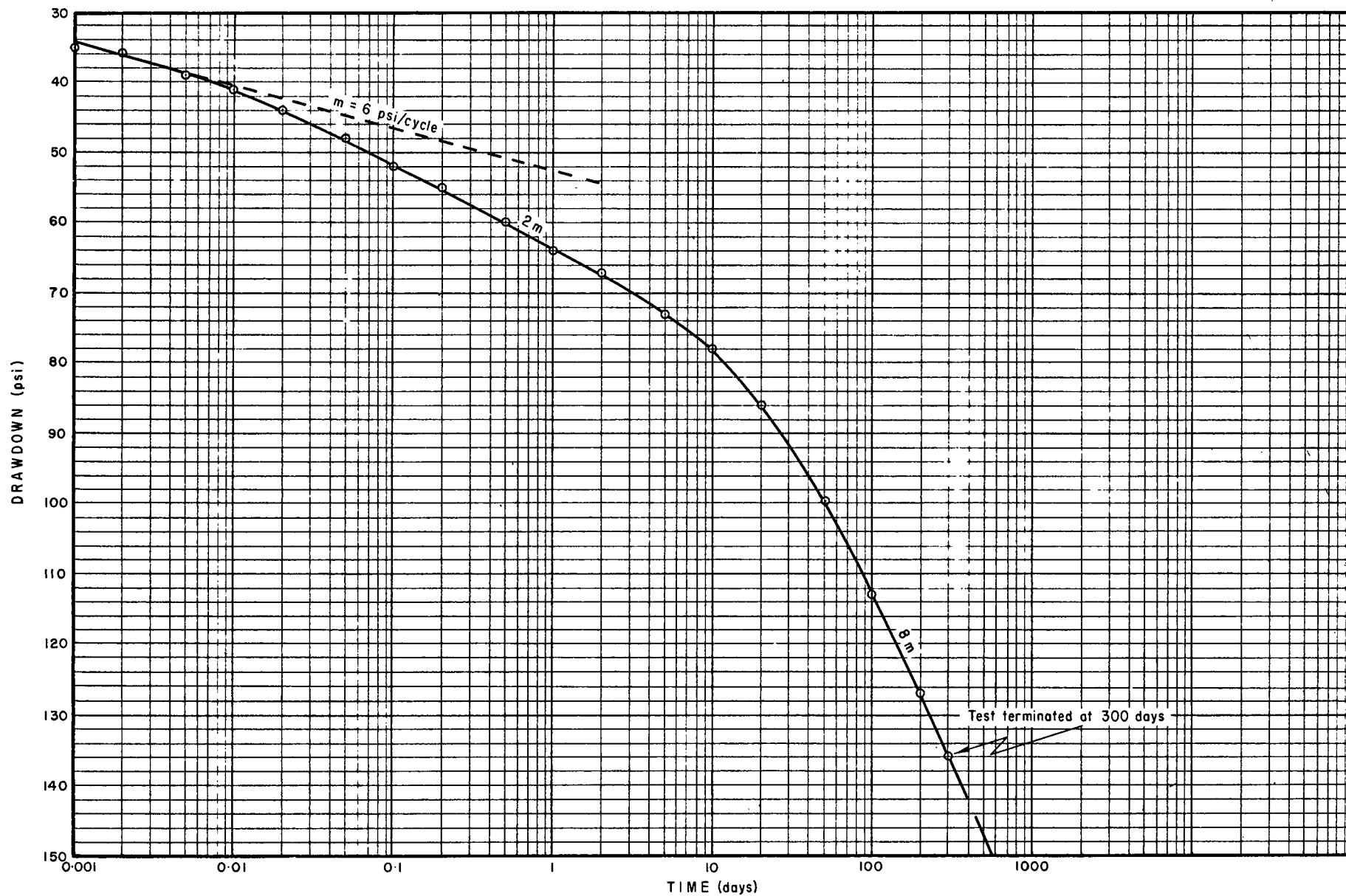


FIGURE 11  
SUBSURFACE FAULT MAPPING  
EXAMPLE No.1  
DRAWDOWN CURVE

From equation (III - 2) :

$$\begin{aligned}
 D &= \frac{m}{1.15 \text{ BQ}} \\
 &= \frac{6}{1.15 \times 100} \\
 &= 0.0522 \text{ psi/bpd}
 \end{aligned}$$

From equation (III - 3) :

$$\begin{aligned}
 k &= \frac{0.1626 \mu \text{BQ}}{hm} \\
 &= \frac{0.1626 \times 5.25 \times 100}{62 \times 6} \\
 &= 0.229 \text{ darcies}
 \end{aligned}$$

From equation (III - 4) :

$$\begin{aligned}
 \eta &= \frac{0.8935}{Dhc\phi} \\
 &= \frac{0.8935}{0.0522 \times 62 \times 8 \times 10^{-6} \times 0.3} \\
 &= 1.15 \times 10^5 \text{ sq. ft/day}
 \end{aligned}$$

From equation (II - 8) :

$$j_i = m \log \frac{2.25 \eta t}{r_w^2}$$

Therefore, at one day :

$$\begin{aligned}
 j_i &= 6 \log \frac{2.25 \times 1.15 \times 10^5}{0.111} \\
 &= 38 \text{ psi}
 \end{aligned}$$

But, at one day, the actual drawdown on the line of slope  $m$  is :

$$j_w = 53 \text{ psi}$$

Therefore, the skin effect, from equation (II - 17) ,  
is :

$$\begin{aligned} j_s &= (53 - 38) \\ &= + 15 \text{ psi} \end{aligned}$$

Thus, field drawdown measurements may be converted to ideal measurements by subtracting 15 psi throughout.

Conversion of field data to ideal dimensionless data.

From equation (II - 10) :

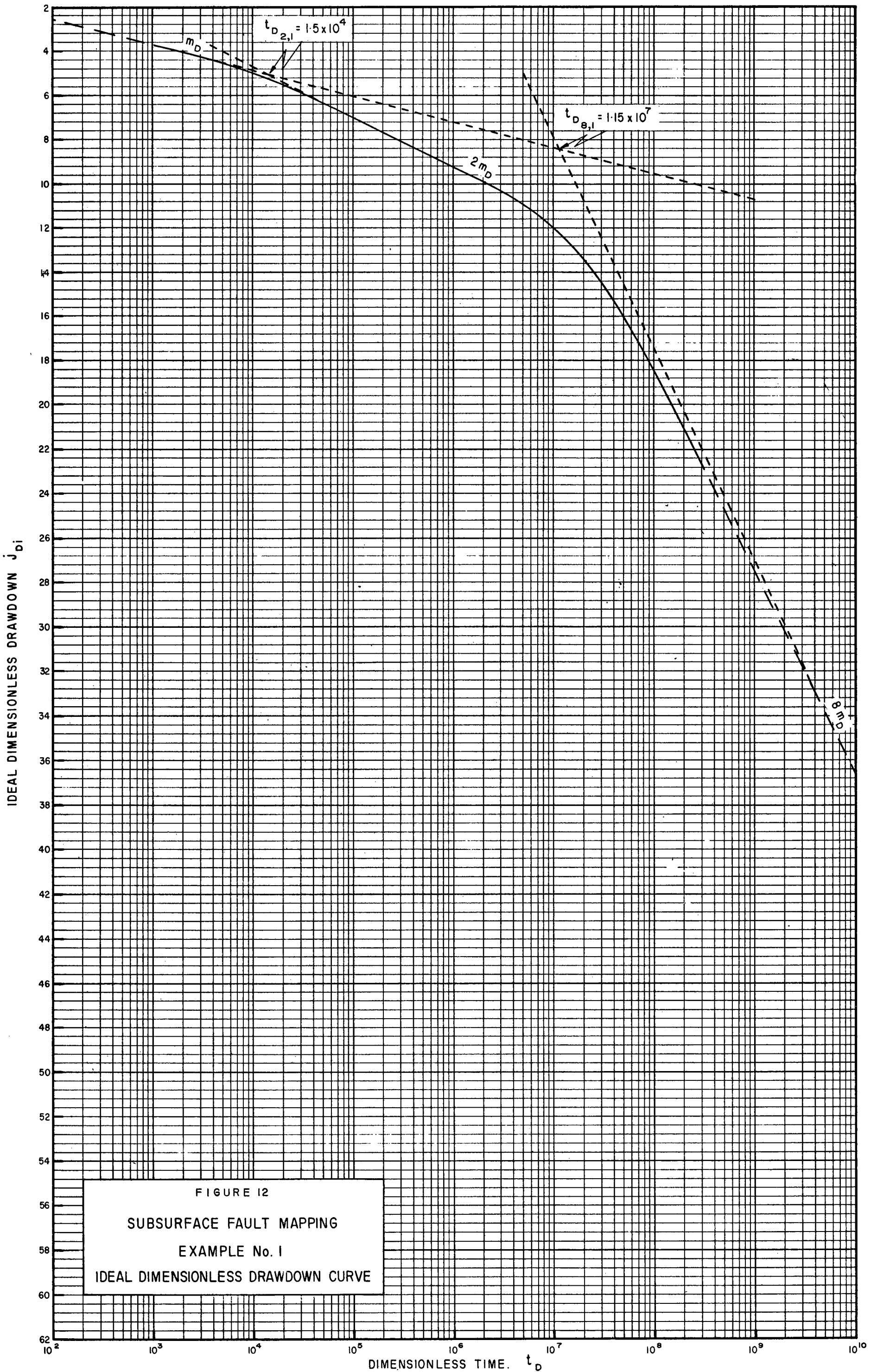
$$\begin{aligned} j_{Di} &= \frac{j_i}{BDQ} \\ &= \frac{j_i}{5.22} \\ &= 0.19 (j_w - 15) \end{aligned}$$

From equation (II - 11) :

$$\begin{aligned} t_D &= \frac{\eta t}{r_w^2} \\ &= \frac{1.15 \times 10^5 t}{0.111} \\ &= 1.04 \times 10^6 t \end{aligned}$$

Using the above, the field measurements were converted to ideal dimensionless data and plotted in Figure 12 , on the same scale as that used in Appendix E . Straight-line portions of the curve, and dimensionless times at which the straight-line portions intersect, are clearly marked. The curve was extrapolated using Appendix E - 6 .





Analysis of the dimensionless drawdown curve. A comparison of Figure 12 with the library of curves in Appendix E indicates that the well is situated in a  $45^\circ$  fault block in which  $r_{D2}/r_{D1} > 20$ .

From Figure 12 :

$$t_{D2,1} = 1.5 \times 10^4$$

Therefore, from Appendix F - 1 :

$$r_{D1} = 90$$

Also, from Figure 12 :

$$t_{D8,1} = 1.15 \times 10^7$$

Therefore, from Appendix F - 1 :

$$r_{D2}/r_{D1} = 42$$

from which :

$$r_{D2} = 3780$$

Therefore, from equations (V - 18) and (V - 19) , the distances to the two faults are :

$$\begin{aligned} g_1 &= 90 \times 0.333 \\ &= 30 \text{ ft.} \end{aligned}$$

$$\begin{aligned} \text{and } g_2 &= 3780 \times 0.333 \\ &= 1260 \text{ ft.} \end{aligned}$$

Jones (5 : 2) has shown that the proved distance seen out into a reservoir during a Reservoir Limit Test, is :

$$d = 2\sqrt{\eta t_{fin}}$$

where  $t_{fin}$  is the duration of the test, in days.

Thus, as no interference, other than that due to the two faults intersecting at  $45^\circ$ , had been felt at the conclusion of the above test, i.e. at 300 days, the distance seen out into the reservoir is given by :

$$\begin{aligned} d &= 2\sqrt{1.15 \times 10^5 \times 300} \\ &= 11,750 \text{ ft.} \end{aligned}$$

Figure 13 shows the complete solution and defines the area proved up during the test.

Discussion of results. (i) It is most unlikely that a Reservoir Limit Test would actually be run for as long as 300 days, since the chances of maintaining a constant producing rate and controlling the gas/oil ratio over such a long period would be remote. It is therefore of interest to re-examine the above data, assuming that the test had been terminated at an earlier time. If the test had been stopped at 10 days (i.e.  $t_D = 1.04 \times 10^7$ ), interference from the second fault would have been seen, because the straight line of slope  $2m_D$ , on the dimensionless curve, begins to bend over at  $t_D = \text{circa } 3 \times 10^6$ , indicating interference from the second image well. However, determination of the angle of intersection between the two faults would not have been possible because the data obtained up to 10 days give no indication of the slope of the final straight-line portion of the curve. Using equation (II - 16) and the above dimensionless interference time, the dimensionless distance to the second fault is given by :

A B C is the area proved up  
during the test

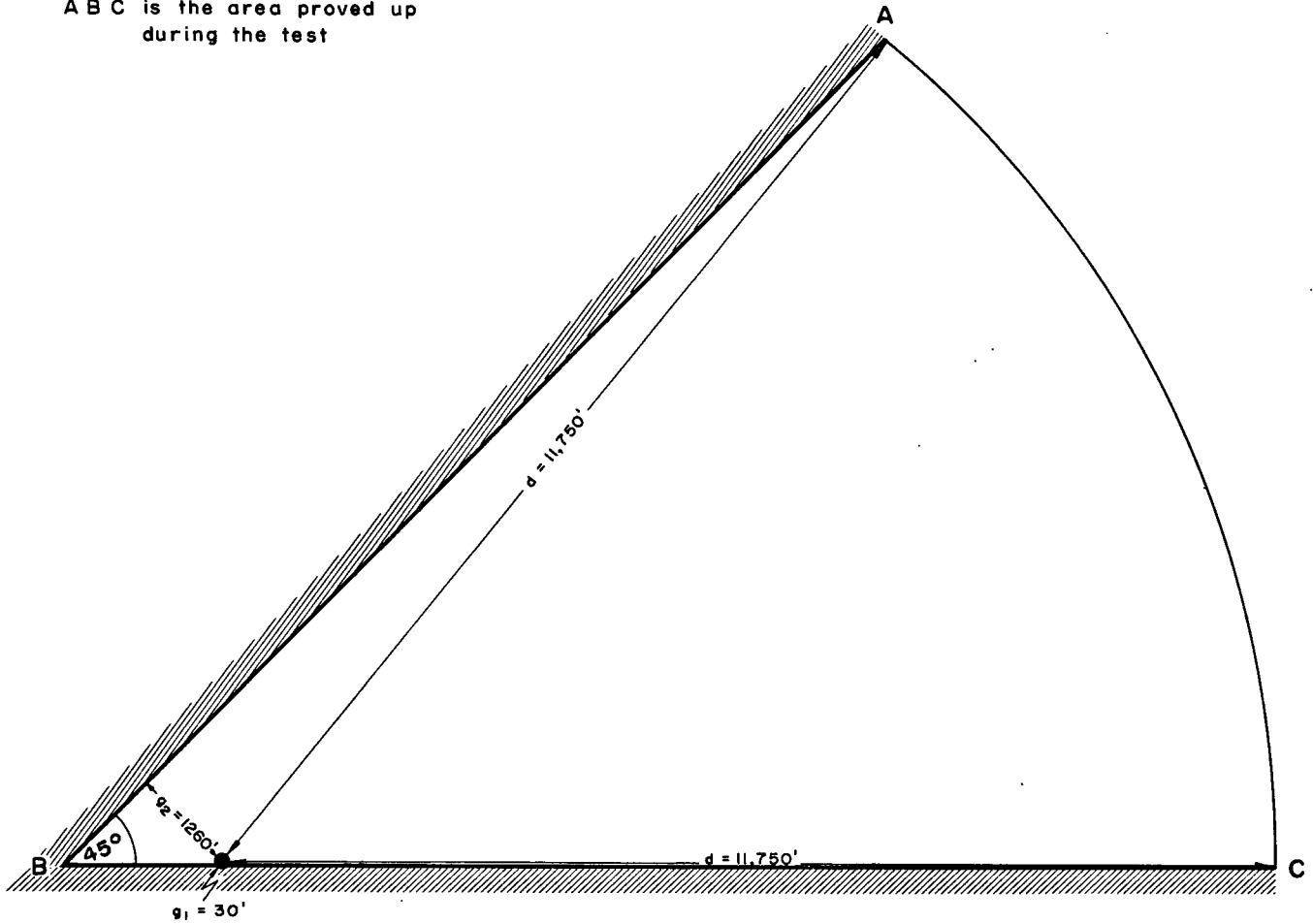


FIGURE 13  
SUBSURFACE FAULT MAPPING  
SOLUTION TO EXAMPLE No. 1

$$\begin{aligned} r_{D2} &= 2 \sqrt{3 \times 10^6} \\ &= 3460 \end{aligned}$$

which agrees fairly closely with that calculated above.

A comparison of Figure 12 with the library of curves in Appendix E indicates that the minimum dimensionless time required to determine the angle of intersection between the faults is :

$$t_{D_{\min}} = \text{circa } 5.0 \times 10^7$$

This corresponds to a minimum testing time of 48 days.

(ii) It is also unlikely that the initial slope  $m$  would have been seen in practice in this example, since data obtained before 0.01 days is usually unreliable due to the effects of the skin and unloading of the well i.e. the time before 0.01 days may be regarded as the "settling-down" period.

(iii) In general, for values of  $r_{D1}$  less than fifty to a hundred, the curve will begin with a slope of  $2m_D$ , unless the diffusivity is so low that interference from the first fault is not felt until after 0.01 days.

(iv) For a given reservoir shape, the area proved up during a Reservoir Limit Test is a function of the diffusivity,  $\eta$ . For example, if the diffusivity in this example had been ten times as great as the calculated value above, then the proved distance seen out into the reservoir at the conclusion of the test, i.e. at 300 days, would have been :

$$\begin{aligned} d &= 2 \sqrt{1.15 \times 10^5 \times 10 \times 300} \\ &= 37,140 \text{ ft.} \end{aligned}$$

compared with a value of 11,750 ft. calculated above.

( v) To summarize, low values of diffusivity will enable faults close to the wellbore to be picked up on the drawdown curve, but the area proved up will be small unless the Reservoir Limit Test is run for a long period of time. Conversely, large values of diffusivity will enable a large area to be proved up in a short time, but faults situated close to the producing well will, for practical purposes, affect the drawdown from commencement of production, and the initial slope of the draw-down curve will be greater than  $m$  . This is illustrated further in later examples.

#### Example number 2

Measured data. An oil well was produced at a constant reservoir production rate of 250 barrels per day and the bottom hole pressure was continually recorded for 10 days as follows :

<u>Time</u> (days)	<u>Bottom hole pressure</u> (psig)	<u>Drawdown</u> (psi)
0.00	1500	Initial shut-in pressure
0.01	1443	57
0.02	1439	61
0.05	1435	65
0.1	1432	68
0.2	1427	73
0.5	1421	79
1.0	1415	85
2.0	1409	91
5.0	1399	101
10.0	1393	107

The following data were known from other sources :

$$\begin{aligned}
 \phi &= 25\% \\
 h &= 210 \text{ ft.} \\
 \mu &= 3.5 \text{ cps.} \\
 c &= 9 \times 10^{-6} \text{ vol/vol/psi.} \\
 r_w &= 0.5 \text{ ft.}
 \end{aligned}$$

Calculation of resistivity, diffusivity and skin effect.

The drawdown measurements are plotted in Figure 14 which contains only two straight-line portions as indicated, the slope of the second line being twice that of the first.

Assuming that the first line represents the drawdown before interference from any barriers has been felt, then :

$$m = 11.5 \text{ psi/log cycle}$$

From equation (III - 2) :

$$\begin{aligned}
 D &= \frac{m}{1.15 \text{ BQ}} \\
 &= \frac{11.5}{1.15 \times 250} \\
 &= 0.04 \text{ psi/bpd}
 \end{aligned}$$

From equation (III - 3) :

$$\begin{aligned}
 k &= \frac{0.1626 \mu \text{BQ}}{hm} \\
 &= \frac{0.1626 \times 3.5 \times 250}{210 \times 11.5} \\
 &= 0.059 \text{ darcies}
 \end{aligned}$$

From equation (III - 4) :

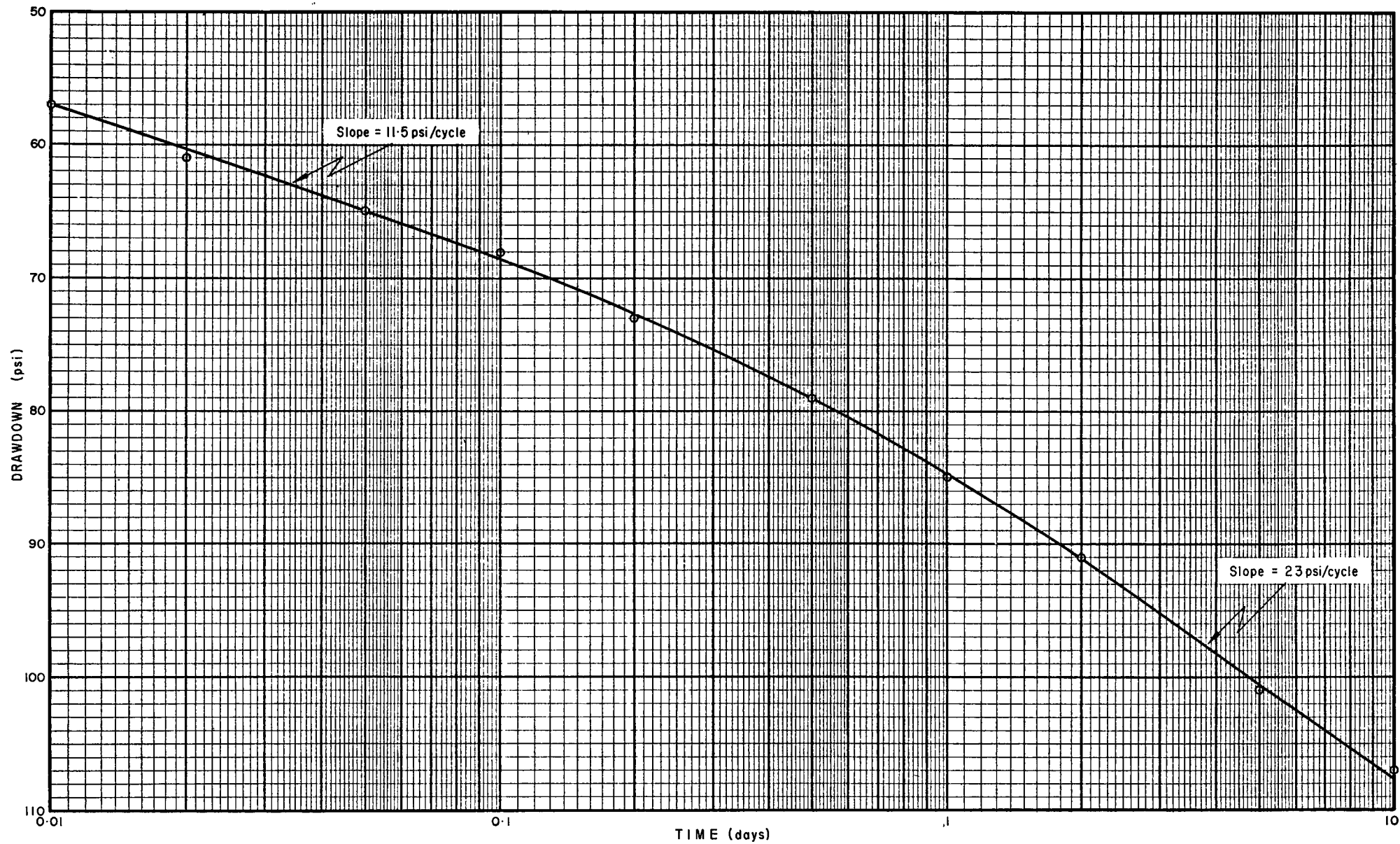


FIGURE 14  
SUBSURFACE FAULT MAPPING  
EXAMPLE No. 2  
DRAWDOWN CURVE



$$\begin{aligned}
 \eta &= \frac{0.8935}{Dhc\phi} \\
 &= \frac{0.8935}{0.04 \times 210 \times 9 \times 10^{-6} \times 0.25} \\
 &= 4.73 \times 10^4 \text{ sq.ft./day}
 \end{aligned}$$

From equation (II - 8) :

$$j_i = m \log \frac{2.25 \eta t}{r_w^2}$$

Therefore, at one day :

$$\begin{aligned}
 j_i &= 11.5 \log \frac{2.25 \times 4.73 \times 10^4}{0.25} \\
 &= 65 \text{ psi}
 \end{aligned}$$

But, at one day, the actual drawdown on the line of slope  $m$  is :

$$j_w = 80 \text{ psi}$$

Therefore, the skin effect, from equation (II - 17) ,  
is :

$$\begin{aligned}
 j_s &= (80 - 65) \\
 &= + 15 \text{ psi}
 \end{aligned}$$

Thus, field drawdown measurements may be converted to ideal measurements by subtracting 15 psi throughout.

#### Conversion of field data to ideal dimensionless data.

From equation (II - 10) :

$$\begin{aligned}
 j_{Di} &= \frac{j_i}{BDQ} \\
 &= 0.1 (j_w - 15)
 \end{aligned}$$

From equation (II - 11) :

$$\begin{aligned} t_D &= \frac{\eta t}{r_w^2} \\ &= \frac{4.73 \times 10^4 t}{0.25} \\ &= 1.89 \times 10^5 t \end{aligned}$$

Using the above, the ideal dimensionless drawdown curve was constructed (Figure 15) on the same scale as that used in Appendix E , and extrapolated using Appendix E - 1 .

Analysis of the dimensionless drawdown curve. From Appendix E , a possible solution is that the well is situated near a single linear barrier.

From Figure 15 :

$$t_{D2,1} = 7.5 \times 10^4$$

Therefore, from Appendix F - 1 :

$$r_{D1} = 205$$

Therefore, the distance to the barrier is :

$$s_1 = 205 \times 0.5 = 103 \text{ ft.}$$

As in the previous example, the proved distance seen out into the reservoir is given by :

$$\begin{aligned} d &= 2 \sqrt{\eta t_{\text{end of test}}} \\ &= 2 \sqrt{4.73 \times 10^4 \times 10} \\ &= 1375 \text{ ft.} \end{aligned}$$

Thus, a possible complete solution is as shown in Figure 17 (a) .

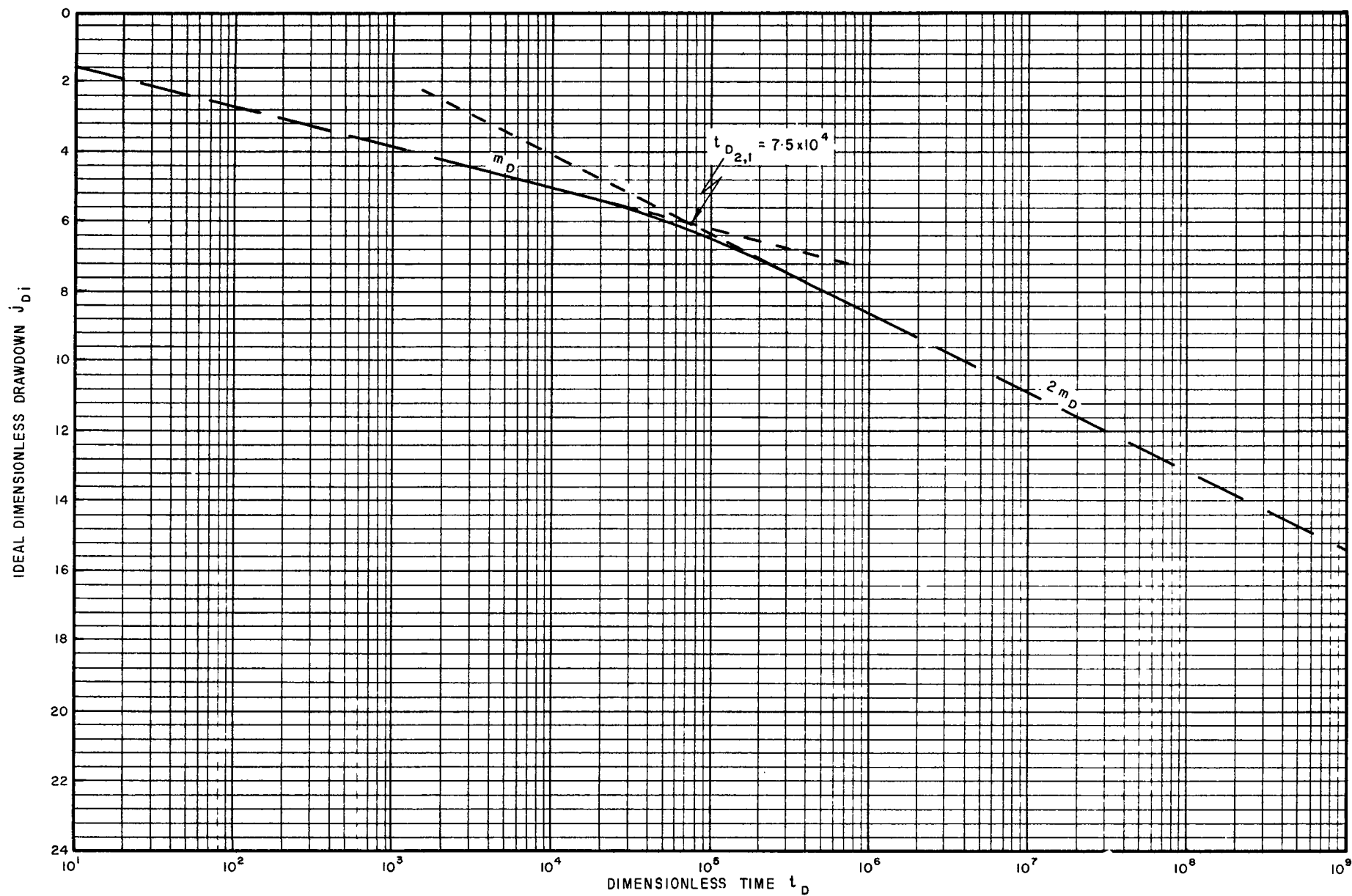


FIGURE 15

SUBSURFACE FAULT MAPPING

EXAMPLE No. 2

IDEAL DIMENSIONLESS DRAWDOWN CURVE FOR SOLUTION No. 1

However, this is not the only solution, because it was assumed that the slope of the first straight-line portion of the curve was  $m$  and this is not necessarily correct. It is quite possible that the well was situated so close to a barrier that the slope of the drawdown curve was  $2m$  from the start.

If this is so, then  $m = 5.75$  psi/cycle i.e. half the value previously accepted. This has the effect of halving the value of  $D$  and doubling the value of  $\eta$ . Using this value of  $m$ , the following results are obtained :

$$D = 0.02 \text{ psi/bpd}$$

$$k = 0.118 \text{ darcies}$$

$$\eta = 9.46 \times 10^4 \text{ sq. ft./day}$$

$$j_s = + 12 \text{ psi}$$

$$j_{Di} = 0.2 (j_w - 12)$$

$$\text{and } t_D = 3.78 \times 10^5 t$$

The corresponding ideal dimensionless drawdown curve is shown in Figure 16. Comparison of this curve with those contained in Appendix E indicates that the well is situated in a  $90^\circ$  fault block, at or close to one of the faults.

From Figure 16 :

$$t_{D4,2} = 1.5 \times 10^5$$

Therefore, from Appendix F - 2 :

$$r_{D2} = 290$$

Therefore, the distance to the second barrier is :

$$g_2 = 290 \times 0.5 = 145 \text{ ft.}$$

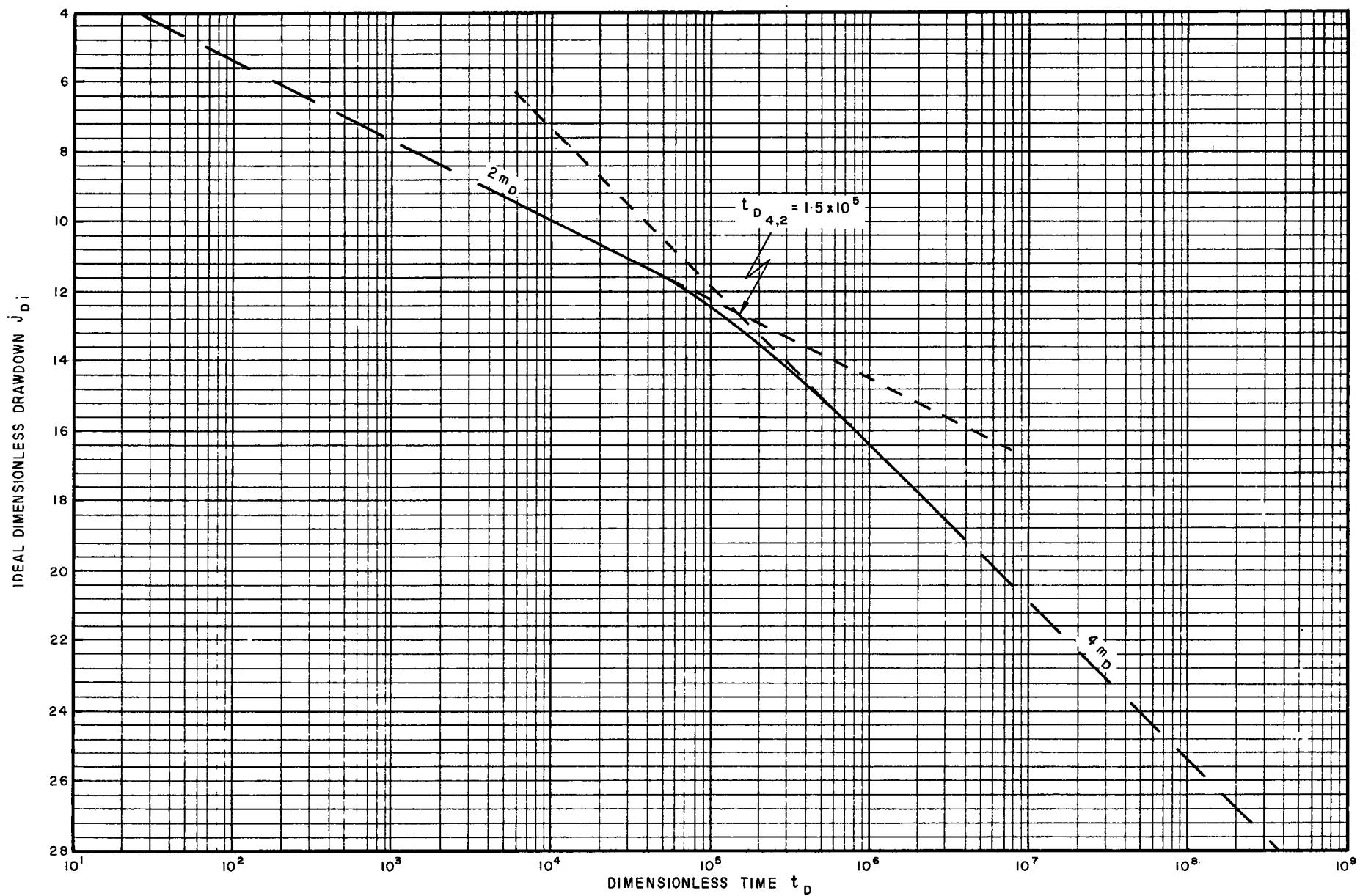


FIGURE 16

SUBSURFACE FAULT MAPPING

EXAMPLE No.2

IDEAL DIMENSIONLESS DRAWDOWN CURVE FOR SOLUTION No.2

As above, the distance seen out into the reservoir is :

$$\begin{aligned} d &= 2 \sqrt{9.46 \times 10^4 \times 10} \\ &= 1945 \text{ ft.} \end{aligned}$$

Thus, a second possible solution is as shown in Figure 17 (b) .

Discussion of results. The above example illustrates one of the major difficulties encountered during the interpretation of a Reservoir Limit Test, namely the selection of  $m$  . Unless an approximate value of the permeability is known from other sources, there is no way of checking the value of  $m$  calculated from the drawdown curve and several solutions may be possible. If the permeability is known, however, the value of  $m$  may be checked and the most probable solution chosen.

For example, if the permeability from core measurements is 65 mds , then from equation (III - 3) :

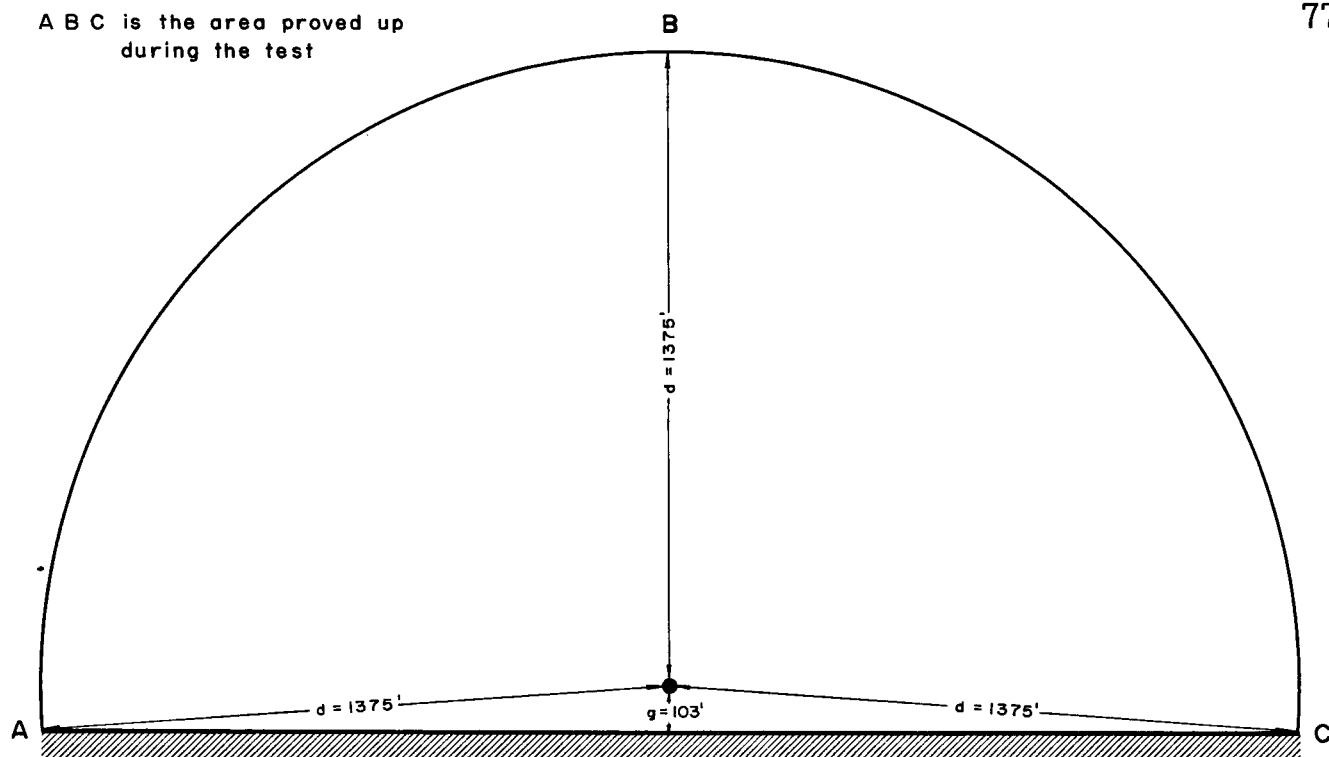
$$\begin{aligned} m &= \frac{0.1626 \mu BQ}{hk} \\ &= \frac{0.1626 \times 3.5 \times 250}{210 \times 0.065} \\ &= 10.4 \text{ psi/cycle} \end{aligned}$$

which agrees closely with the value used in the first interpretation. Solution number 1 is therefore the more probable of the two.

### Example number 3

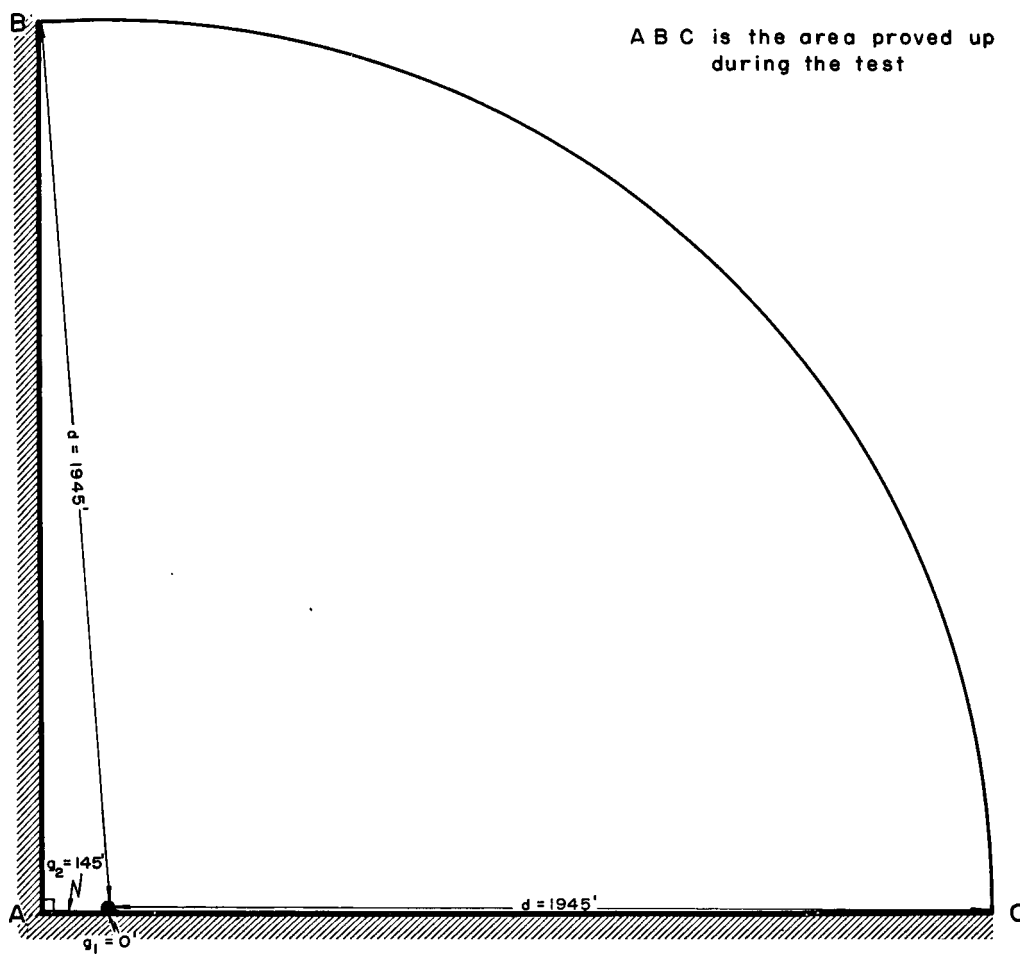
Measured data. A gas well was produced at a constant

A B C is the area proved up  
during the test



(a) SOLUTION No.1

A B C is the area proved up  
during the test



(b) SOLUTION No.2

FIGURE 17

SUBSURFACE FAULT MAPPING  
SOLUTIONS TO EXAMPLE No.2

rate of 500 mscf/day and the bottom hole pressure was continually recorded for 10 days as follows :

<u>Time</u> (days)	<u>Bottom hole pressure</u> (psig)	<u>Drawdown</u> (psi)
0.00	3000	Initial shut-in pressure
0.01	2954	46
0.02	2951	49
0.05	2945	55
0.1	2942	58
0.2	2938	62
0.5	2934	66
1.0	2930	70
2.0	2926	74
5.0	2922	78
10.0	2918	82

The following data were known from other sources :

$$\begin{aligned}
 \phi &= 15\% \\
 h &= 110 \text{ ft.} \\
 \mu &= 0.02 \text{ cps.} \\
 k &= 10 \text{ mds.} \\
 c &= 200 \times 10^{-6} \text{ vol/vol/psi.} \\
 r_w &= 0.25 \text{ ft.} \\
 B &= 0.806 \text{ res. bbls/mscf.}
 \end{aligned}$$

Calculation of resistivity, diffusivity and skin effect;  
and interpretation of the drawdown curve. Since the permeability is known from core analysis, values of resistivity and diffusivity may be calculated without reference to the drawdown data.

From equation (II - 1) :

$$\begin{aligned}
 D &= \frac{0.1412\mu}{hk} \\
 &= \frac{0.1412 \times 0.02}{110 \times 0.01} \\
 &= 0.00257 \text{ psi/bpd.}
 \end{aligned}$$



From equation (III - 1) :

$$\begin{aligned}
 m &= 1.15 \text{ BDQ} \\
 &= 1.15 \times 0.806 \times 0.00257 \times 500 \\
 &= 1.19 \text{ psi/log cycle.}
 \end{aligned}$$

But the slope of the drawdown curve, which is a single straight line in this case (Figure 18) , is 12 psi/log cycle, which is approximately ten times the value calculated from the permeability obtained from core samples.

Thus, since the slope of the drawdown curve is 10m from commencement of the test, the well is situated at or very close to two faults which intersect at an angle ( $\theta$ ) given by :

$$\begin{aligned}
 \theta &= \frac{360}{10} \\
 &= 36^\circ
 \end{aligned}$$

From equation (III - 4) :

$$\begin{aligned}
 \eta &= \frac{0.8935}{Dhc\phi} \\
 &= \frac{0.8935}{0.00257 \times 110 \times 200 \times 10^{-6} \times 0.15} \\
 &= 1.05 \times 10^5 \text{ sq. ft./day}
 \end{aligned}$$

As in previous examples, the distance seen out into the reservoir is :

$$\begin{aligned}
 d &= 2 \sqrt{\eta \ t_{\text{end of test}}} \\
 &= 2 \sqrt{1.05 \times 10^5 \times 10} \\
 &= 2050 \text{ ft.}
 \end{aligned}$$

Thus, the complete solution is as shown in Figure 19 .

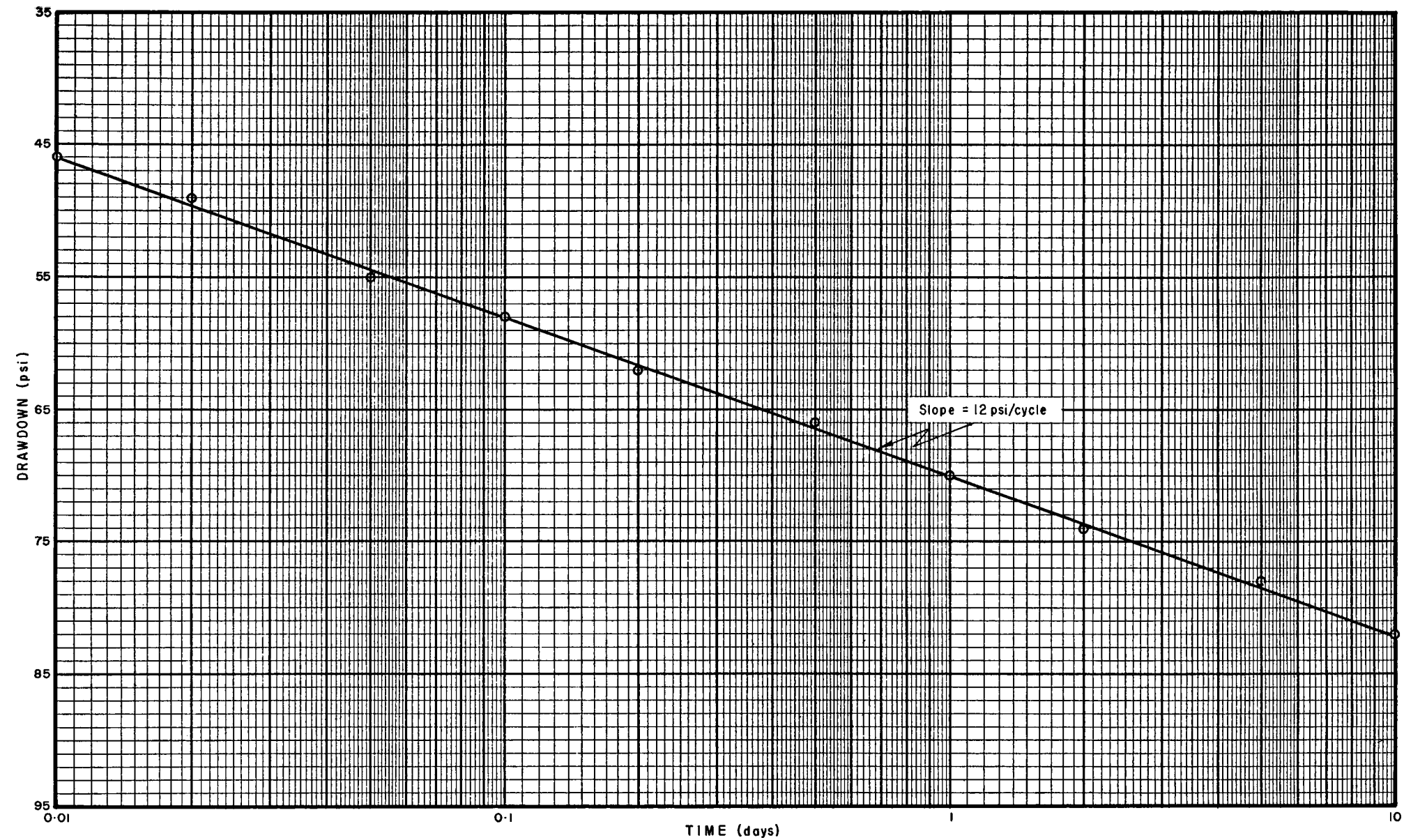


FIGURE 18  
SUBSURFACE FAULT MAPPING  
EXAMPLE No. 3  
DRAWDOWN CURVE

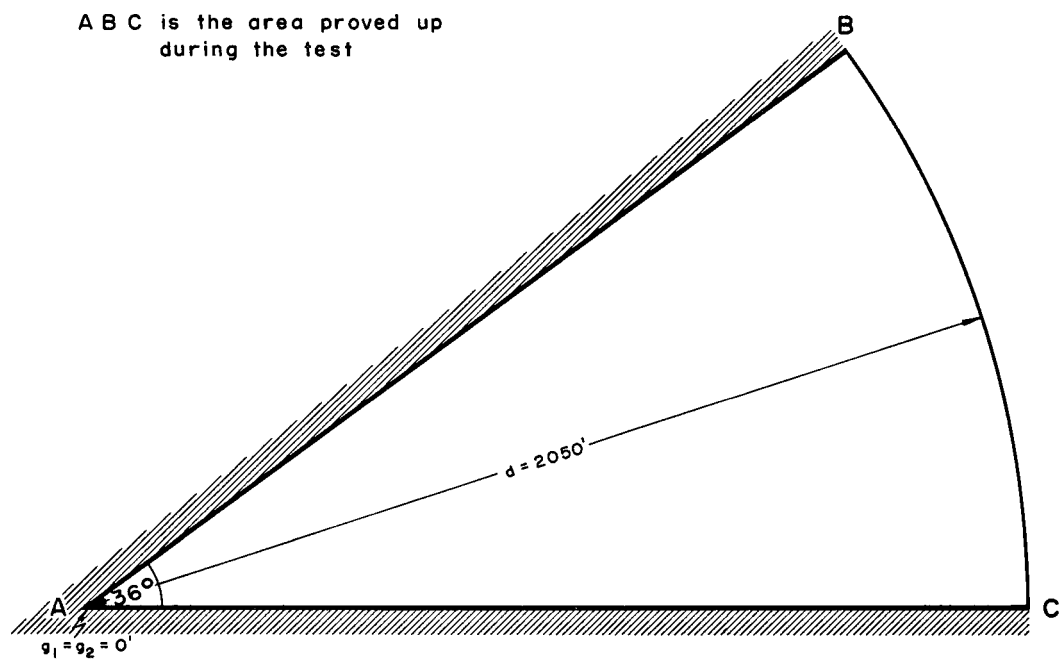


FIGURE 19  
SUBSURFACE FAULT MAPPING  
SOLUTION TO EXAMPLE No. 3

The ideal drawdown in this case will be ten times that in an ideal well situated in an infinite reservoir.

Therefore, from equation (II - 8) :

$$j_i = 10m \log \frac{2.25 \eta t}{r_w^2}$$

Therefore, at one day :

$$\begin{aligned} j_i &= 12 \log \frac{2.25 \times 1.05 \times 10^5}{0.0625} \\ &= 79 \text{ psi.} \end{aligned}$$

But the actual drawdown at one day, from Figure 18 , is :

$$j_w = 70 \text{ psi.}$$

Therefore, the skin effect, from equation (II - 17) ,  
is :

$$\begin{aligned} j_s &= (70 - 79) \\ &= -9 \text{ psi.} \end{aligned}$$

i.e. the skin effect is negative, indicating a zone of stimulated permeability around the wellbore.

Discussion of results. Since the drawdown curve in the above example consisted of one straight-line portion only, the use of dimensionless data was not necessary.

A single interpretation would not have been possible without a knowledge of the permeability from measurements on cores. The reliability of the above solution is therefore totally dependent upon the accuracy of the core analysis.

In the case of a gas well, the formation volume factor will actually change gradually throughout the test due to the

change in pressure at the sand face. This should be investigated before commencement of the test in order to calculate what changes in flow rate will be necessary to maintain a constant reservoir production rate throughout. A constant formation volume factor was assumed above in order to simplify the example.

#### Example number 4

Measured data. An oil well was produced at a constant reservoir production rate of 150 barrels per day and the bottom hole pressure was continually recorded for 30 days as follows :

<u>Time</u> (days)	<u>Bottom hole pressure</u> (psig)	<u>Drawdown</u> (psi)
0.0000	2500	Initial shut-in pressure
0.0006	2365	135
0.001	2293	207
0.002	2257	243
0.005	2207	293
0.01	2183	317
0.02	2167	333
0.05	2147	353
0.1	2131	369
0.2	2111	389
0.5	2072	428
1.0	2023	477
2.0	1953	547
5.0	1827	673
10.0	1712	788
20.0	1573	927
30.0	1492	1008

The following data were known from other sources :

$$\phi = 12\%$$

$$h = 50 \text{ ft.}$$

$$\mu = 5.00 \text{ cps.}$$

$$\begin{aligned}
 k &= 50 \text{ mds.} \\
 c &= 10.0 \times 10^{-6} \text{ vol/vol/psi.} \\
 r_w &= 0.5 \text{ ft.}
 \end{aligned}$$

Calculation of resistivity, diffusivity and skin effect.

The drawdown measurements are plotted in Figure 20 . From a visual examination of the curve, the part before 0.01 days is due to the skin effect and may be ignored. The remainder of the curve contains two straight-line portions, the second of which has a slope equal to approximately nine times that of the first.

Assuming that the slope of the first straight line is  $m$  , then from equation (III - 3) :

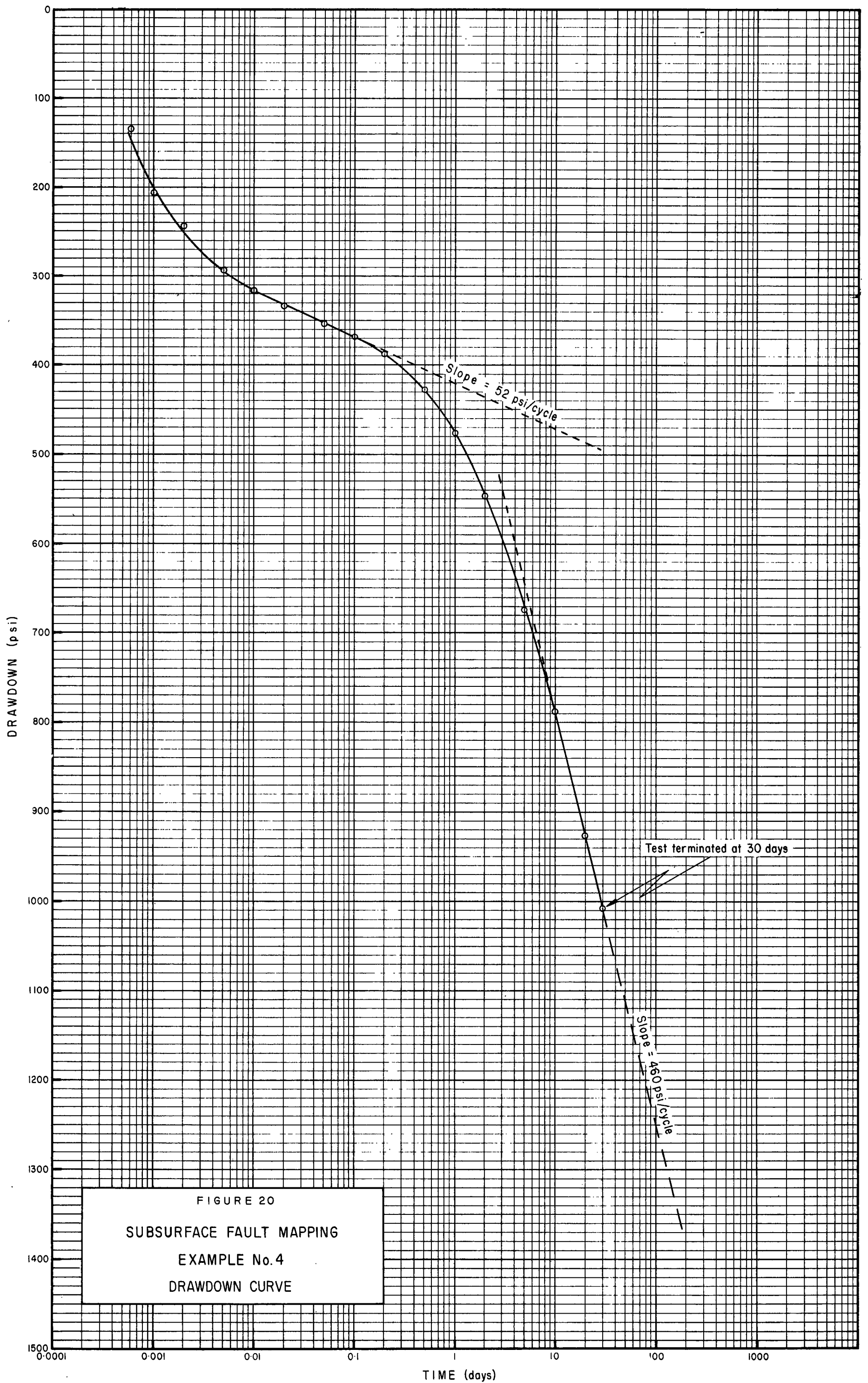
$$\begin{aligned}
 k &= \frac{0.1626 \mu BQ}{hm} \\
 &= \frac{0.1626 \times 5 \times 150}{50 \times 52} \\
 &= 0.047 \text{ darcies}
 \end{aligned}$$

which agrees closely with that known from other sources. Thus, the assumed value of  $m$  is correct.

Since the final slope of the drawdown curve is equal to  $9m$  , the well is situated between two faults which intersect at an angle  $(\theta)$  given by :

$$\begin{aligned}
 \theta &= \frac{360}{9} \\
 &= 40^\circ
 \end{aligned}$$

From equation (III - 2) :



$$\begin{aligned}
 D &= \frac{m}{1.15 \text{ BQ}} \\
 &= \frac{52}{1.15 \times 150} \\
 &= 0.3014 \text{ psi/bpd.}
 \end{aligned}$$

From equation (III - 4) :

$$\begin{aligned}
 \eta &= \frac{0.8935}{Dhc\phi} \\
 &= \frac{0.8935}{0.3014 \times 50 \times 10^{-5} \times 0.12} \\
 &= 4.94 \times 10^4 \text{ sq.ft./day}
 \end{aligned}$$

From equation (II - 8) :

$$j_i = m \log \frac{2.25 \eta t}{r_w^2}$$

Therefore, at one day :

$$\begin{aligned}
 j_i &= 52 \log \frac{2.25 \times 4.94 \times 10^4}{0.25} \\
 &= 294 \text{ psi.}
 \end{aligned}$$

But, at one day, the actual drawdown on the line of slope  $m$  is :

$$j_w = 421 \text{ psi.}$$

Therefore, the skin effect, from equation (II - 17) , is :

$$\begin{aligned}
 j_s &= (421 - 294) \\
 &= 127 \text{ psi.}
 \end{aligned}$$



Thus, field drawdown measurements may be converted to ideal measurements by subtracting 127 psi throughout.

Conversion of field data to ideal dimensionless data.

From equation (II - 10) :

$$\begin{aligned} j_{Di} &= \frac{j_i}{BDQ} \\ &= \frac{(j_w - 127)}{45.21} \\ &= 0.022 (j_w - 127) \end{aligned}$$

From equation (II - 11) :

$$\begin{aligned} t_D &= \frac{\eta t}{r_w^2} \\ &= \frac{4.94 \times 10^4 t}{0.25} \\ &= 1.98 \times 10^5 t \end{aligned}$$

Using the above, the field data obtained after 0.01 days were converted to ideal dimensionless data and plotted in Figure 21, on the same scale as that used in Appendix E.

Analysis of the dimensionless drawdown curve. A comparison of Figure 21 with the library of curves in Appendix E indicates that the well is situated in a  $40^\circ$  fault block in which  $r_{D2}/r_{D1} = 1$ .

From Figure 21 :

$$t_{D9,1} = 3.5 \times 10^5$$

Entering the values of  $r_{D2}/r_{D1}$  and  $t_{D9,1}$  into

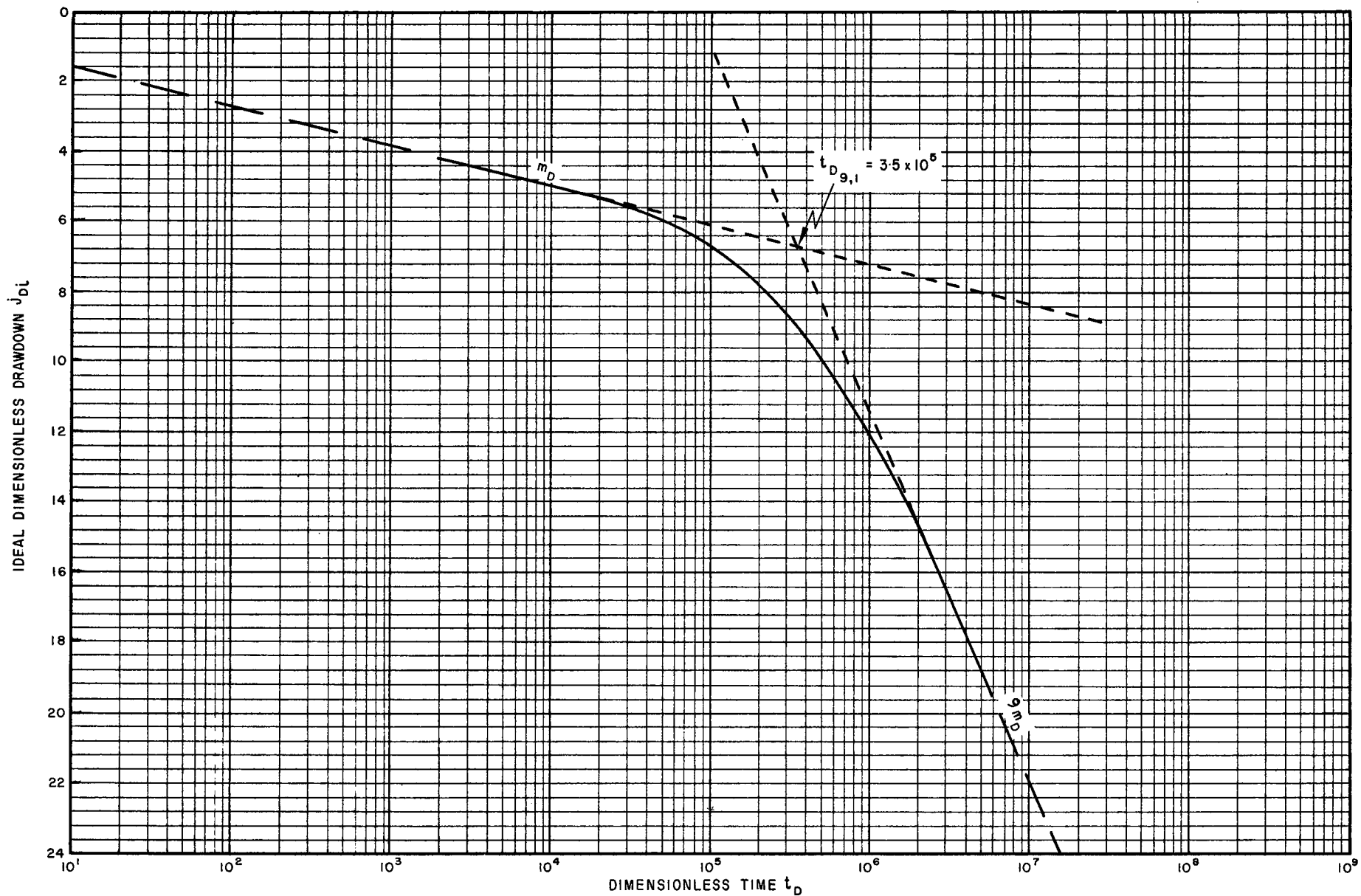


FIGURE 21  
 SUBSURFACE FAULT MAPPING  
 EXAMPLE No. 4  
 IDEAL DIMENSIONLESS DRAWDOWN CURVE

Appendix F - 1 , we obtain :

$$r_{D1} = 240$$

But :

$$r_{D2}/r_{D1} = 1$$

Therefore :

$$r_{D2} = 240$$

Therefore, from equations (V - 18) and (V - 19) ,  
the distances to the faults are :

$$\begin{aligned} g_1 &= g_2 \\ &= 240 \times 0.5 \\ &= 120 \text{ ft.} \end{aligned}$$

As in previous examples, the distance seen out into  
the reservoir, is :

$$\begin{aligned} d &= 2 \sqrt{4.94 \times 10^4 \times 30} \\ &= 2,440 \text{ ft.} \end{aligned}$$

Thus, the complete solution is as shown in Figure 22 .

Discussion of results. The above interpretation was straightforward and no difficulties were encountered. Since Appendices E and F do not contain curves for a  $40^\circ$  fault block, it was necessary to interpolate between  $30^\circ$  and  $45^\circ$  type curves.

#### Example number 5

Measured data. An oil well was produced at a constant reservoir production rate of 164 barrels per day and the bottom hole pressure was continually recorded for 10 days as

A B C is the area proved up  
during the test

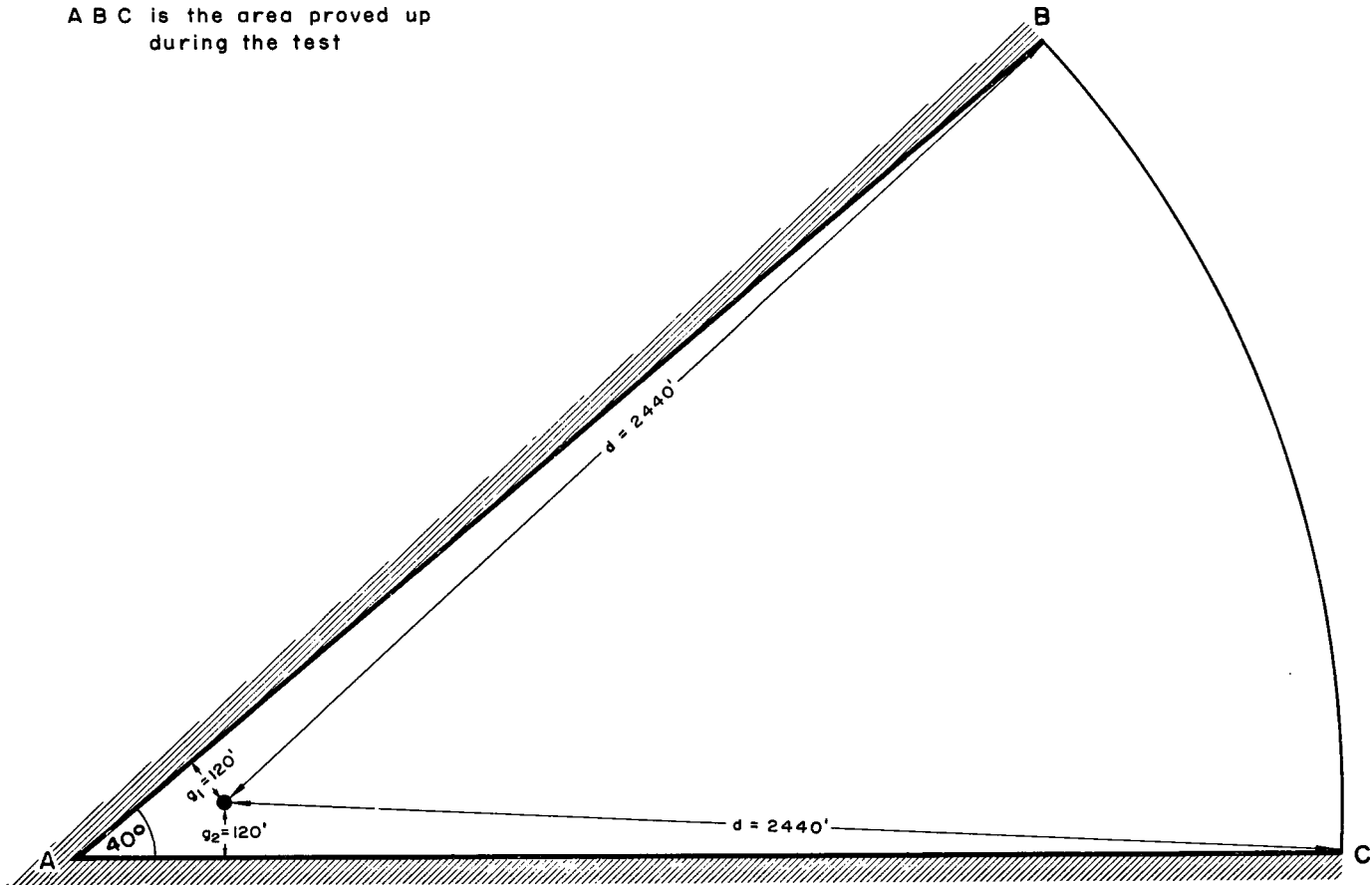


FIGURE 22  
SUBSURFACE FAULT MAPPING  
SOLUTION TO EXAMPLE No. 4

follows :

<u>Time</u> (days)	<u>Bottom hole pressure</u> (psig)	<u>Drawdown</u> (psi)
0.00	2500	Initial shut-in pressure
0.01	2114	386
0.02	2080	420
0.05	2033	467
0.1	1994	506
0.2	1948	552
0.5	1866	634
1.0	1778	722
2.0	1654	846
5.0	1409	1091
10.0	1132	1368

The following data were known from other sources :

$$\phi = 20\%$$

$$h = 80 \text{ ft.}$$

$$\mu = 8.0 \text{ cps.}$$

$$k \approx 25 \text{ mds.}$$

$$c = 6.5 \times 10^{-6} \text{ vol/vol/psi.}$$

$$r_w = 0.375 \text{ ft.}$$

#### Calculation of resistivity, diffusivity and skin effect.

The drawdown measurements are plotted in Figure 23 . The curve contains one straight-line portion only, and then bends over sharply, suggesting the presence of parallel faults. No final straight-line portion is apparent.

Assuming that the slope of the initial straight line is  $m$  , then from equation (III - 3) :

$$\begin{aligned}
 k &= \frac{0.1626 \mu BQ}{hm} \\
 &= \frac{0.1626 \times 8 \times 164}{80 \times 115} \\
 &= 0.023 \text{ darcies.}
 \end{aligned}$$

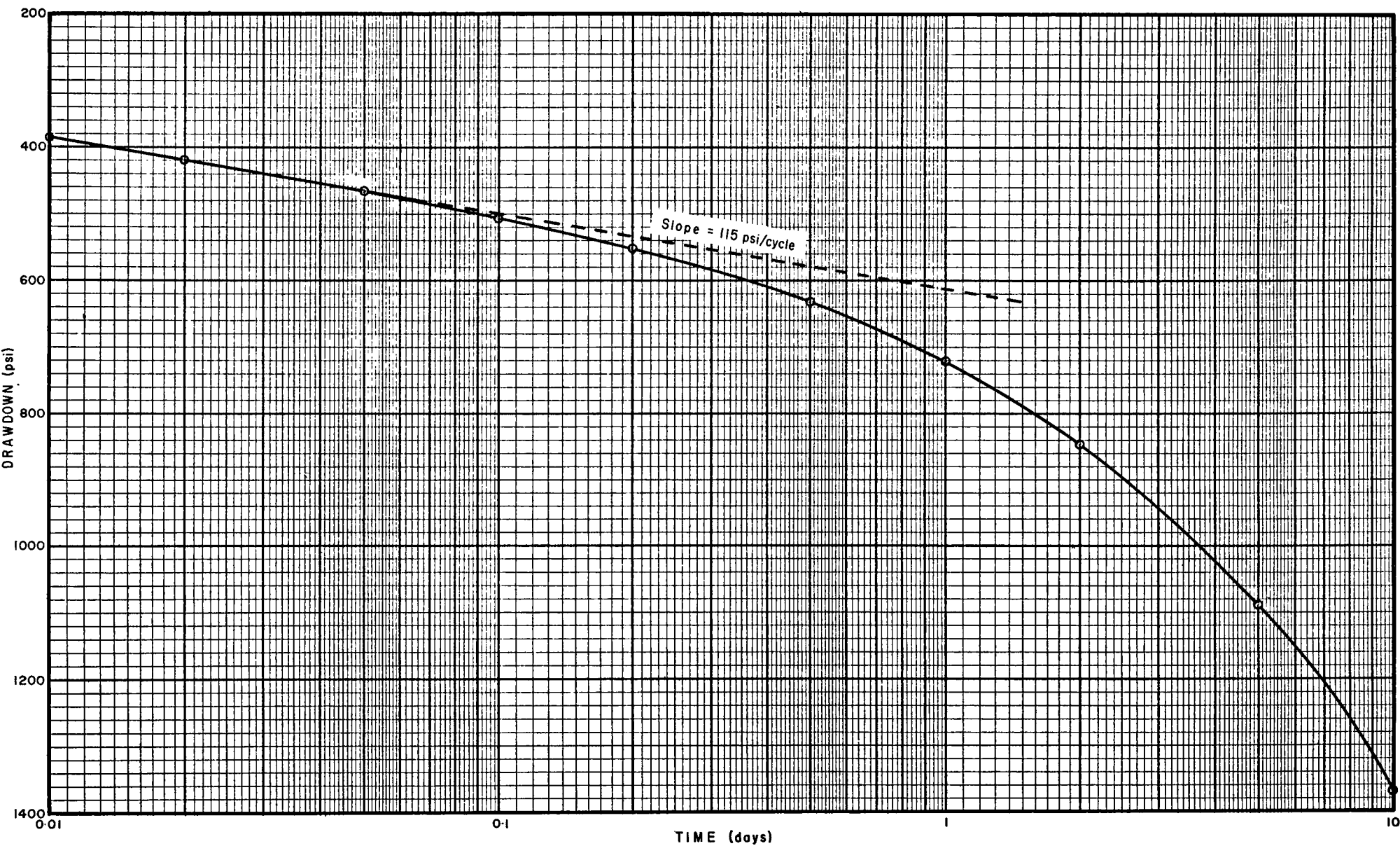


FIGURE 23  
SUBSURFACE FAULT MAPPING  
EXAMPLE No. 5  
DRAWDOWN CURVE

which agrees with that known from other sources. Thus, the assumed value of  $m$  is correct.

From equation (III - 2) :

$$\begin{aligned} D &= \frac{m}{1.15 \text{ BQ}} \\ &= \frac{115}{1.15 \times 164} \\ &= 0.6098 \text{ psi/bpd.} \end{aligned}$$

From equation (III - 4) :

$$\begin{aligned} \eta &= \frac{0.8935}{Dhc\phi} \\ &= \frac{0.8935}{0.6098 \times 80 \times 6.5 \times 10^{-6} \times 0.2} \\ &= 1.41 \times 10^4 \text{ sq.ft/day.} \end{aligned}$$

From equation (II - 8) :

$$j_i = m \log \frac{2.25 \eta t}{r_w^2}$$

Therefore, at one day :

$$\begin{aligned} j_i &= 115 \log \frac{2.25 \times 1.41 \times 10^4}{0.141} \\ &= 616 \text{ psi.} \end{aligned}$$

But, at one day, the actual drawdown on the line of slope  $m$  is :

$$j_w = 616 \text{ psi.}$$

Therefore, the skin effect, from equation (II - 17) ,  
is :

$$\begin{aligned} j_s &= (616 - 616) \\ &= 0 \text{ psi.} \end{aligned}$$

Conversion of field data to ideal dimensionless data.

From equation (II - 10) :

$$\begin{aligned} j_{Di} &= \frac{j_i}{BDQ} \\ &= 0.01 j_w \end{aligned}$$

From equation (II - 11) :

$$\begin{aligned} t_D &= \frac{\eta t}{r_w^2} \\ &= \frac{1.41 \times 10^4 t}{0.141} \\ &= 1 \times 10^5 t \end{aligned}$$

Using the above, the field data were converted to ideal dimensionless data and plotted in Figure 24 . Since it was suspected that the well was situated between parallel faults, the curve was plotted on the same scale as that used in Appendix E - 9 .

Analysis of the dimensionless drawdown curve. A comparison of Figure 24 with Appendix E - 9 indicates that the well is situated between parallel faults with  $r_{D2}/r_{D1} = 2$  .

As explained in Chapter V , there is no final straight-line portion on the dimensionless drawdown curve of a well situated between parallel faults. Furthermore, since  $r_{D2}/r_{D1} < 20$  in this example, the straight line of slope  $2m_D$



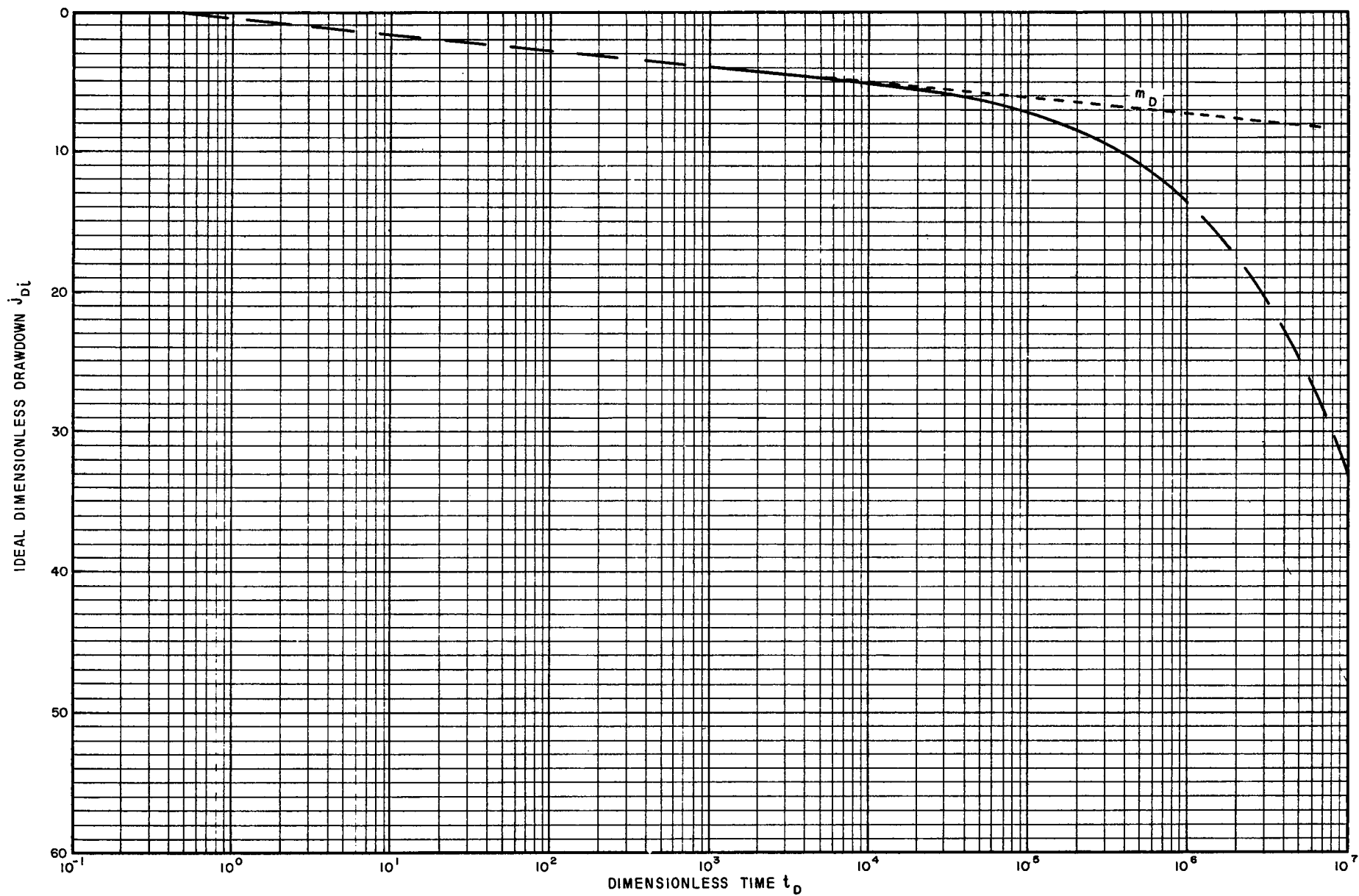


FIGURE 24  
 SUBSURFACE FAULT MAPPING  
 EXAMPLE No. 5  
 IDEAL DIMENSIONLESS DRAWDOWN CURVE

is also absent.

The dimensionless distance to the first fault must therefore be calculated from the dimensionless time of interference, using equation (II - 16) .

However, this is difficult to see on the dimensionless drawdown curve and might be anywhere between  $t_D = 3 \times 10^3$  and  $t_D = 6 \times 10^3$  , indicating a value of  $r_{D1}$  somewhere between 110 and 156 .

In this case, the computer program (Appendix D - 9) should be run for values of  $r_{D1}$  equal to 110, 120, 130, 140, 150 and 160 , and  $r_{D2}/r_{D1}$  equal to two, to determine the correct values of  $r_{D1}$  and  $r_{D2}$  . In this example, computer output indicated that :

$$r_{D1} = 125$$

and :

$$r_{D2} = 250$$

from which :

$$g_1 = 47 \text{ ft.}$$

and :

$$g_2 = 94 \text{ ft.}$$

As in previous examples :

$$\begin{aligned} d &= 2 \sqrt{1.41 \times 10^4 \times 10} \\ &= 750 \text{ ft.} \end{aligned}$$

The complete solution is shown in Figure 25 .

Discussion of results. The above example illustrates the difficulty of selecting interference times from drawdown

A B C D is the area proved up  
during the test

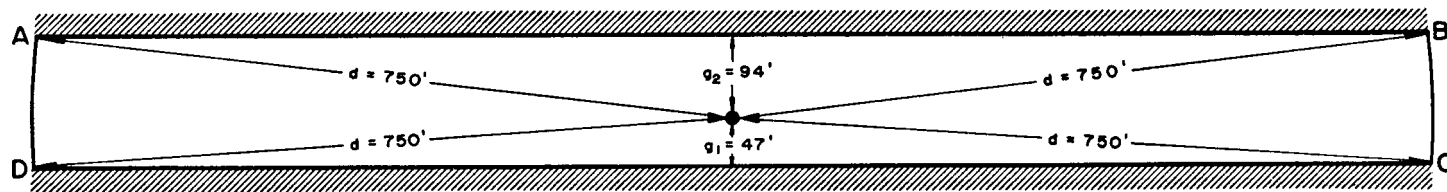


FIGURE 25  
SUBSURFACE FAULT MAPPING  
SOLUTION TO EXAMPLE No. 5

curves. This practice should be avoided whenever intersection times can be used instead.

The high resistivity and the presence of parallel faults at small distances from the producing well resulted in a very high drawdown, amounting to 55 per cent of the initial shut-in pressure after 10 days of production.

If the faults had been absent, the drawdown at 10 days would have been 731 psi. Thus, the faults resulted in an additional drawdown of  $(1368 - 731)$  psi = 637 psi.

The extrapolation of the dimensionless drawdown curve may be used to predict the future drawdown, provided no interference from a third barrier is felt.

For example, suppose it is calculated that the well will cease flowing when the bottom hole pressure drops to 500 psig. Then, the time at which the well will cease flowing, on the assumption that a constant reservoir production rate of 164 barrels per day can be maintained, may be found as follows :

When :  $p_{wf} = 500$  psig,  $j_w = j_i = 2000$  psi.

Therefore :

$$j_{Di} = 20$$

Therefore, from Figure 24 :

$$t_D = 2.9 \times 10^6$$

Therefore :

$$t = 29 \text{ days.}$$

i.e. the well will cease flowing 29 days after being opened up or 19 days after completion of the Reservoir Limit Test.

## CHAPTER VII

### AN APPRAISAL OF THE RESERVOIR LIMIT TEST, AND CONCLUSIONS

The Reservoir Limit Test can be an excellent tool for the determination of the size and shape of hydrocarbon reservoirs. However, the following points should be borne in mind :

( i) The basic equations were derived for flow of a single, slightly compressible fluid through a homogeneous, isotropic reservoir. There are few reservoirs which are completely homogeneous, but experience has shown that this does not seriously affect the results provided the degree of heterogeneity is not too great. Furthermore, the equations may be used for gas flow provided the drawdown is not excessive. The effect of two phase flow on the Reservoir Limit Test is not yet fully understood, and further work is necessary in this direction. However, it is apparent that a changing gas/oil ratio could have a marked effect upon the drawdown curve, since this implies a change in relative permeability which would cause a change of slope, even in the absence of reservoir limits.

( ii) Interpretation of a Reservoir Limit Test is difficult, unless a constant reservoir production rate can be maintained. Odeh and Jones (7 : 960) have developed a method for obtaining the value of  $m$  from drawdown data obtained during a variable-rate test, but their analysis applies to an infinite reservoir only. A future investigation of the effects of variable flow rates on the transient pressure behavior of a well situated between two sealing faults, or in a closed reservoir, would be

of immense value for future analyses of Reservoir Limit Tests.

(iii) Interpretation of a Reservoir Limit Test depends upon a knowledge of several reservoir rock and fluid properties. The accuracy of results therefore depends upon the quality of the basic data, and every effort should be made to ensure that these have been obtained from reliable sources.

A method for mapping two subsurface faults, using data obtained during a Reservoir Limit Test, has been developed in this thesis. A future extension of this work to cover closed reservoirs would contribute significantly to our understanding of drawdown data observed in the field. The effects of reservoir shape on the pressure behavior of a producing well would be of particular interest.

The construction of Appendices E and F has made it possible to analyze many drawdown curves which were difficult, or virtually impossible, to interpret in the past. The method of approach is straightforward and it is hoped that its simplicity will encourage further use of the Reservoir Limit Test in the future.

## BIBLIOGRAPHY

1. Carslaw, H.S. and Jaeger, J.C. Conduction of Heat in Solids. Oxford at the Clarendon Press, 1959.
2. van Everdingen, A.F. "The Skin Effect and Its Influence on the Productive Capacity of a Well", Trans. AIME, 198 (1953).
3. Hurst, W. "Establishment of the Skin Effect and Its Impediment to Fluid-Flow into a Well Bore", Petroleum Engineer, 25 (11) (October, 1953).
4. Hurst, William. "Interference Between Oil Fields", Trans. AIME, 219 (1960).
5. Jones, Park J. "Formation Evaluation by the Reservoir Limit Test", Paper SPE - 385 presented at the Society of Petroleum Engineers of AIME Rocky Mountain Joint Regional Meeting, Billings, Montana (May, 1962).
6. Muskat, M. The Flow of Homogeneous Fluids through Porous Media. New York : McGraw - Hill Book Company, Inc, 1937.
7. Odeh, A.S. and Jones, L.G. "Pressure Drawdown Analysis, Variable - Rate Case", Journal of Petroleum Technology, 17 (8) (August, 1965).
8. Ramey, H.J., Jr. "Non - Darcy Flow and Wellbore Storage Effects in Pressure Build - Up and Drawdown of Gas Wells", Journal of Petroleum Technology, 17 (2) (February, 1965).



## APPENDIX A

## NOMENCLATURE

## I. SYMBOLS

B	formation volume factor	res.bbls/stock tank bbl oil or res.bbls/mscf gas
c	average coefficient of compressibility	vol/vol/psi
D	formation resistivity	psi/res.bpd
d	proved distance seen out into a reservoir	ft.
g	distance between the prod- ucing well and a fault	ft.
h	formation thickness	ft.
j	drawdown	psi
k	effective permeability to the mobile phase	darcies
m	slope of the drawdown curve for a well situated in an infinite reservoir	psi/log cycle
p	pressure	psig
Q	flow rate	stock tank bbls oil per day or mscf gas per day
R	radius of a circle on which image wells are located	ft.
r	radius	ft.
r	distance between the prod- ucing well and an image well	ft.
S	skin	dimensionless
t	time	days
W(u)	Well Function of u	dimensionless
$\eta$	diffusivity	sq.ft./day
$\theta$	angle of intersection between two faults	degrees

$\mu$	viscosity of the mobile phase	cps
$\phi$	porosity	per cent

## II. SUBSCRIPTS

D	dimensionless
i	ideal
int	interference
s	skin
w	well
wf	bottom hole, flowing
ws	bottom hole, static
x,y	point of intersection of two straight-line portions of a dimensionless drawdown curve with slopes equal to $x_{mD}$ and $y_{mD}$ .

## APPENDIX B

## THE WELL FUNCTION

The Well Function is identically equal to the Exponential Integral, and defined as follows :

$$\begin{aligned}
 W(u) &\equiv -\text{Ei}(-u) \\
 &= \int_u^{\infty} \frac{e^{-v}}{v} dv \\
 &= -\ln u - 0.5772 + \sum_{n=1}^{\infty} (-1)^{n+1} \frac{u^n}{n \cdot n!}
 \end{aligned}$$

A plot of  $W(u)$  versus  $u$  is shown in Figure B - 1 . For a given value of  $u$  ,  $W(u)$  may be read from appropriate tables.

For  $u < 0.01$  , the series above may be taken as zero, and the value of the Well Function becomes :

$$\begin{aligned}
 W(u) &= -\ln u - 0.5772 \\
 &= -\ln u + \ln 0.5616 \\
 &= \ln \frac{1}{1.78u}
 \end{aligned}$$

But :

$$\ln x = 2.3 \log x$$

Therefore, for  $u < 0.01$  :

$$W(u) = 2.3 \log \frac{1}{1.78u}$$

For practical purposes,  $W(u)$  may be taken as zero when  $u > 4$  . This is compatible with equation (II - 15) , for when  $u = 4$  :

$$\frac{r^2}{4\eta t} = 4$$

and :

$$t = \frac{r^2}{16\eta}$$

The Well Function was programmed as an external function in the MAD language, for use on a digital computer, as shown in Figure B - 2 .

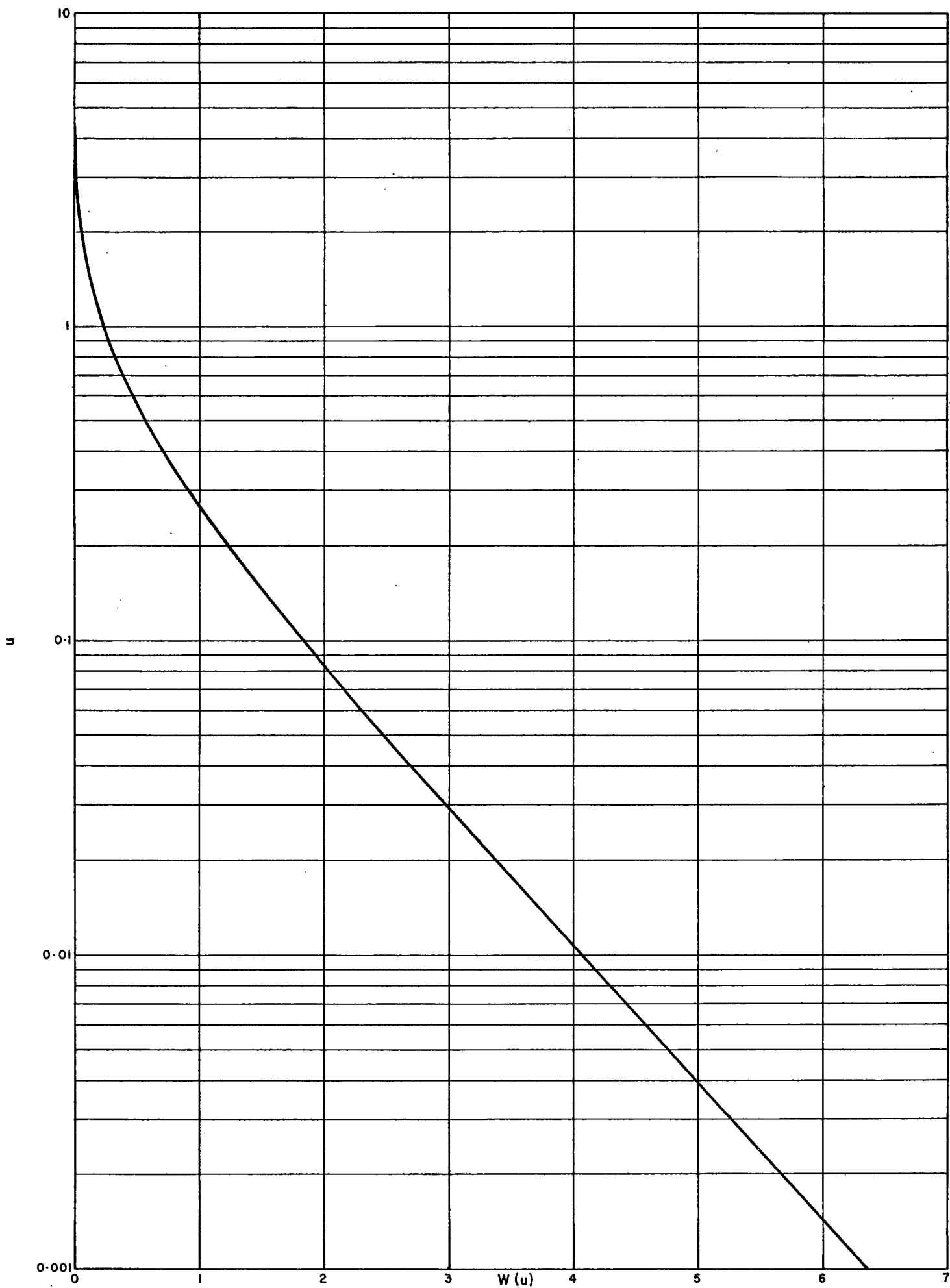


FIGURE B-1  
 $W(u)$  VERSUS  $u$

```

$ COMPILE MAD
R
R      WELL FUNCTION
R
  EXTERNAL FUNCTION(U)
  ENTRY TO W.
  INTEGER I
  WHENEVER U.G.4.
    WF = 0.
    TRANSFER TO FINISH
  OR WHENEVER U.L.0.01
    WF = -ELOG.(U)-0.5772
    TRANSFER TO FINISH
  OTHERWISE
    WF = -ELOG.(U)-0.5772+U
    TERM = U
    THROUGH ALPHA, FOR I = 2,1,I.G.30
    TERM = -(TERM*U*(I-1)/I.P.2)
    WHENEVER .ABS.TERM.L.0.0001
      TRANSFER TO FINISH
    OTHERWISE
      WF = WF+TERM
  ALPHA
    END OF CONDITIONAL
  END OF CONDITIONAL
  FINISH
    FUNCTION RETURN WF
    END OF FUNCTION

```

FIGURE B - 2  
THE WELL FUNCTION  
COMPUTER PROGRAM



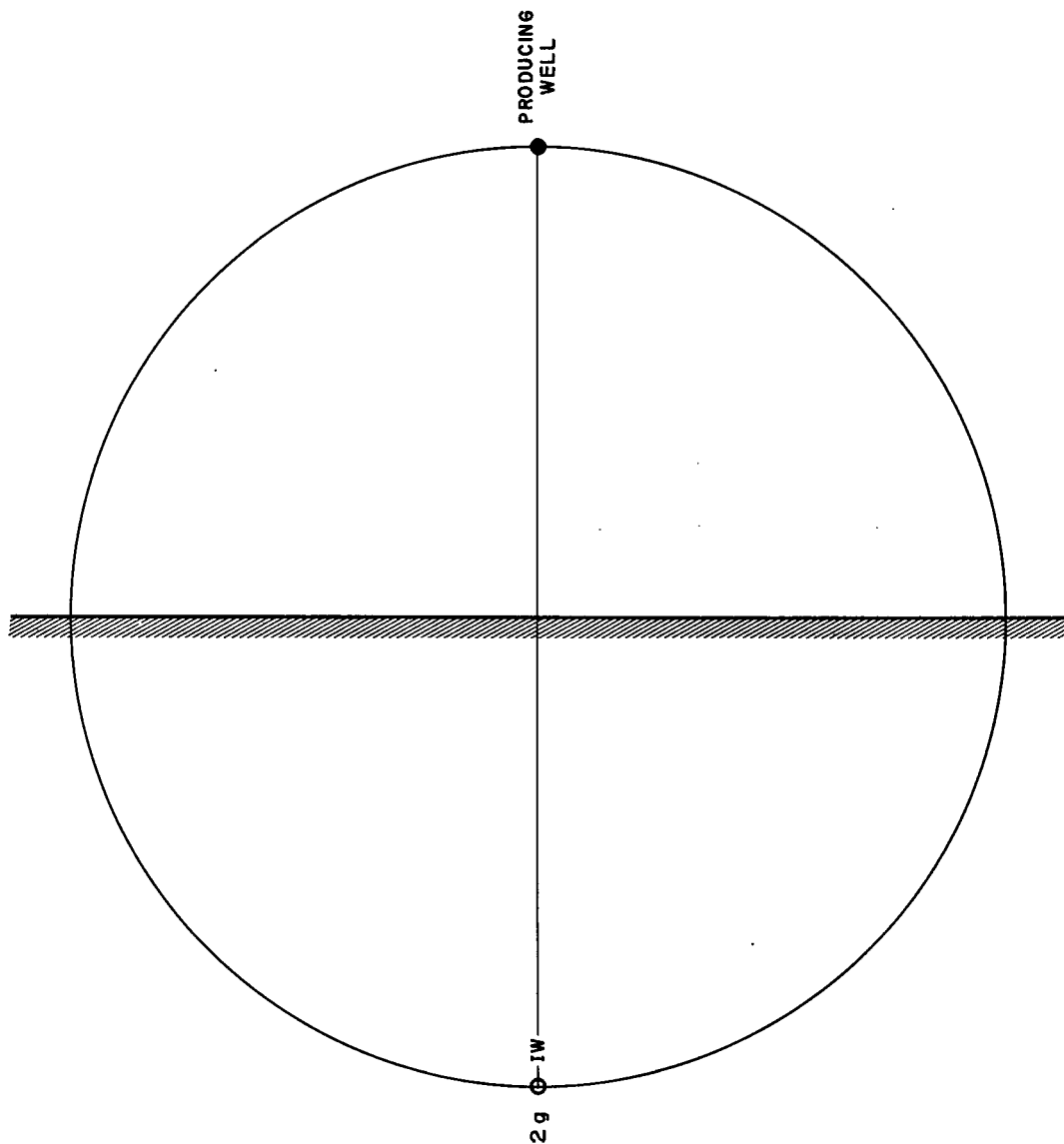
## APPENDIX C

## IMAGE SYSTEMS

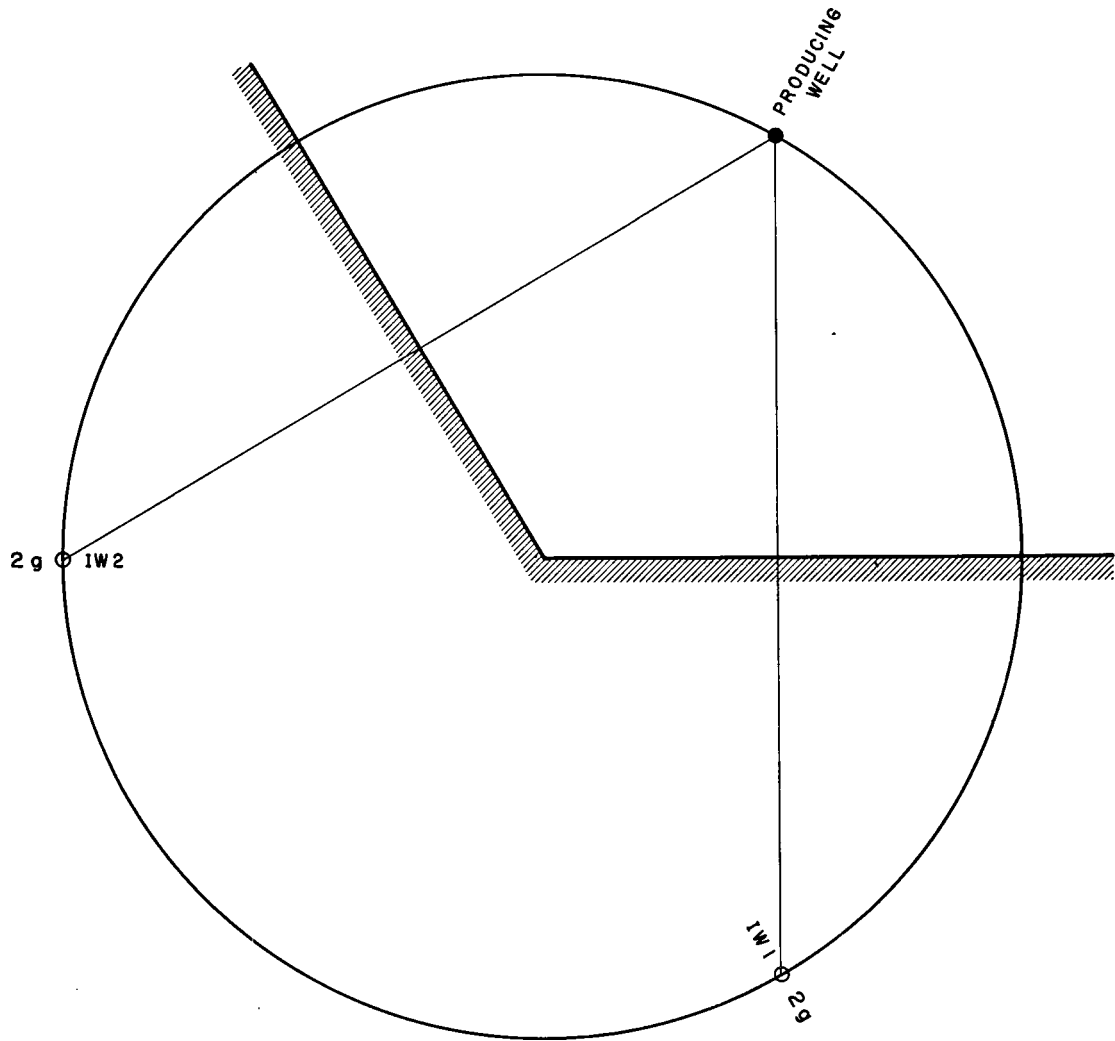
## CONTENTS

APPENDIX		PAGE
C - 1	180° Fault Block .....	113
C - 2	120° Fault Block .....	114
C - 3	90° Fault Block .....	115
C - 4	72° Fault Block .....	116
C - 5	60° Fault Block .....	117
C - 6	45° Fault Block .....	118
C - 7	30° Fault Block .....	119
C - 8	15° Fault Block .....	120
C - 9	Parallel Faults .....	121

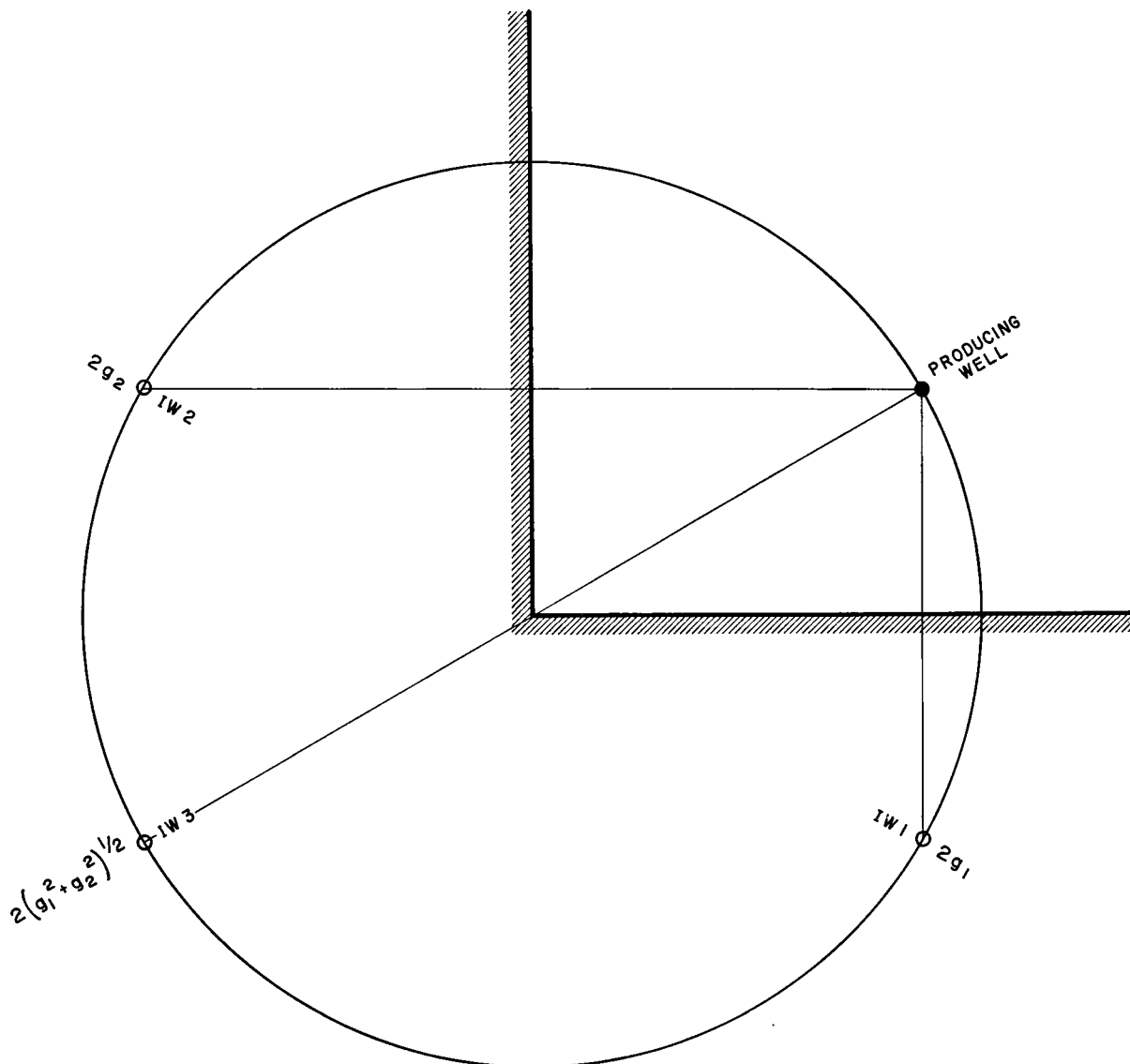
Image wells are numbered, and the distance between the producing well and each image well is given, in terms of the distances between the producing well and the two faults.



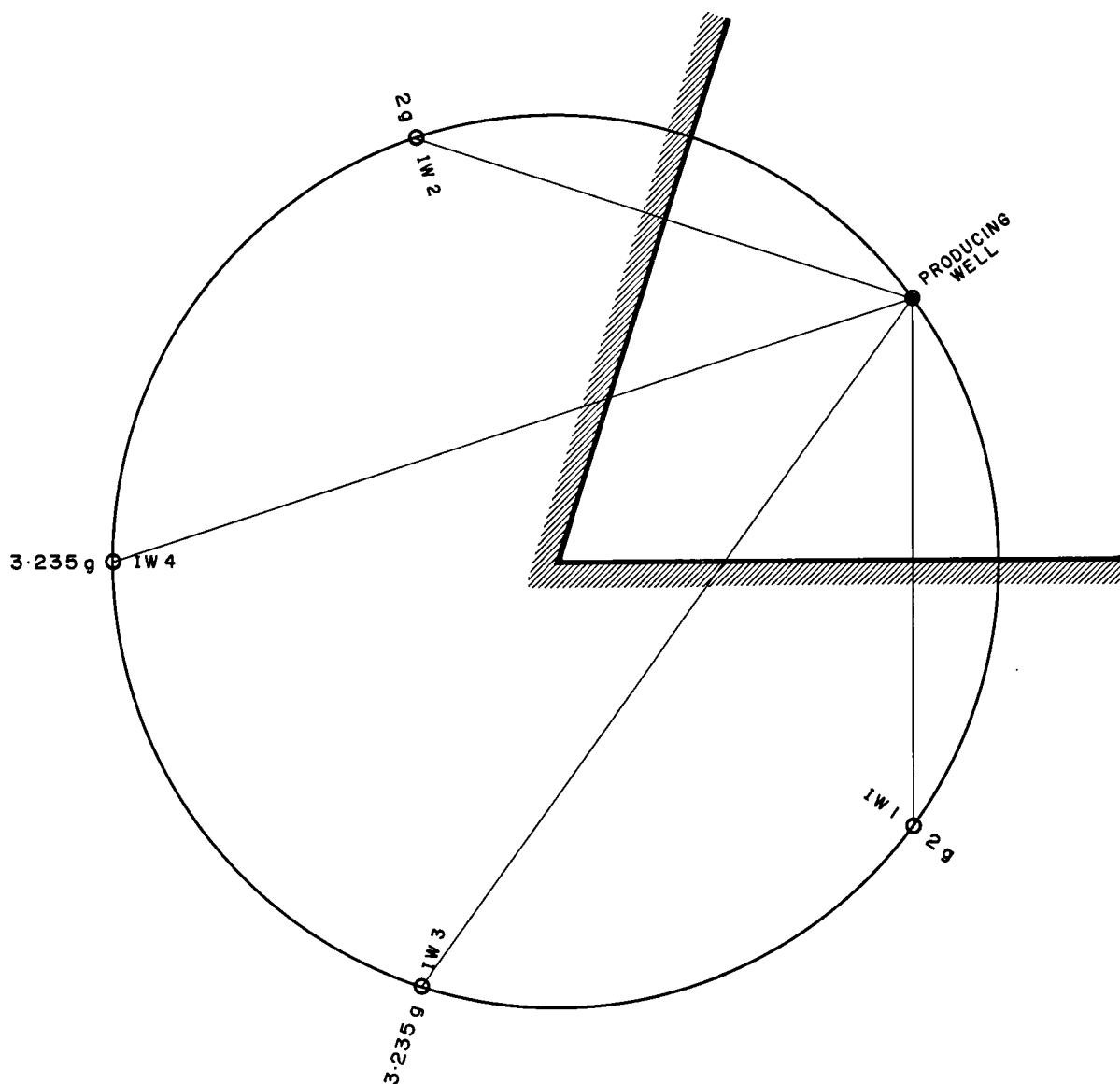
APPENDIX C-1  
180° FAULT BLOCK  
IMAGE SYSTEM



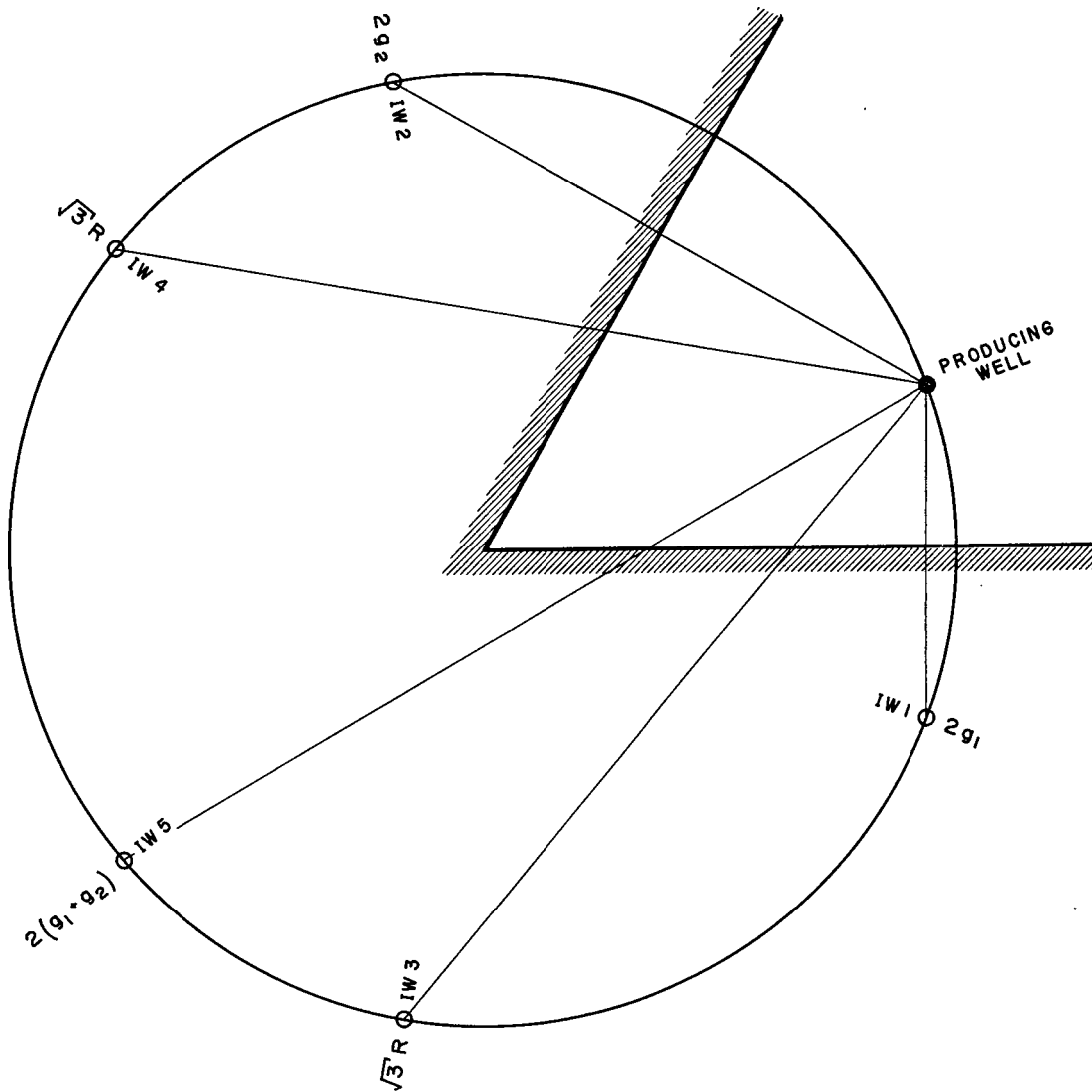
APPENDIX C-2  
120° FAULT BLOCK  
IMAGE SYSTEM



APPENDIX C-3  
 90° FAULT BLOCK  
 IMAGE SYSTEM

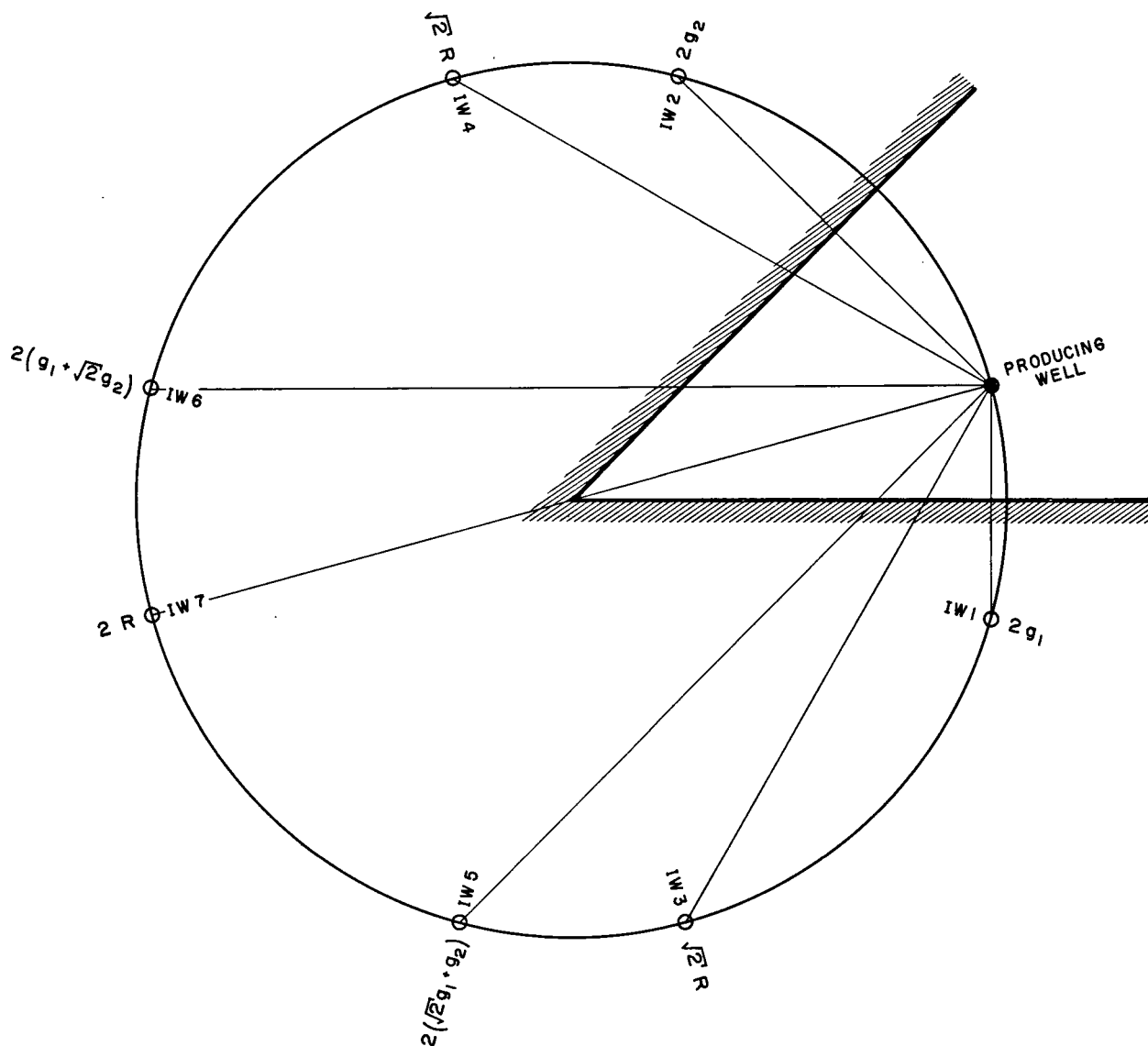


APPENDIX C-4  
72° FAULT BLOCK  
IMAGE SYSTEM



$$R = \frac{2}{\sqrt{3}} (g_1^2 + g_1 g_2 + g_2^2)^{1/2}$$

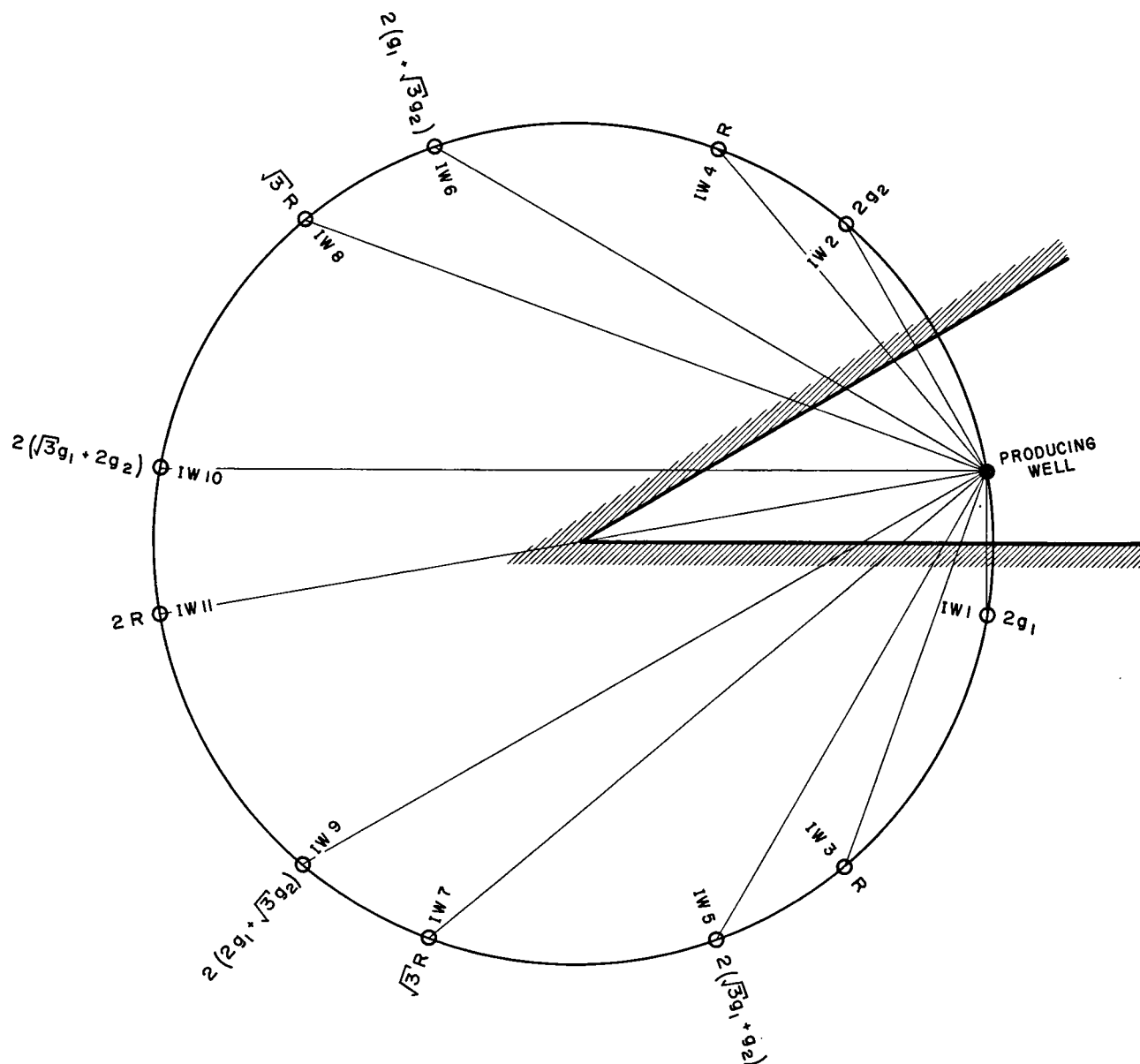
APPENDIX C-5  
60° FAULT BLOCK  
IMAGE SYSTEM



$$R = [2(g_1^2 + g_2^2 + \sqrt{2}g_1 g_2)]^{1/2}$$

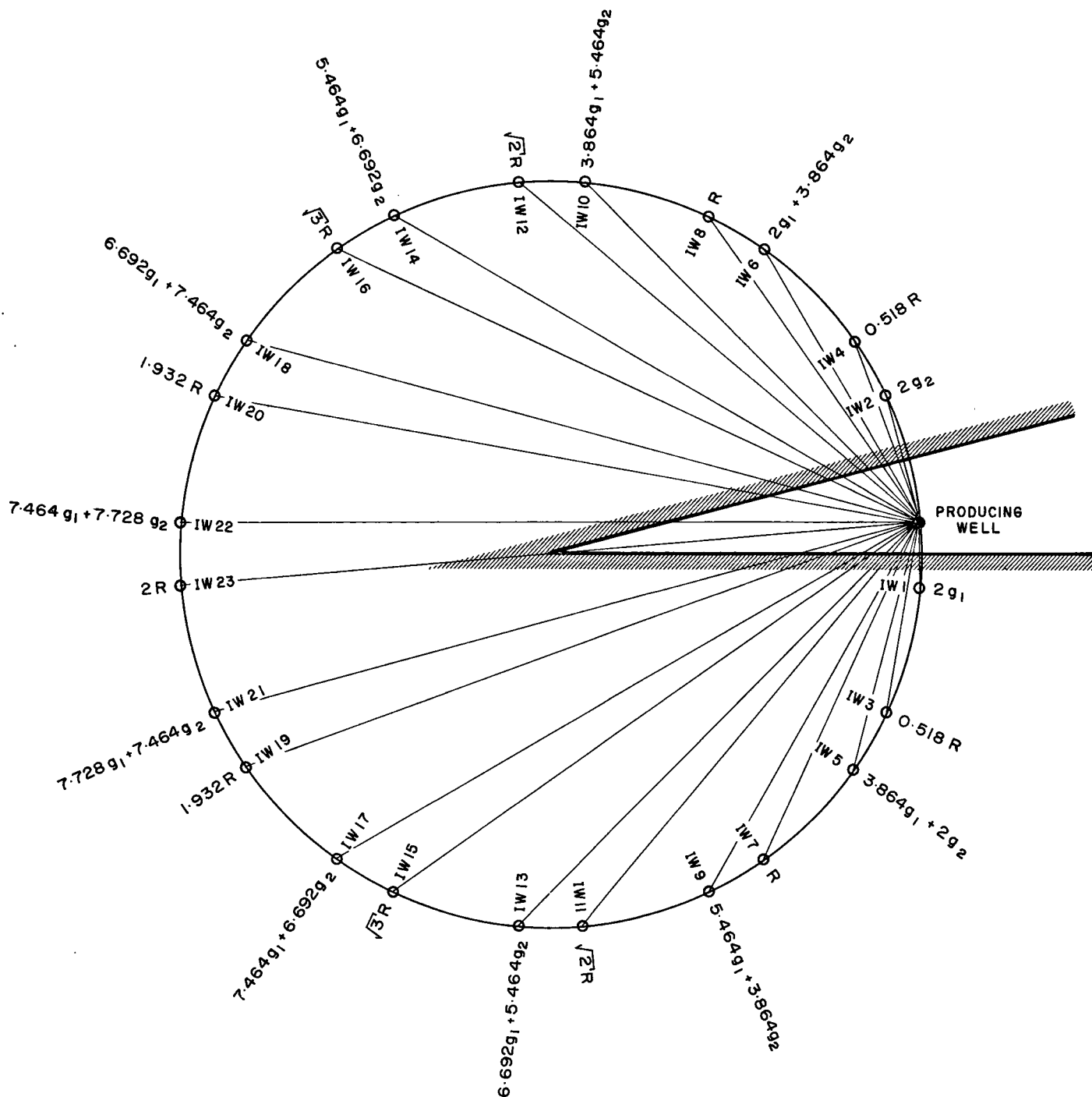
APPENDIX C-6  
45° FAULT BLOCK  
IMAGE SYSTEM





$$R = 2(g_1^2 + g_2^2 + \sqrt{3}g_1g_2)^{1/2}$$

APPENDIX C-7  
30° FAULT BLOCK  
IMAGE SYSTEM



$$R = \left( 14.928g_1^2 + 14.928g_2^2 + 28.839g_1g_2 \right)^{1/2}$$

APPENDIX C - 8

15° FAULT BLOCK  
IMAGE SYSTEM

\_\_\_\_\_

.....

APPENDIX C-9

PARALLEL FAULTS

IMAGE SYSTEM

## APPENDIX D

COMPUTER PROGRAMS FOR IDEAL  
DIMENSIONLESS DRAWDOWN CURVES

CONTENTS

APPENDIX	PAGE
D - 1      180° Fault Block .....	124
D - 2      120° Fault Block .....	125
D - 3      90° Fault Block .....	126
D - 4      72° Fault Block .....	127
D - 5      60° Fault Block .....	128
D - 6      45° Fault Block .....	129
D - 7      30° Fault Block .....	130
D - 8      15° Fault Block .....	131
D - 9      Parallel Faults .....	132

The above programs, which are written in the MAD language, require the use of the Well Function, and are therefore run together with the external function shown in Figure B - 2 .

The dimensionless distances to the two faults ( $r_{D1}$  and  $r_{D2}$ ) are fed in as data, but the programs are only applicable when  $r_{D2} > 0$  .

```

$ COMPILE MAD,EXECUTE
R
R      ONE HUNDRED AND EIGHTY DEGREE FAULT BLOCK
R  DIMENSIONLESS DRAWDOWN CURVES FOR RD GREATER THAN ZERO
R
START  READ DATA RD
        PRINT FORMAT TITLE
        PRINT FORMAT DIMRAD,RD
        A = RD.P.2
        THROUGH BETA, FOR VALUES OF TD = 1E1,2E1,5E1,1E2,2E2,5E2,1E3,
12E3,5E3,1E4,2E4,5E4,1E5,2E5,5E5,1E6,2E6,5E6,1E7,2E7,5E7,1E8,
22E8,5E8,1E9,2E9,5E9,1E10,2E10,5E10,1E11,2E11,5E11,1E12
        JD = 0.5*(W.(0.25/TD)+W.(A/TD))
BETA   PRINT FORMAT JDVSTD,TD,JD
        TRANSFER TO START
        VECTOR VALUES TITLE = $1H1,S39,41H ONE HUNDRED AND EIGHTY DEGR
1EE FAULT BLOCK*$
        VECTOR VALUES DIMRAD = $////S54,5HRD = F7.2////S48,2HTD,S20,
12HJD//*$
        VECTOR VALUES JDVSTD = $1H ,S40,E12.1,S15,F6.2*$
        END OF PROGRAM

```

APPENDIX D - 1

180° FAULT BLOCK

COMPUTER PROGRAM

```

$ COMPILE MAD,EXECUTE
R
R          ONE HUNDRED AND TWENTY DEGREE FAULT BLOCK
R DIMENSIONLESS DRAWDOWN CURVES FOR RD GREATER THAN ZERO
R
START      READ DATA RD
           PRINT FORMAT TITLE
           PRINT FORMAT DIMRAD,RD
           A = RD.P.2
           THROUGH BETA, FOR VALUES OF TD = 1E1,2E1,5E1,1E2,2E2,5E2,1E3,
12E3,5E3,1E4,2E4,5E4,1E5,2E5,5E5,1E6,2E6,5E6,1E7,2E7,5E7,1E8,
22E8,5E8,1E9,2E9,5E9,1E10,2E10,5E10,1E11,2E11,5E11,1E12
           JD = 0.5*W.(0.25/TD)+W.(A/TD)
BETA       PRINT FORMAT JDVSTD,TD,JD
           TRANSFER TO START
           VECTOR VALUES TITLE = $1H1,S39,41H ONE HUNDRED AND TWENTY DEGR
1EE FAULT BLOCK*$
           VECTOR VALUES DIMRAD = $////S54,5HRD = F7.2///S48,2HTD,S20,
12HJD//*$
           VECTOR VALUES JDVSTD = $1H ,S40,E12.1,S15,F6.2*$
           END OF PROGRAM

```

APPENDIX D - 2

120° FAULT BLOCK

COMPUTER PROGRAM

```

$ COMPILE MAD,EXECUTE
R
R                               NINETY DEGREE FAULT BLOCK
R  DIMENSIONLESS DRAWDOWN CURVES FOR RD2 GREATER THAN ZERO
R
START  READ DATA RD2,RD1
        PRINT FORMAT TITLE
        PRINT FORMAT DIMRAD,RD2,RD1
        WHENEVER RD1.E.O.
        A = RD2.P.2
        THROUGH ALPHA, FOR VALUES OF TD = 1E1,2E1,5E1,1E2,2E2,5E2,1E3,
12E3,5E3,1E4,2E4,5E4,1E5,2E5,5E5,1E6,2E6,5E6,1E7,2E7,5E7,1E8,
22E8,5E8,1E9,2E9,5E9,1E10,2E10,5E10,1E11,2E11,5E11,1E12
        JD = W.(0.25/TD)+W.(A/TD)
ALPHA  PRINT FORMAT JDVSTD,TD,JD
        OTHERWISE
        A = RD1.P.2
        B = RD2.P.2
        C = A+B
        THROUGH BETA, FOR VALUES OF TD = 1E1,2E1,5E1,1E2,2E2,5E2,1E3,
12E3,5E3,1E4,2E4,5E4,1E5,2E5,5E5,1E6,2E6,5E6,1E7,2E7,5E7,1E8,
22E8,5E8,1E9,2E9,5E9,1E10,2E10,5E10,1E11,2E11,5E11,1E12
        JD = 0.5*(W.(0.25/TD)+W.(A/TD)+W.(B/TD)+W.(C/TD))
BETA  PRINT FORMAT JDVSTD,TD,JD
        END OF CONDITIONAL
        TRANSFER TO START
        VECTOR VALUES TITLE = $1H1,S47,25HNINETY DEGREE FAULT BLOCK*$
        VECTOR VALUES DIMRAD = $////S43,6HRD2 = F7.2,S9,6HRD1 = F7.2/
1//S48,2HTD,S20,2HJD//*$
        VECTOR VALUES JDVSTD = $1H ,S40,E12.1,S15,F6.2*$
        END OF PROGRAM

```

APPENDIX D - 3

90° FAULT BLOCK

COMPUTER PROGRAM



```

$ COMPILE MAD,EXECUTE
R
R              SEVENTY TWO DEGREE FAULT BLOCK
R  DIMENSIONLESS DRAWDOWN CURVES FOR RD GREATER THAN ZERO
R
START          READ DATA RD
                PRINT FORMAT TITLE
                PRINT FORMAT DIMRAD,RD
                A = RD.P.2
                B = 2.616*A
                THROUGH BETA, FOR VALUES OF TD = 1E1,2E1,5E1,1E2,2E2,5E2,1E3,
12E3,5E3,1E4,2E4,5E4,1E5,2E5,5E5,1E6,2E6,5E6,1E7,2E7,5E7,1E8,
22E8,5E8,1E9,2E9,5E9,1E10,2E10,5E10,1E11,2E11,5E11,1E12
                JD = 0.5*W.(0.25/TD)+W.(A/TD)+W.(B/TD)
BETA           PRINT FORMAT JDVSTD,TD,JD
                TRANSFER TO START
                VECTOR VALUES TITLE = $1H1,S45,30HSEVENTY TWO DEGREE FAULT BL
10CK*$
                VECTOR VALUES DIMRAD = $////S54,5HRD = F7.2///S48,2HTD,S20,
12HJD//*$
                VECTOR VALUES JDVSTD = $1H ,S40,E12.1,S15,F6.2*$
                END OF PROGRAM

```

APPENDIX D - 4

72° FAULT BLOCK

COMPUTER PROGRAM

```

$ COMPILE MAD,EXECUTE
R
R                               SIXTY DEGREE FAULT BLOCK
R  DIMENSIONLESS DRAWDOWN CURVES FOR RD2 GREATER THAN ZERO
R
START  READ DATA RD2,RD1
        PRINT FORMAT TITLE
        PRINT FORMAT DIMRAD,RD2,RD1
        WHENEVER RD1.E.O.
        A = RD2.P.2
        THROUGH ALPHA, FOR VALUES OF TD = 1E1,2E1,5E1,1E2,2E2,5E2,1E3,
12E3,5E3,1E4,2E4,5E4,1E5,2E5,5E5,1E6,2E6,5E6,1E7,2E7,5E7,1E8,
22E8,5E8,1E9,2E9,5E9,1E10,2E10,5E10,1E11,2E11,5E11,1E12
        JD = W.(0.25/TD)+2.*W.(A/TD)
ALPHA  PRINT FORMAT JDVSTD,TD,JD
        OTHERWISE
        A = RD1.P.2
        B = RD2.P.2
        C = A+B+RD1*RD2
        D = (RD1+RD2).P.2
        THROUGH BETA, FOR VALUES OF TD = 1E1,2E1,5E1,1E2,2E2,5E2,1E3,
12E3,5E3,1E4,2E4,5E4,1E5,2E5,5E5,1E6,2E6,5E6,1E7,2E7,5E7,1E8,
22E8,5E8,1E9,2E9,5E9,1E10,2E10,5E10,1E11,2E11,5E11,1E12
        JD = 0.5*(W.(0.25/TD)+W.(A/TD)+W.(B/TD)+2.*W.(C/TD)+W.(D/TD))
BETA  PRINT FORMAT JDVSTD,TD,JD
        END OF CONDITIONAL
        TRANSFER TO START
        VECTOR VALUES TITLE = $1H1,S48,24HSIXTY DEGREE FAULT BLOCK*$
        VECTOR VALUES DIMRAD = $////S43,6HRD2 = F7.2,S9,6HRD1 = F7.2/
1//S48,2HTD,S20,2HJD//*$
        VECTOR VALUES JDVSTD = $1H ,S40,E12 .1,S15,F6.2*$
        END OF PROGRAM

```

APPENDIX D - 5

60° FAULT BLOCK

COMPUTER PROGRAM

```

$ COMPILE MAD,EXECUTE
R
R                                     FORTY FIVE DEGREE FAULT BLOCK
R  DIMENSIONLESS DRAWDOWN CURVES FOR RD2 GREATER THAN ZERO
R
START  READ DATA RD2,RD1
        PRINT FORMAT TITLE
        PRINT FORMAT DIMRAD,RD2,RD1
        WHENEVER RD1.E.O.
        A = RD2.P.2
        B = 2.*A
        THROUGH ALPHA, FOR VALUES OF TD = 1E1,2E1,5E1,1E2,2E2,5E2,1E3,
12E3,5E3,1E4,2E4,5E4,1E5,2E5,5E5,1E6,2E6,5E6,1E7,2E7,5E7,1E8,
22E8,5E8,1E9,2E9,5E9,1E10,2E10,5E10,1E11,2E11,5E11,1E12
        JD = W.(0.25/TD)+2.*W.(A/TD)+W.(B/TD)
ALPHA  PRINT FORMAT JDVSTD,TD,JD
        OTHERWISE
        A = RD1.P.2
        B = RD2.P.2
        C = A+B+1.414*RD1*RD2
        D = (1.414*RD1+RD2).P.2
        E = (RD1+1.414*RD2).P.2
        F = 2.*C
        THROUGH BETA, FOR VALUES OF TD = 1E1,2E1,5E1,1E2,2E2,5E2,1E3,
12E3,5E3,1E4,2E4,5E4,1E5,2E5,5E5,1E6,2E6,5E6,1E7,2E7,5E7,1E8,
22E8,5E8,1E9,2E9,5E9,1E10,2E10,5E10,1E11,2E11,5E11,1E12
        JD = 0.5*(W.(0.25/TD)+W.(A/TD)+W.(B/TD)+2.*W.(C/TD)+W.(D/TD)
1+W.(E/TD)+W.(F/TD))
BETA  PRINT FORMAT JDVSTD,TD,JD
        END OF CONDITIONAL
        TRANSFER TO START
        VECTOR VALUES TITLE = $1H1,S45,29H FORTY FIVE DEGREE FAULT BLO
1CK*$
        VECTOR VALUES DIMRAD = $////S43,6HRD2 = F7.2,S9,6HRD1 = F7.2/
1//S48,2HTD,S20,2HJD//*$
        VECTOR VALUES JDVSTD = $1H ,S40,E12.1,S15,F6.2*$
        END OF PROGRAM

```

APPENDIX D - 6

45° FAULT BLOCK

COMPUTER PROGRAM

\$ COMPILE MAD,EXECUTE

R

R

THIRTY DEGREE FAULT BLOCK

R DIMENSIONLESS DRAWDOWN CURVES FOR RD2 GREATER THAN ZERO

R

START

READ DATA RD2,RD1

PRINT FORMAT TITLE

PRINT FORMAT DIMRAD,RD2,RD1

WHENEVER RD1.E.O.

A = RD2.P.2

B = 3.\*A

C = 4.\*A

THROUGH ALPHA, FOR VALUES OF TD = 1E1,2E1,5E1,1E2,2E2,5E2,1E3,  
12E3,5E3,1E4,2E4,5E4,1E5,2E5,5E5,1E6,2E6,5E6,1E7,2E7,5E7,1E8,  
22E8,5E8,1E9,2E9,5E9,1E10,2E10,5E10,1E11,2E11,5E11,1E12

JD = W.(0.25/TD)+2.\*W.(A/TD)+2.\*W.(B/TD)+W.(C/TD)

ALPHA

PRINT FORMAT JDVSTD,TD,JD

OTHERWISE

A = RD1.P.2

B = RD2.P.2

C = A+B+1.732\*RD1\*RD2

D = (1.732\*RD1+RD2).P.2

E = (RD1+1.732\*RD2).P.2

F = 3.\*C

G = (2.\*RD1+1.732\*RD2).P.2

H = (1.732\*RD1+2.\*RD2).P.2

I = 4.\*C

THROUGH BETA, FOR VALUES OF TD = 1E1,2E1,5E1,1E2,2E2,5E2,1E3,  
12E3,5E3,1E4,2E4,5E4,1E5,2E5,5E5,1E6,2E6,5E6,1E7,2E7,5E7,1E8,  
22E8,5E8,1E9,2E9,5E9,1E10,2E10,5E10,1E11,2E11,5E11,1E12

JD = 0.5\*(W.(0.25/TD)+W.(A/TD)+W.(B/TD)+2.\*W.(C/TD)+W.(D/TD)  
1+W.(E/TD)+2.\*W.(F/TD)+W.(G/TD)+W.(H/TD)+W.(I/TD))

BETA

PRINT FORMAT JDVSTD,TD,JD

END OF CONDITIONAL

TRANSFER TO START

VECTOR VALUES TITLE = \$1H1,S47,25H THIRTY DEGREE FAULT BLOCK\*\$

VECTOR VALUES DIMRAD = \$////S43,6HRD2 = F7.2,S9,6HRD1 = F7.2/  
1//S48,2HTD,S20,2HJD//\*\$

VECTOR VALUES JDVSTD = \$1H ,S40,E12.1,S15,F6.2\*\$

END OF PROGRAM

APPENDIX D - 7

30° FAULT BLOCK

COMPUTER PROGRAM

```

R
R                                     FIFTEEN DEGREE FAULT BLOCK
R   DIMENSIONLESS DRAWDOWN CURVES FOR RD2 GREATER THAN ZERO
R
START   READ DATA RD2,RD1
        PRINT FORMAT TITLE
        PRINT FORMAT DIMRAD,RD2,RD1
        WHENEVER RD1.E.O.
        A = RD2.P.2
        B = 3.732*A
        C = 7.464*A
        D = 11.196*A
        E = 13.928*A
        F = 14.928*A
        THROUGH ALPHA, FOR VALUES OF TD = 1E1,2E1,5E1,1E2,2E2,5E2,1E3,
        12E3,5E3,1E4,2E4,5E4,1E5,2E5,5E5,1E6,2E6,5E6,1E7,2E7,5E7,1E8,
        22E8,5E8,1E9,2E9,5E9,1E10,2E10,5E10,1E11,2E11,5E11,1E12
        JD = W.(0.25/TD)+2.*W.(A/TD)+2.*W.(B/TD)+2.*W.(C/TD)
        1+2.*W.(D/TD)+2.*W.(E/TD)+W.(F/TD)
ALPHA   PRINT FORMAT JDVSTD,TD,JD
        OTHERWISE
        X = 14.928*RD1.P.2+14.928*RD2.P.2+28.839*RD1*RD2
        A = RD1.P.2
        B = RD2.P.2
        C = 0.067*X
        D = (1.932*RD1+RD2).P.2
        E = (RD1+1.932*RD2).P.2
        F = 0.25*X
        G = (2.732*RD1+1.932*RD2).P.2
        H = (1.932*RD1+2.732*RD2).P.2
        I = 0.5*X
        J = (3.346*RD1+2.732*RD2).P.2
        K = (2.732*RD1+3.346*RD2).P.2
        L = 0.75*X
        M = (3.732*RD1+3.346*RD2).P.2
        N = (3.346*RD1+3.732*RD2).P.2
        O = 0.933*X
        P = (3.864*RD1+3.732*RD2).P.2
        Q = (3.732*RD1+3.864*RD2).P.2
        THROUGH BETA, FOR VALUES OF TD = 1E1,2E1,5E1,1E2,2E2,5E2,1E3,
        12E3,5E3,1E4,2E4,5E4,1E5,2E5,5E5,1E6,2E6,5E6,1E7,2E7,5E7,1E8,
        22E8,5E8,1E9,2E9,5E9,1E10,2E10,5E10,1E11,2E11,5E11,1E12
        JD = 0.5*(W.(0.25/TD)+W.(A/TD)+W.(B/TD)+2.*W.(C/TD)+W.(D/TD)
        1+W.(E/TD)+2.*W.(F/TD)+W.(G/TD)+W.(H/TD)+2.*W.(I/TD)+W.(J/TD)
        2+W.(K/TD)+2.*W.(L/TD)+W.(M/TD)+W.(N/TD)+2.*W.(O/TD)+W.(P/TD)
        3+W.(Q/TD)+W.(X/TD))
BETA   PRINT FORMAT JDVSTD,TD,JD
        END OF CONDITIONAL
        TRANSFER TO START
        VECTOR VALUES TITLE=$1H1,S47,26HFIFTEEN DEGREE FAULT BLOCK*$
        VECTOR VALUES DIMRAD = $////S43,6HRD2 = F7.2,S9,6HRD1 = F7.2/
        1//S48,2HTD,S20,2HJD//*$
        VECTOR VALUES JDVSTD = $1H ,S40,E12.1,S15,F6.2*$
        END OF PROGRAM

```

APPENDIX D - 8

15° FAULT BLOCK

COMPUTER PROGRAM

R  
R  
R  
R  
TWO PARALLEL FAULTS  
DIMENSIONLESS DRAWDOWN CURVES

START

INTEGER N  
READ DATA RD2,RD1  
PRINT FORMAT TITLE  
PRINT FORMAT DIMRAD,RD2,RD1  
WHENEVER RD1.E.0.  
THROUGH ALPHA, FOR VALUES OF TD = 1.1,2E1,5E1,1E2,2E2,5E2,1E3,  
1.2E3,5E3,1E4,2E4,5E4,1E5,2E5,5E5,1E6,2E6,5E6,1E7,2E7,5E7,1E8,  
2.2E8,5E8,1E9  
N = 1  
JD = W.(0.25/TD)  
THROUGH THETA, FOR I = RD2,RD2,I.G.1E6  
A = I.P.2/TD  
WHENEVER A.LE.4.  
JD = JD+2.\*W.(A)  
N = N+4  
OTHERWISE  
TRANSFER TO ALPHA  
END OF CONDITIONAL  
PRINT FORMAT RESULTS,TD,JD,N  
OTHERWISE  
C = RD1+RD2  
THROUGH BETA, FOR VALUES OF TD = 1E1,2E1,5E1,1E2,2E2,5E2,1E3,  
1.2E3,5E3,1E4,2E4,5E4,1E5,2E5,5E5,1E6,2E6,5E6,1E7,2E7,5E7,1E8,  
2.2E8,5E8,1E9  
N = 0  
JD = 0.5\*W.(0.25/TD)  
THROUGH PHI, FOR I = 0.,C,I.G.1E6  
D = (RD1+I).P.2/TD  
E = (RD2+I).P.2/TD  
F = (C+I).P.2/TD  
WHENEVER F.LE.4.  
JD = JD+0.5\*(W.(D)+W.(E))+W.(F)  
N = N+4  
OR WHENEVER E.LE.4.  
JD = JD+0.5\*(W.(D)+W.(E))  
N = N+2  
TRANSFER TO BETA  
OR WHENEVER D.LE.4.  
JD = JD+0.5\*W.(D)  
N = N+1  
TRANSFER TO BETA  
OTHERWISE  
TRANSFER TO BETA  
END OF CONDITIONAL  
PRINT FORMAT RESULTS,TD,JD,N  
END OF CONDITIONAL  
TRANSFER TO START  
VECTOR VALUES TITLE = \$1H1,S52,15HPARALLEL FAULTS\*\$  
VECTOR VALUES DIMRAD = \$////S42,6HRD2 = F7.2,S9,6HRD1 = F7.2  
1///S35,2HTD,S20,2HJD,S20,6HIMAGES//\*\$  
VECTOR VALUES RESULTS = \$1H ,S27,E12.1,S14,F7.2,S19,I5\*\$  
END OF PROGRAM

THETA  
ALPHA

PHI  
BETA

APPENDIX D - 9

PARALLEL FAULTS

COMPUTER PROGRAM

## APPENDIX E

LIBRARY OF TYPE DIMENSIONLESS  
DRAWDOWN CURVES

CONTENTS

APPENDIX	PAGE
E - 1      180° Fault Block .....	135
E - 2      120° Fault Block .....	136
E - 3      90° Fault Block .....	137
E - 4      72° Fault Block .....	138
E - 5      60° Fault Block .....	139
E - 6      45° Fault Block .....	140
E - 7      30° Fault Block .....	141
E - 8      15° Fault Block .....	142
E - 9      Parallel Faults .....	143

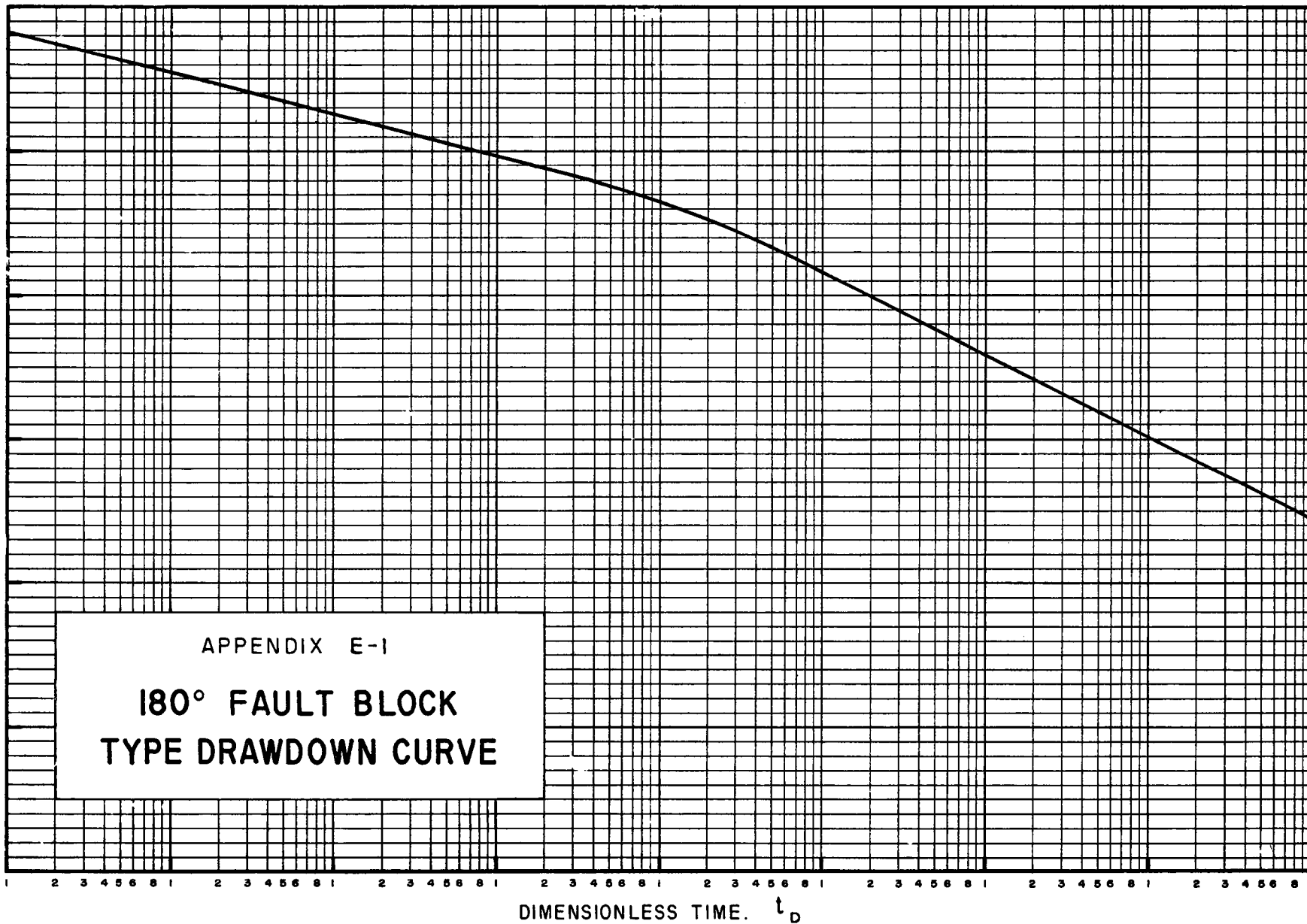
It should be noted that the scale used for Appendix E - 9 is different from that used for the remaining curves.

Actual values of dimensionless drawdown and dimensionless time are omitted, since only the shape of each curve is significant.

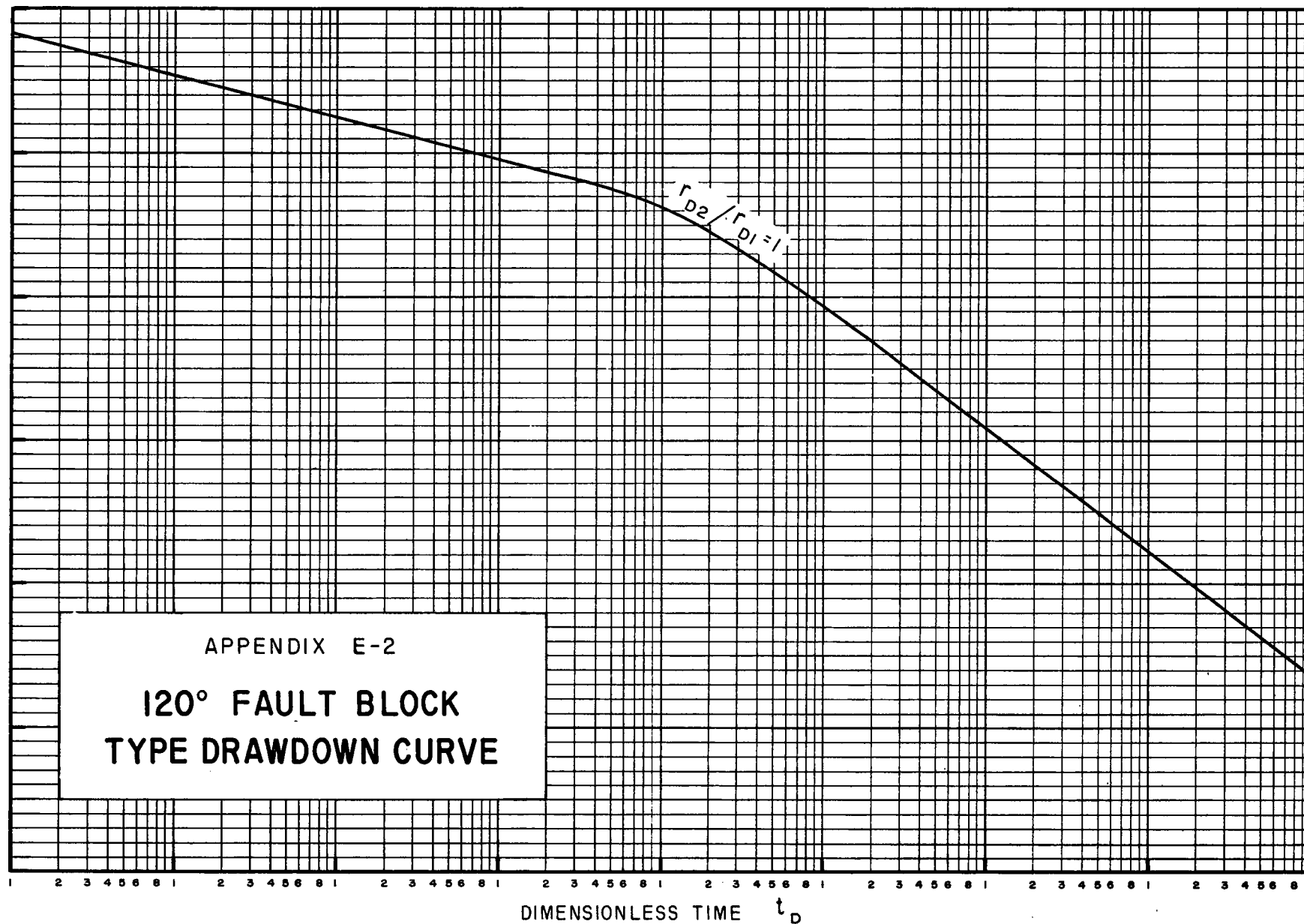
Although the curves were constructed from equations pertaining to an ideal well, they also apply to a well with a skin, provided the part of the drawdown curve due to the skin is recognized and ignored.



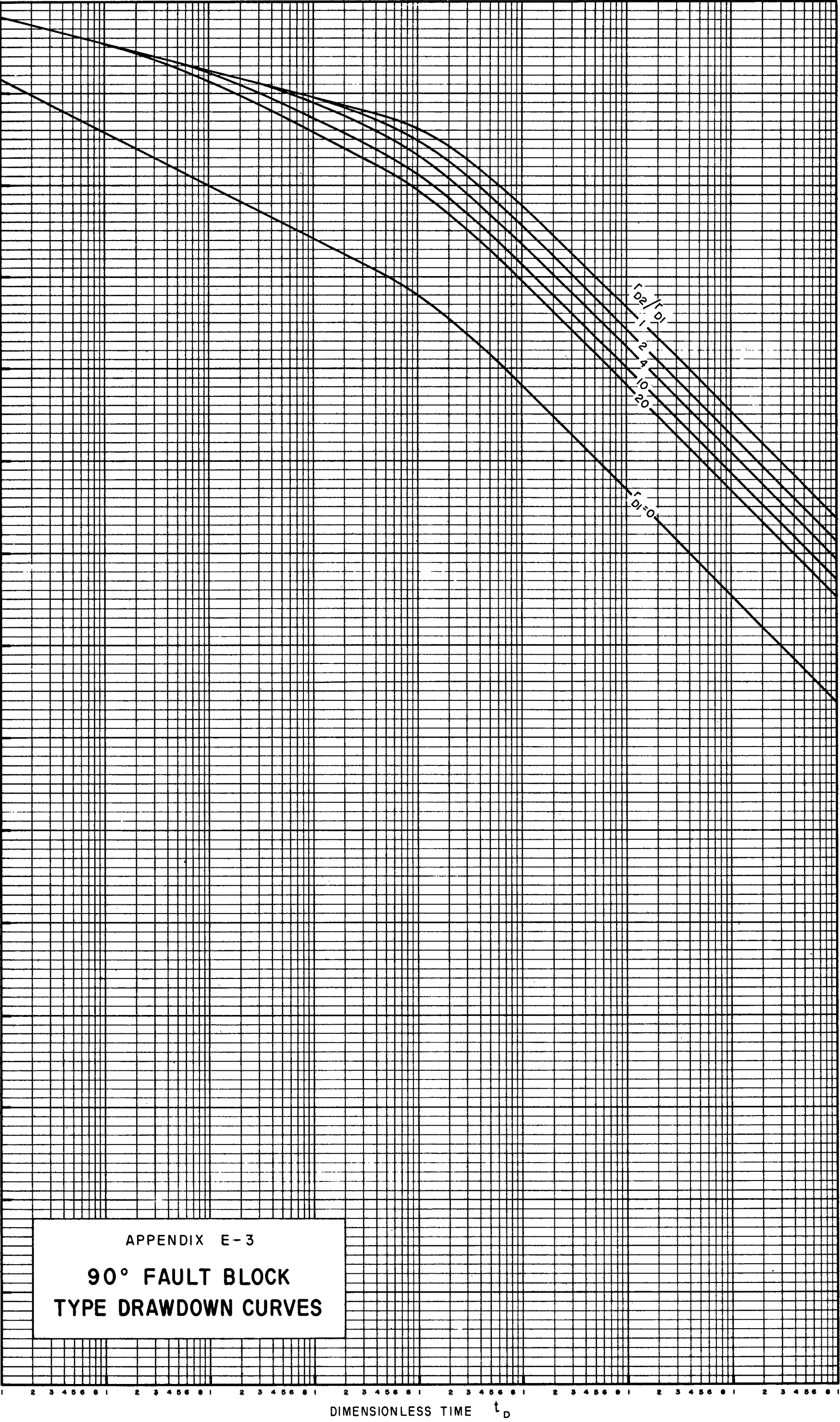
DIMENSIONLESS DRAWDOWN,  $J_D$  (SCALE - 1" = 4 Units)



DIMENSIONLESS DRAWDOWN  $J_D$  (SCALE - 1" = 4 Units)

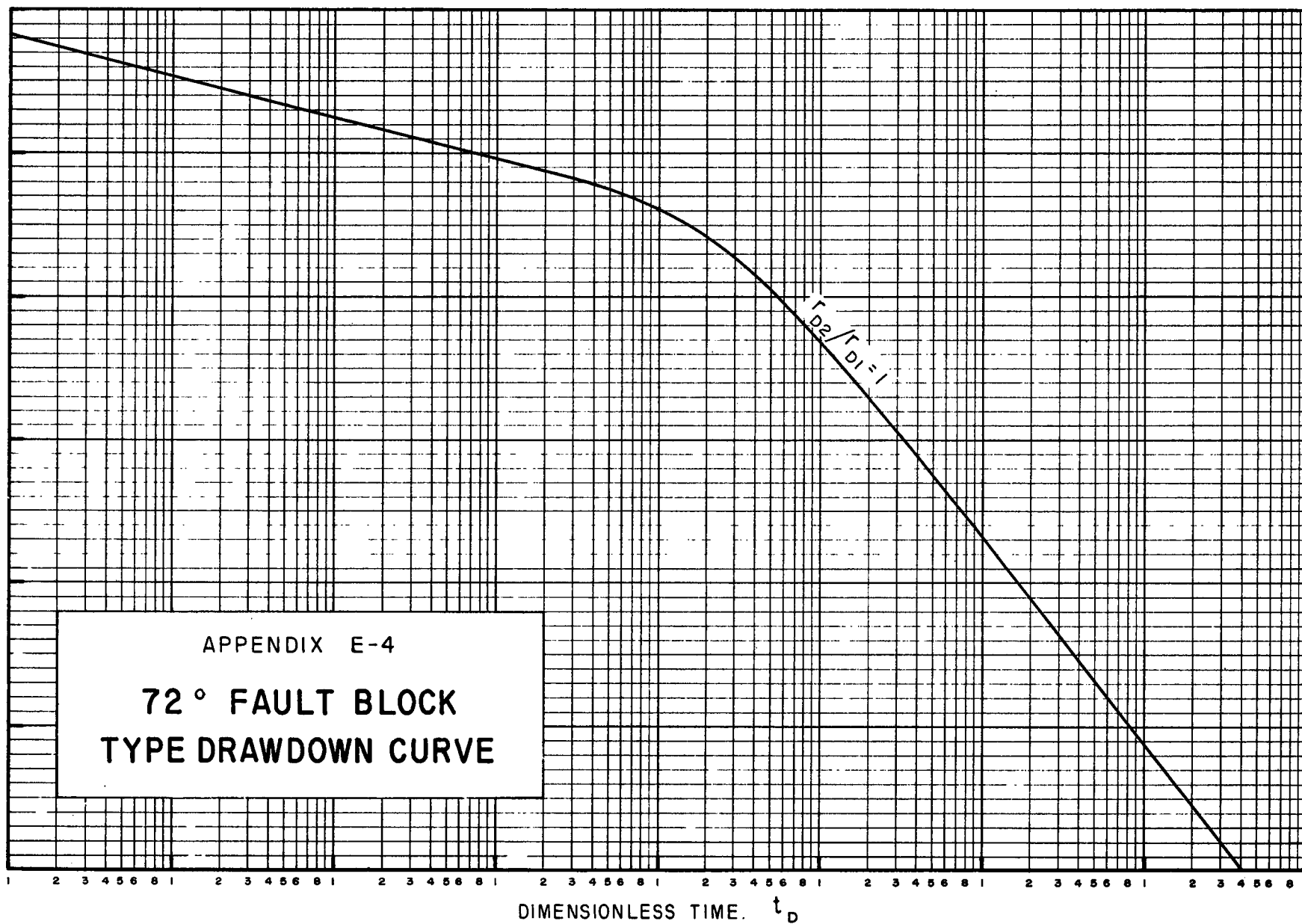


DIMENSIONLESS DRAWDOWN,  $J_D$  (SCALE -  $r' = 4$  Units)

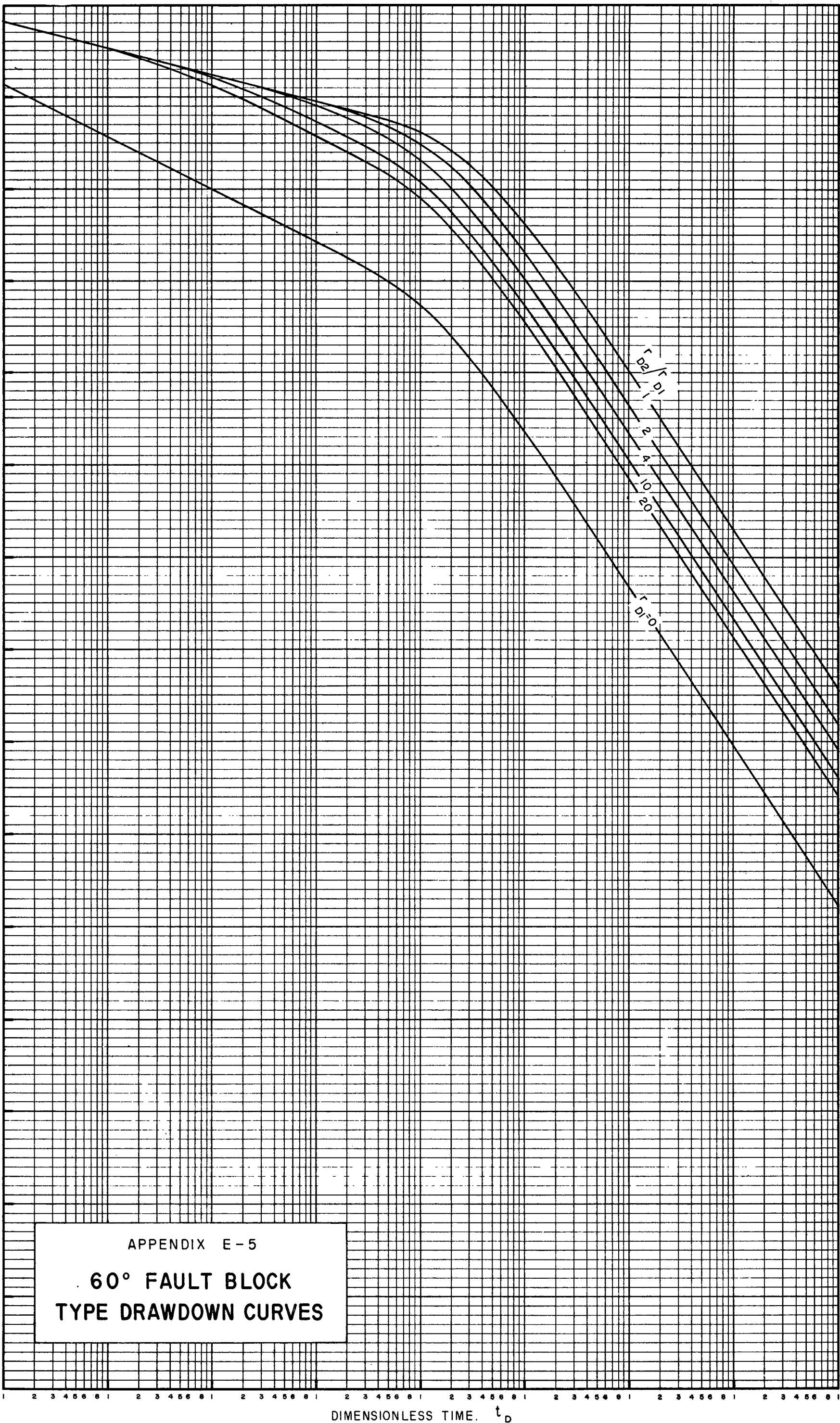


APPENDIX E-3  
90° FAULT BLOCK  
TYPE DRAWDOWN CURVES

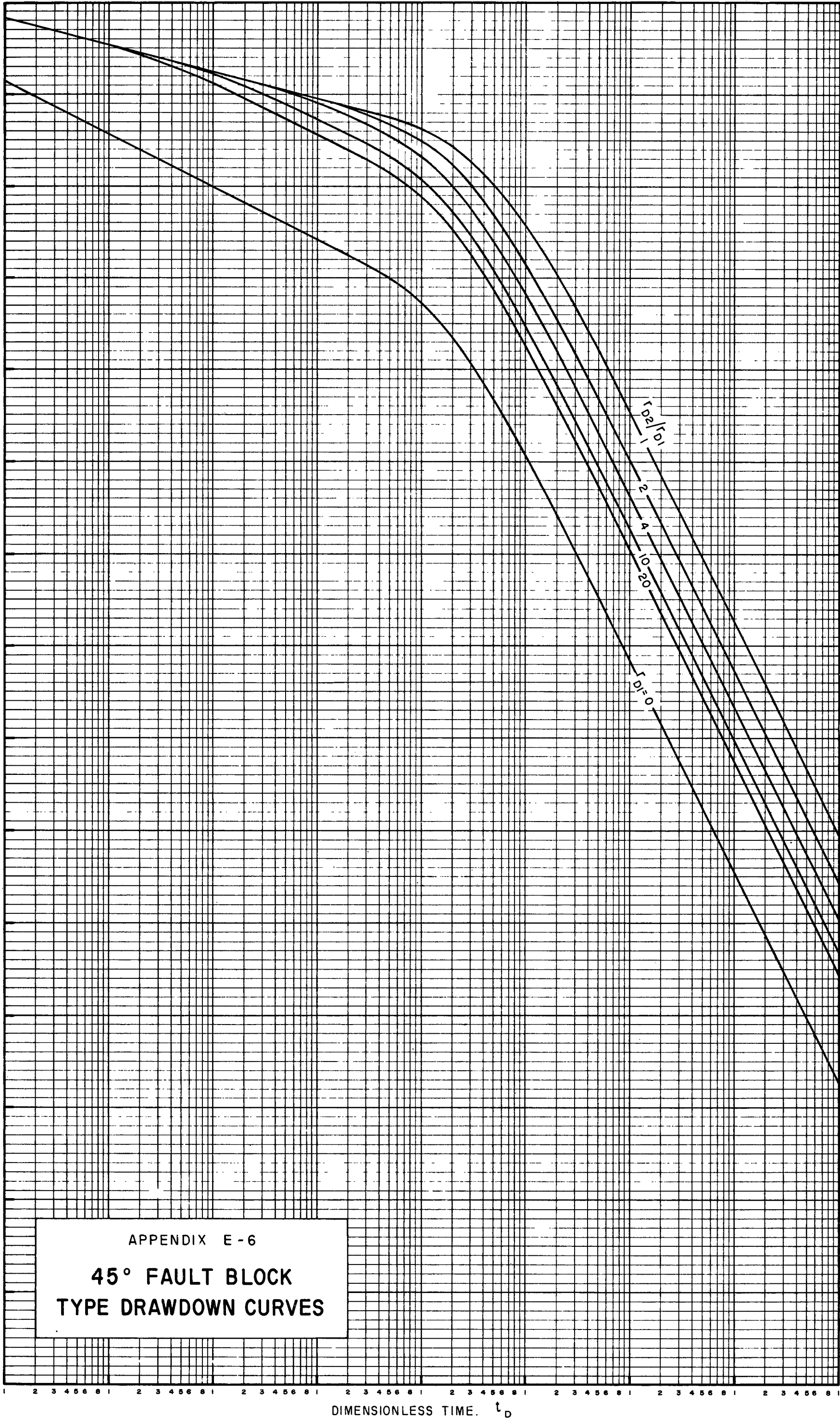
DIMENSIONLESS DRAWDOWN  $J_D$  (SCALE - 1" = 4 Units)



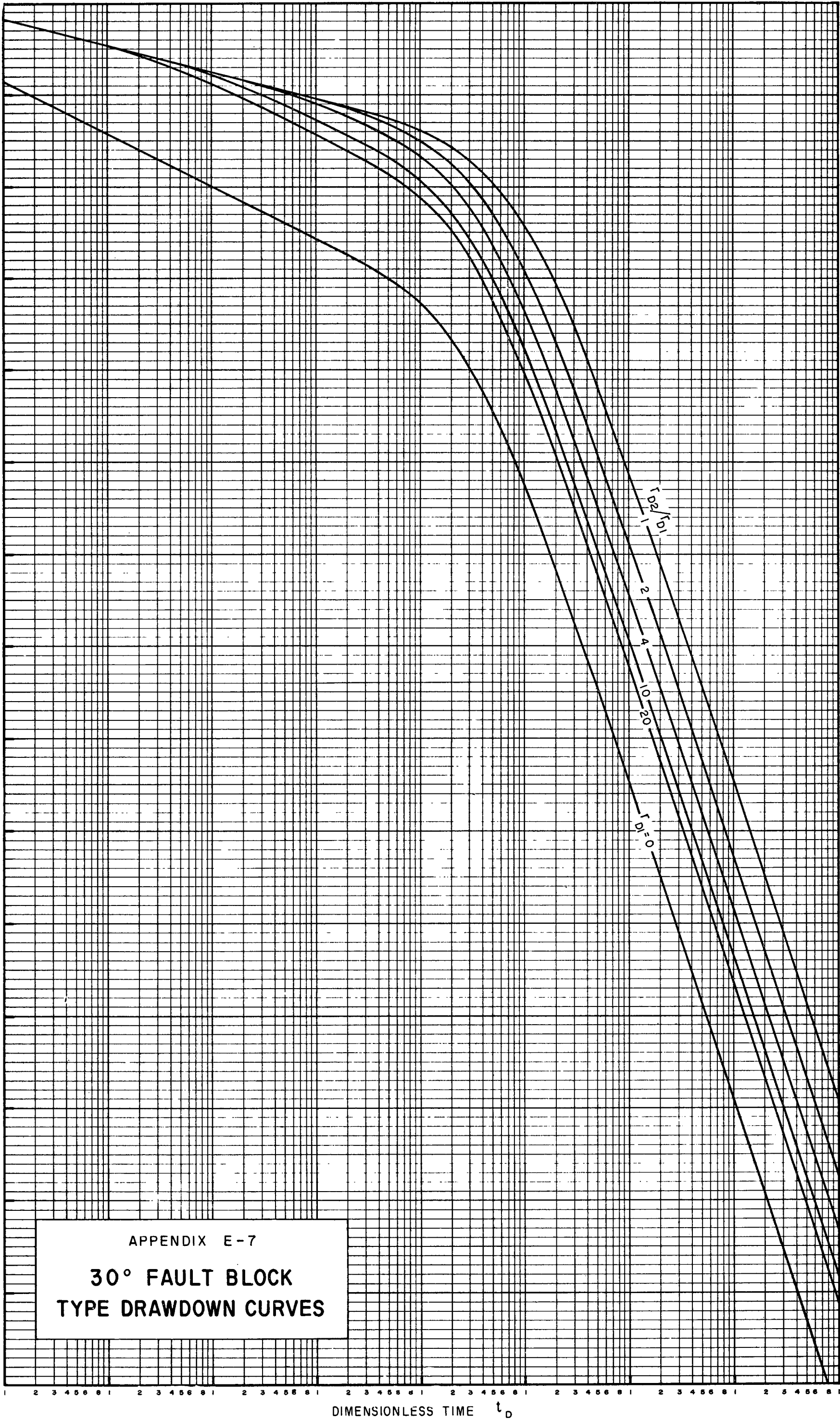
DIMENSIONLESS DRAWDOWN,  $J_D$  (SCALE -  $r' = 4$  Units)



DIMENSIONLESS DRAWDOWN,  $J_D$  (SCALE -  $r' = 4$  Units)



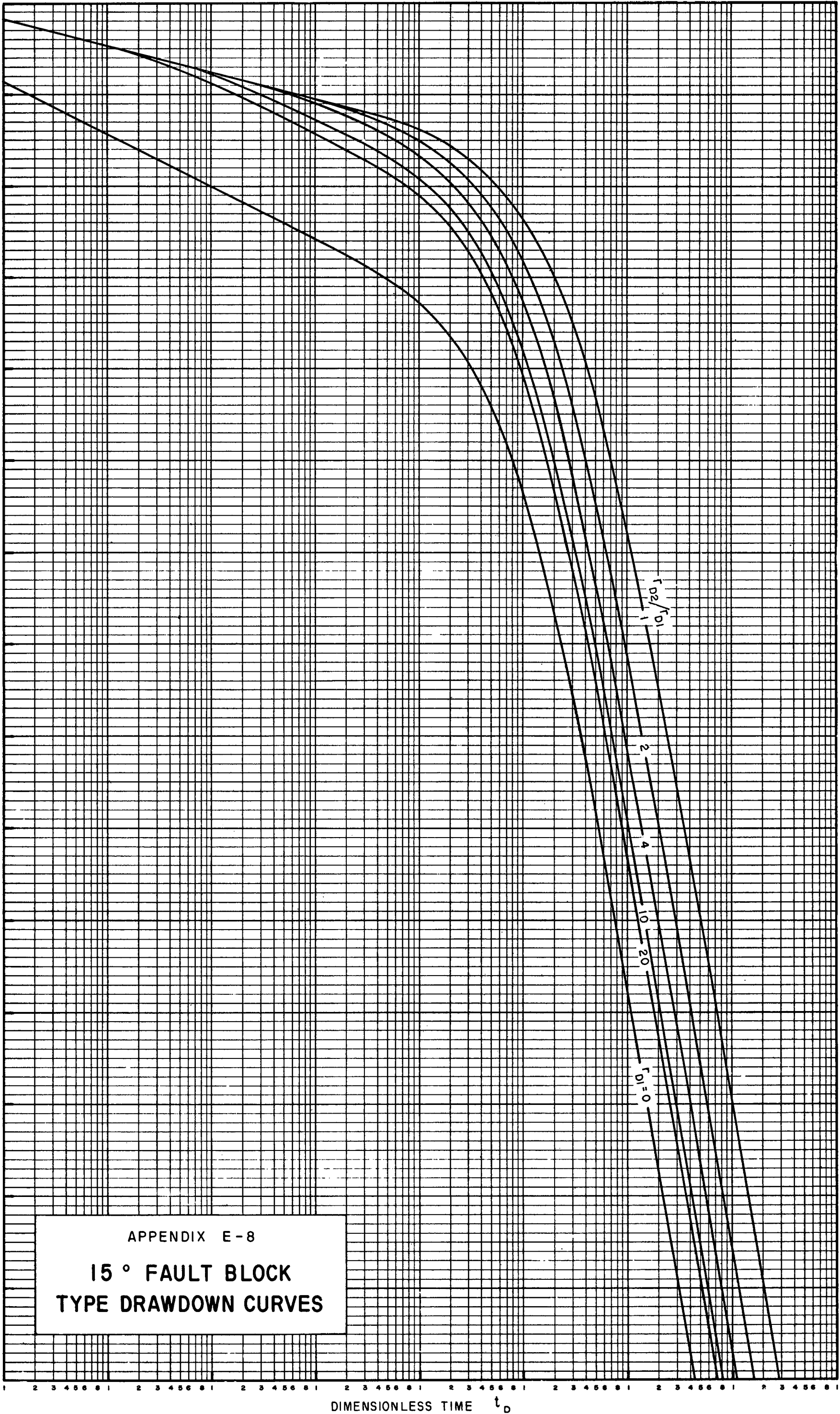
DIMENSIONLESS DRAWDOWN,  $J_D$  (SCALE  $\sim r' = 4$  Units)



APPENDIX E-7  
30° FAULT BLOCK  
TYPE DRAWDOWN CURVES



DIMENSIONLESS DRAWDOWN,  $J_D$  (SCALE -  $r' = 4$  Units)



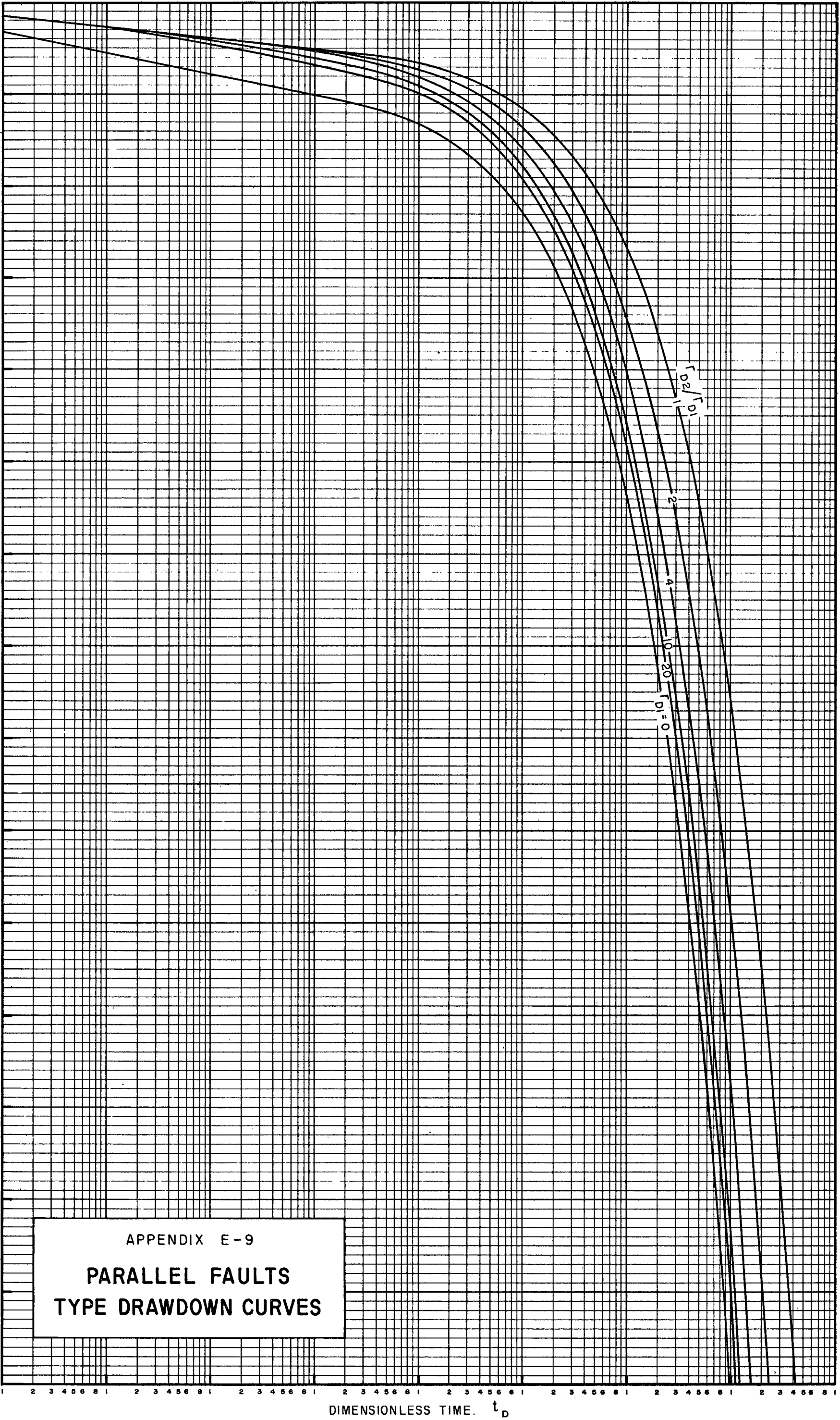
APPENDIX E-8

15 ° FAULT BLOCK  
TYPE DRAWDOWN CURVES

DIMENSIONLESS TIME  $t_D$



DIMENSIONLESS DRAWDOWN,  $J_D$  (SCALE -  $r^2 = 10$  Units)



## APPENDIX F

## CHARTS FOR SUBSURFACE FAULT MAPPING

The following two charts are used to determine the dimensionless distances to the two faults ( $r_{D1}$  and  $r_{D2}$ ), when the angle of intersection between the faults, and the dimensionless times at which straight-line portions of the drawdown curve intersect, are known.

Appendix F - 1 is applicable when  $r_{D1} > 0$ , and is used in two ways as follows :

( i ) When  $r_{D2}/r_{D1} \geq 20$ , measure the dimensionless time at which the straight lines of slope  $m_D$  and  $2m_D$  intersect ( $t_{D2,1}$ ) and also the dimensionless time at which the straight lines of slope  $m_D$  and  $nm_D$  intersect ( $t_{Dn,1}$ ), where  $nm_D$  is the slope of the final straight-line portion of the dimensionless drawdown curve.

Using the right-hand side of the chart, enter the value of  $t_{D2,1}$  and determine the value of  $r_{D1}$ .

Using the left-hand side of the chart, pass a straight line through the values of  $t_{D2,1}$  and  $t_{Dn,1}$ , to determine the value of  $t_{Dn,1}/t_{D2,1}$ . Proceed horizontally from this point to the appropriate curve, depending upon the angle of intersection between the faults, as determined from Appendix E. Then proceed vertically down to determine the value of  $r_{D2}/r_{D1}$ .

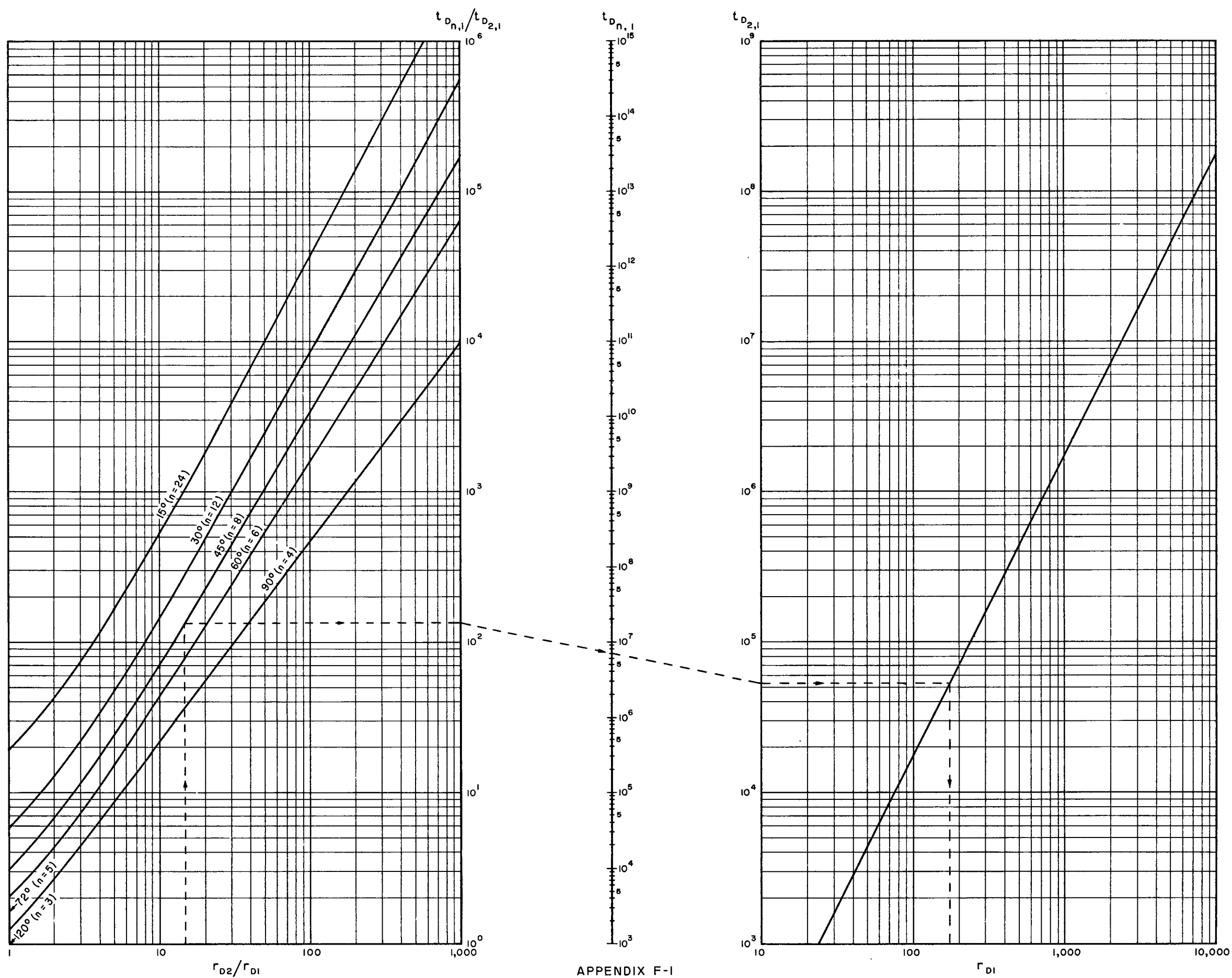
Knowing  $r_{D1}$  and  $r_{D2}/r_{D1}$ , calculate the value of  $r_{D2}$ .

(ii) When  $r_{D2}/r_{D1} < 20$ , determine the value of  $r_{D2}/r_{D1}$  from Appendix E and measure  $t_{Dn,1}$  on the dimensionless drawdown curve. Enter  $r_{D2}/r_{D1}$  where indicated, proceed vertically to the appropriate curve, then horizontally to obtain the value of  $t_{Dn,1}/t_{D2,1}$ . Pass a straight line from this point through the measured value of  $t_{Dn,1}$  to obtain  $t_{D2,1}$ . Using the right-hand side of the chart, determine  $r_{D1}$ .

Knowing  $r_{D1}$  and  $r_{D2}/r_{D1}$ , calculate the value of  $r_{D2}$ .

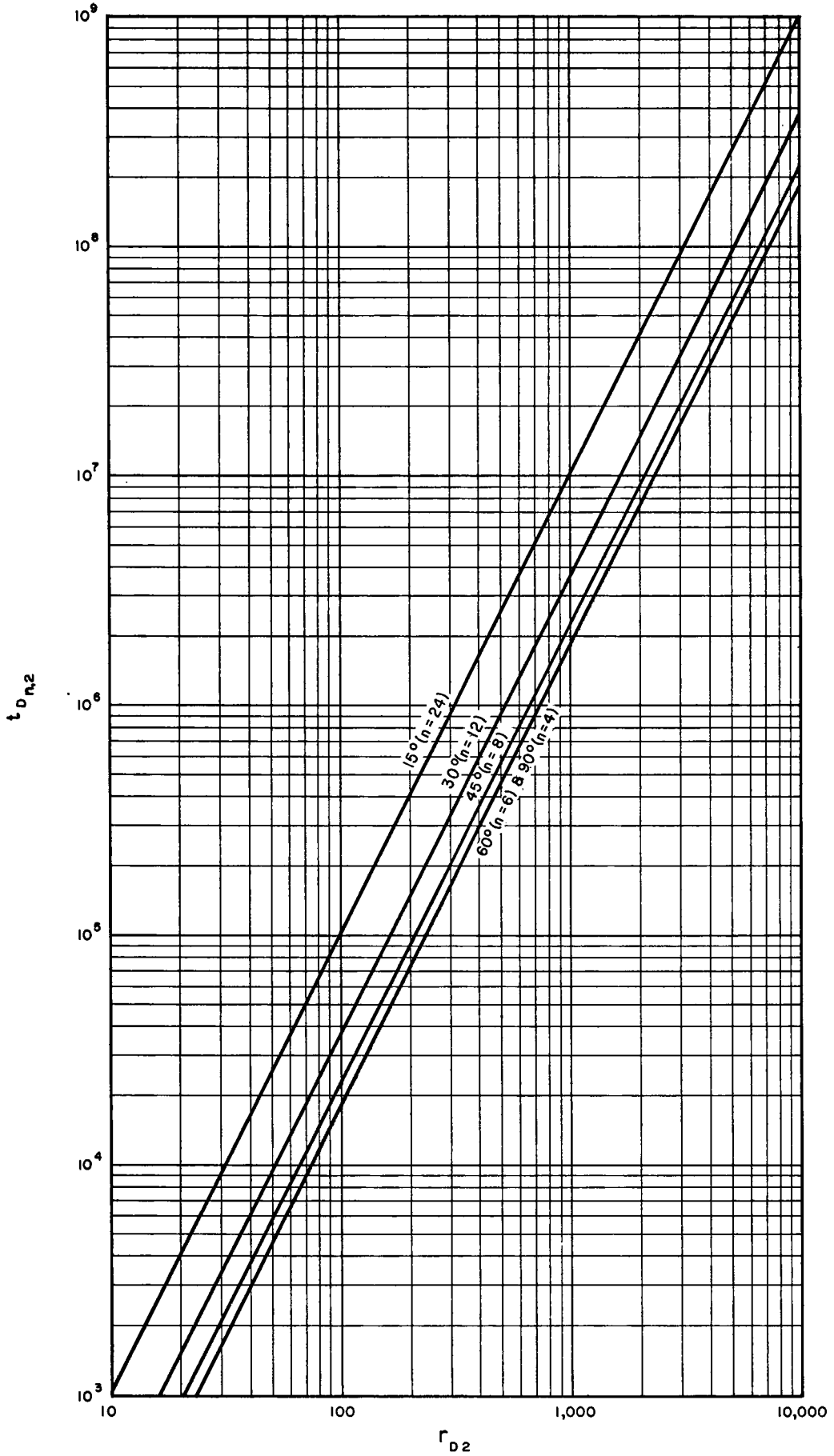
The example illustrated on the chart is for a  $45^\circ$  fault block in which  $r_{D2}/r_{D1} = 15$  and  $t_{D8,1} = 7 \times 10^6$ . Using the chart as above,  $r_{D1}$  is found to be 180. Thus, since  $r_{D2}/r_{D1} = 15$ ,  $r_{D2} = 15 \times 180 = 2700$ .

Appendix F - 2, the use of which is self-explanatory, is applicable when  $r_{D1} = 0$ .



APPENDIX F-1

CHART No.1 FOR  
SUBSURFACE FAULT MAPPING  
( $r_{D1} > 0$ )



APPENDIX F-2

CHART No. 2 FOR  
SUBSURFACE FAULT MAPPING  
( $r_{D1} = 0$ )